Extracellular vesicle miRNAs are regulators of lung adenocarcinoma tumor progression and are important tumor-stromal communicators

by

James Lawson

B.Sc., The University of Guelph, 2013

A THESIS SUBMITTED IN PARTIAL FULFILLMENT OF

THE REQUIREMENTS FOR THE DEGREE OF

DOCTOR OF PHILOSOPHY

in

THE FACULTY OF GRADUATE AND POSTDOCTORAL STUDIES

(Interdisciplinary Oncology)

THE UNIVERSITY OF BRITISH COLUMBIA

(Vancouver)

April 2018

Abstract

Lung adenocarcinoma (LAC) is the most common subtype of non-small cell lung cancer and is the leading cause of cancer death worldwide. Five-year survival rates of LAC remain dismally low at ~17%, due to the late stage of diagnosis. MicroRNAs (miRNAs) are small RNAs 17-22 nucleotides long and are stable within the serum and when present within extracellular vesicles (EVs), additionally EV miRNAs contribute to tumor-stromal communication. Determining non-invasive novel biomarkers for early disease detection and understanding EV miRNA tumor-stromal communication may aid in improving overall survival.

In this thesis, I identify miRNAs that are differentially detected within the serum of patients with LAC using miRNA profiling of patient serum samples and demographically matched controls. I additionally characterize the function of LAC secreted miRNA within EVs when entering normal fibroblast and endothelial cells. My hypotheses are that miRNAs within the serum of LAC patients will show a unique signature that will be distinguishable from non-cancer high risk individuals, and that miRNAs selectively released from LAC cells within EVs will promote tumorigenesis in endothelial cells through stimulating angiogenesis and in fibroblasts through promoting the cancer associated fibroblast phenotype. A unique signature of miRNAs within the serum of LAC patients is found and miRNAs within patient serum is dependent on sex. Several miRNAs within LAC EVs are then functionally characterized in the role they play when signaling to normal stromal cells.

Together, this thesis provides a comprehensive analysis of LAC miRNAs and the roles they play as biomarkers within the serum and as tumor-stromal signals when within EVs.

Lay Summary

Lung cancer is the leading cause of cancer death worldwide. A better understanding of the biological mechanisms that drive this disease are required to improve lung cancer survival. MicroRNAs are a group of small molecules that regulate processes within cells. When deregulated, they can play a role in driving cancer growth and development. Cells have been shown to selectively package and release specific microRNAs into small cellular containers called extracellular vesicles. The released vesicles can then affect the surrounding environment, including transforming neighboring cells into become more cancer-like. In my thesis, I examine whether cancer cell secreted microRNAs can be used to detect lung cancer early in development within the blood of patients. In addition, I determine the function of specific microRNAs within extracellular vesicles when they enter neighboring normal cells and how this mechanism contributes to transforming those cells into become more cancer-like.

Preface

The research conducted within this thesis has been approved by the University of British Columbia Research Ethics Board (Certificate Number: H10-02846)

Chapters 3 and 4 were co-authored for publication. The full author lists are as follows.

A version of Chapter 3 has been published as:

Lawson, J., Dickman, C., MacLellan, S., Towle, R., Jabalee, J., Lam, S., & Garnis, C. (2017). Selective secretion of microRNAs from lung cancer cells via extracellular vesicles promotes CAMK1D-mediated tube formation in endothelial cells. Oncotarget, 8:83913-83924.

I am first author of this work. I conducted experiments, wrote manuscript, analyzed data, interpreted the results and constructed figures. Dickman, C., Maclellan, S., Towle, R., Jabalee, J. and Garnis C. were critical in conceptualizing the project.

A version of Chapter 4 is currently submitted:

Lawson, J., Dickman, C., Towle, R., Jabalee, J., & Garnis, C. (2017). Secretion of miR-142-3p from lung adenocarcinoma cells through extracellular vesicles promotes tumor associated changes in the stroma.

I am first author of this work. I conducted 95% of experiments, wrote manuscript, analyzed data, interpreted the results and constructed figures. Dickman, C. conducted the experiment for Figure 4.5. Towle, R., Jabalee, J. and Garnis C. were critical in conceptualizing the project.

Table of Contents

List of Tables

List of Figures

List of Abbreviations

ARHGAP	Rho GTPase activating proteins
CAF	Cancer associated fibroblast
CAMK1D	Calcium/calmodulin-dependent protein kinase ID
CT Scan	Computed tomography scan
DNA	Deoxyribonucleic acid
dFBS	Depleted fetal bovine serum
EGFR	Epidermal growth factor receptor
ESCRT	Endosomal sorting complex required for transport
EV	Extracellular vesicle
FBS	Fetal bovine serum
hnRNPs	Heterogeneous nuclear riboproteins
HMEC-1	Human microvascular endothelial cell line-1
HRS	Hepatocyte growth factor-regulated tyrosine kinase substrate
IGF1R	Insulin-like growth factor 1 receptor
ILV	Intraluminal vesicle
LAC	Lung adenocarcinoma
LNA	Locked nucleic acid
MDM2	Mouse double minute 2 homolog
miRNA/miR	MicroRNA
MUC4	Mucin 4
MVB	Multivesicular bodies

NKG2D	Natural-killer group 2, member D
NSCLC	Non-small cell lung cancer
NTA	Nanoparticle tracking analysis
PCR	Polymerase chain reaction
PET Scan	Positron electron tomography scan
PNEC	Pulmonary neuroendocrine cells
qRT-PCR	Quantitative real time polymerase chain reaction
RAB14	Ras-related protein Rab-14
RNA	Ribonucleic acid
ROC Curve	Receiver operating characteristic curve
SCLC	Small cell lung cancer
SMAD2	SMAD family member 2
SMAD3	SMAD family member 3
SqCC	Squamous cell carcinoma
TGF-β	Transforming growth factor beta
TGFβR	Transforming growth factor beta receptor
TSG101	Tumor suppressor gene 101
VEGF	Vascular endothelial growth factor

Acknowledgements

I am so grateful to all of those who have supported me throughout my PhD, I could not have done this without you.

I would especially like to thank Dr. Cathie Garnis, who gave me a wonderful opportunity and fostered my passion for science and medicine providing support and guidance along the way. I would also like to thank my committee Dr. Martial Guillaud, Dr. Kevin Bennewith and Dr. Will Lockwood for their words of wisdom, scientific criticisms and invaluable support.

I would like to acknowledge the funding support for my research, the Terry Fox Research Institute. Additionally, I would like to acknowledge my scholarship support from the Interdisciplinary Oncology Program.

I want to thank Cathie Garnis lab members for their support and collaborations over the last seven years. Additionally, I would like to thank my peers in the Integrative Oncology Department at the BC Cancer Research Centre who provided advice and support.

Dedication

To my father whose life motivated me to fight against cancer. To my mother who taught me strength and resilience. To my step-father for teaching me passion and commitment. To my sister for teaching me to have fun along the way. To my wonderful girlfriend for her amazing support throughout all of this and for the amazing adventure that we are embarking upon.

Chapter 1: Introduction

1.1 Introduction to Lung Cancer

The lung is an anatomically and histologically complex organ and can generally be divided into two main regions; the conducting airways and the respiratory compartment. The conducting airways consist of two large bronchi entering the lung, which then branch into secondary bronchi and further again into tertiary bronchi. The tertiary bronchioles finally branch into bronchioles and these bronchioles connect with the respiratory compartment, which consists of alveolar ducts and alveolar which are the site of gas exchange. The large bronchial airways are lined with basal, ciliated, goblet and serous cells which are organized into a pseudostratified epithelium, pulmonary neuroendocrine cells (PNEC) are also embedded intermittently within this region[1]. Within the conducting airways goblet cells are replaced by Clara cells and a more structured columnar epithelium becomes present. A transition point appears between the tertiary bronchi and the respiratory compartment, at this point ciliated cuboidal epithelium merge with the squamous epithelium of the alveoli. The alveoli contain type 1 pneumocytes responsible for the transfer of gas between the lungs and blood, and type 2 pneumocytes responsible for surfactant production. Being a large complex organ critical in the transport of oxygen to the body, it is not surprising that lung cancer has a very low survival rate.

In Canada lung cancer is the leading cause of cancer death, responsible for more deaths than the next three major cancer types (breast, prostate and colorectal) combined[2]. It is estimated that in 2017 lung cancer will cause 21,100 deaths in Canada alone[2]. While lung cancer incidence has decreased over the last 40 years, it remains the highest contributor to cancer death in males and females[3]. Lung cancer globally is the leading contributor to new cancer cases, accounting for

an estimated 12.4% or 1,350,000 new cancer cases[4]. It is the largest contributing cancer to cancer deaths, accounting for around 17.6% of total cancer deaths or 1,180,000 deaths. Although targeted therapies have been developed to treat lung cancer, five-year survival rates remain low at ~15%[5].

A major factor contributing to lung cancer survival rates is the late stage of diagnosis. Table 1.1 summarizes lung cancer TMN stages. Stage I lung cancer is localized to the lung with no regional metastasis and is less than 5cm large while stage II lung cancer is either larger than 5cm or contains regional lymph metastasis[6]. Stage III lung cancer is a tumor of any size with local invasion and regional lymph metastasis[6]. Finally stage IV lung cancer is any tumor that has distant metastases and is known to have the worst survival rate[6]. Lung cancer is generally asymptomatic until the disease progresses to a late stage, usually Stage III or IV, manifesting as coughing and shortness of breath which are also common symptoms of heavy smokers[7,8]. This makes it difficult to detect lung cancer early in development as patients are unlikely to seek medical attention for minor symptoms. Considering that diagnosis at earlier stages greatly improves survival it is important that lung cancer is detected early.

Stage	TMN Classification	Description
Ia1	T1a(mi)N0M0 T1aN0M0	Tumor ≤ 1cm in diameter No regional lymph node metastasis or regional metastasis
Ia2	T1bN0M0	Tumor ≤ 2cm in diameter No regional lymph node metastasis or regional metastasis
Ia3	T1cN0M0	Tumor ≤ 3cm in diameter No regional lymph node metastasis or regional metastasis
Ib	T2aN0M0	Tumor > 3cm but ≤ 5cm in diameter No regional lymph metastasis or regional metastasis
IIa	T1aN1M0 T1bN1M0 T2bN0M0	Tumor > 5cm but ≤ 7cm in diameter or metastasis in an ipsilateral peribronchial and/or ipsilateral hilar lymph node and intrapulmonary nodes No distant metastasis
IIb	T1a-cN1M0 T2aN2M0 T2bN1M0 T3N0M0	Tumor > 7cm or metastasis in an ipsilateral peribronchial and/or ipsilateral hilar lymph node and intrapulmonary nodes No distant metastasis
IIIa	T1a-cN2M0 T2a-bN2M0 T3N1M0 T4N0M0 T4N1M0	Tumor < 7cm with metastasis in ipsilateral mediastinal and/or subcarinal lymph nodes; or tumor > 7cm with metastasis in either an ipsilateral peribronchial and/or ipsilateral hilar lymph node and intrapulmonary nodes or metastasis in the ipsilateral mediastinal and/or subcarinal lymph nodes; or any size tumor that has invaded: the mediastinum, heart, great vessels, trachea, recurrent laryngeal nerve, oesophagus, vertebral body or carina or separate tumor nodule in a different ipsilateral lobe with or without metastasis in ipsilateral peribronchial and/or ipsilateral hilar lymph node and intrapulmonary nodes No distant metastasis
IIIb	T1a-cN3M0 T4N2M0 T1N3M0 T2N3M0 T3N2M0	Tumor of any size that has invaded: the mediastinum, heart, great vessels, trachea, recurrent laryngeal nerve, oesophagus, vertebral body or carina or separate tumor nodule in a different ipsilateral lobe and has metastasis in the ipsilateral mediastinal and/or subcarinal lymph nodes; or any size tumor with metastasis in the contralateral mediastinal, contralateral hilar, ipsilateral or contralateral scalene or supraclavicular lymph nodes
IIIc	T3N3M0 T4N3M0	Tumor > 7cm with metastasis in contralateral mediastinal, contralateral hilar, ipsilateral or contralateral scalene or supraclavicular lymph node (s). No distant metastasis
IVa	Any T, Any N, M1a or M1b	Any size tumor with separate nodule in contralateral lobe or single extrathoracic metastasis
IVb	Any T, Any N M1c	Any size tumor with multiple extrathoracic metastases in one or more organs.

Table 1.1 TMN staging of NSCLC. Table adapted from Detterback *et al.* (2017).

The most common causes of lung cancer are smoking tobacco, second-hand smoke, radon exposure and asbestos[4]. Tobacco smoke is the highest contributing factor of lung cancer and is estimated to account for approximately 85% of lung cancer cases in Canada[9]. This includes smoking from pipes, cigars, herbal cigarettes, hookahs, and cigarettes. The risks of developing cigarette smoking related lung cancer increase with an increase in smoking duration, the age at which smoking started and the number of cigarettes each day[10,11].

1.2 Lung Cancer Subtypes

The lung is a heterogeneous organ with a highly complex collection of cell types. Lung cancer is a collection of phenotypically diverse cancers that appear in distinct regions of the lung. Lung cancer is divided into two major subtypes based on clinical and histological criteria: small cell lung cancer (SCLC) and non-small lung cancer (NSCLC).

1.2.1 Small cell lung cancer

SCLC is the most aggressive form of lung cancer and accounts for approximately 15% of all lung cancer cases. SCLC tumors are characterized by their rapid doubling time and the early onset of invasion[12]. The tumors are known to invade the bronchial walls and the parenchyma, given these features, dissemination via lymphatic and blood vessels are common, making SCLC patients generally poor candidates for surgical resection[12]. While chemotherapy treatments are generally successful with a 70-90% objective response rate, resistance and recurrence generally occur rapidly after treatment[13]. Given these features of SCLC, it has the worst 5-year survival of all lung cancers ranging from 31% at stage I to 2% at stage IV. While overall 5-year survival rates have increased over the past three decades from 4.9% (1983-1992) to 5.9% (1993-2002) to

6.4% (2003-2012), the median survival has remained at 7 months for each decade[14]. With general improvement in treatment over the decades survival rates have largely remained unchanged, it is evident that more effective treatment strategies are needed. In addition, early detection may be the best form of SCLC prevention due to the increase in survival if caught early.

The central airways are typically the site of SCLC development, occurring mainly in the secondary bronchi. The cell of origin for SCLC is currently unclear showing both neuroendocrine markers and features of NSCLC [15]. PNECs are proposed as the likely source of SCLC however no identifiable precursory lesion has been identified[16]. Light microscopy is a common tool to identify SCLC as these tumors have distinct histopathological features including, small cells with fine granular nuclear chromatin and an absent nucleoli[17]. SCLC cancers demonstrate features of NSCLC indicating a potential "common" cell of origin, however they generally express a variety of neuroendocrine markers and transcription factors indicating that neuroendocrine cells may be the cell of origin for SCLC[15].

1.2.2 Non-small cell lung cancer

The most common form of lung cancer is NSCLC accounting for 85% of all lung cancer cases. NSCLC is divided into three subtypes, the two most common being lung adenocarcinoma (LAC) and squamous cell carcinoma (SqCC) and the rarer subtype large cell carcinoma[18]. LAC is the most common subtype of lung cancer accounting for 40% of all lung cancer cases. NSCLC treatment is dependent on stage and metastasis, most Stage I and II NSCLC cancers can be treated by surgical resection.

Patients receiving surgical resection of NSCLC tumors are generally prescribed adjuvant chemotherapy, which can reduce recurrence[19]. For Stage III NSCLC, chemotherapy is typically recommended along with high-dose radiation treatments. In Stage IV NSCLC chemotherapy is the primary treatment and radiation is used only for palliative care. The standard chemotherapy regimen includes either cisplatin or carboplatin, combined with docetaxel, gemcitabine, paclitaxel, vinorelbine or pemetrexed[20]. If NSCLC cancer appear with specific markers targeted therapies can be given; in EGFR mutated NSCLC cancer Erlotinib, Afatinib or Gefitinib is recommended dependent on EGFR mutation type[21]. Other therapies currently under investigation include utilizing bevacizumab, an anti-angiogenic therapeutic[22].

LAC develops from uncontrolled growth of epithelial cells generally in the periphery of the lung[23]. LAC is thought to arise from a variety of cell types, in K-Ras driven LAC, alveolar type II cells are the predominant cell of origin but LAC can also arise from club cells, bronchioalveolar stem cells and progenitors of these cells[24]. Tracheal basal cell progenitors are speculated to be the cell of origin in SqCC[15]. Large-cell lung carcinoma is the final subtype of NSCLC and represents around 10% of NSCLC cases, large-cell lung carcinoma generally originates from epithelial cells of the lung[15].

We limited our research to LAC as NSCLC cancers have distinct genomic subtypes and have differing levels of incidence, with LAC being the most common[25]. Additionally, LAC incidence is on the rise and is highly associated with smoking, so this subtype of lung cancer may be the most clinically relevant subtype of lung cancer for designing biomarkers and finding potential therapeutic targets[26].

1.3 Staging of Lung Adenocarcinoma

Using multiple factors LAC can be staged into five stages 0-IV, each with their own variations of the specific stage (Table 1.1). The factors dictating staging are tumor size (T), regional lymph node involvement (N) and distant metastatic sites (M). Current staging guidelines are being replaced by newly constructed guides based on a 90 000-patient collection of data[27]. The newly designed guidelines place less emphasis on tumor size and will cause reclassification of T3 tumors with N2 disease being moved from stage IIIA to stage IIIB and those with N3 disease being moved from stage IIIB to stage IIIC which directly affects treatment and survivability[27]. Reclassification of LAC tumors can result in new staging for tumors and therefore change treatment options. Changing LAC staging based on new patient data can have a positive impact on the effectiveness of treatment for LAC and has the potential to modify treatment options around the world.

1.4 miRNA Biogenesis and Function

MiRNAs are small non-coding RNAs that are on average 17-22 nucleotides long that function in post-transcriptional gene regulation. The biogenesis of miRNAs within humans occurs in a stepwise manner, first miRNAs are transcribed from genomic DNA into pri-miRNAs which are then processed both within the nucleus and the cytoplasm to form mature miRNAs. Beginning in the nucleus miRNAs are transcribed by RNA polymerase II or polymerase III, which results in the production of pri-miRNAs (Figure 1.1)[28,29]. The pri-miRNAs within the nucleus are then processed by the protein RNase III endonuclease Drosha and double-stranded RNA binding protein DiGreorge syndrome crucial region gene 8 (DGCR8) (Figure 1.1)[30,31]. Drosha with the aid of DGCR8 processes the pri-miRNA cutting 60-70 base pairs (bp) and

generating a precursor miRNA (pre-miRNA) (Figure 1.1)[32]. However, miRNAs that are encoded within protein coding genes skip processing by Drosha and are released from their genes through splicing[33]. Pre-miRNAs exit the nucleus using Exportin-5 and enter the cytoplasm where they are processed by RNase II endonuclease Dicer (Dicer) into mature miRNAs approximately 22 nucleotides in length. The RNA induced silencing complex (RISC) forms around the mature miRNAs removing the opposing strand leaving the guide strand within the RISC complex (Figure 1.1). The RISC complex contains a variety of proteins including Argonaute (Ago), the protein into which the single RNA strand is integrated into[34]. Based on the miRNA sequence the RISC complex binds to target mRNAs resulting in: translational repression, mRNA destabilization or mRNA cleavage. Generally binding and targeting of mRNAs is located within the 3' untranslated region (3'UTR) of transcript, however it is noted that some can target beyond the 3'UTR[35,36]. Pre-miRNAs and mature miRNAs have been found within extracellular vesicles, a type of secreted vesicle released from cells, and have been shown to enter the extracellular environment to exert their function within other cells[37].

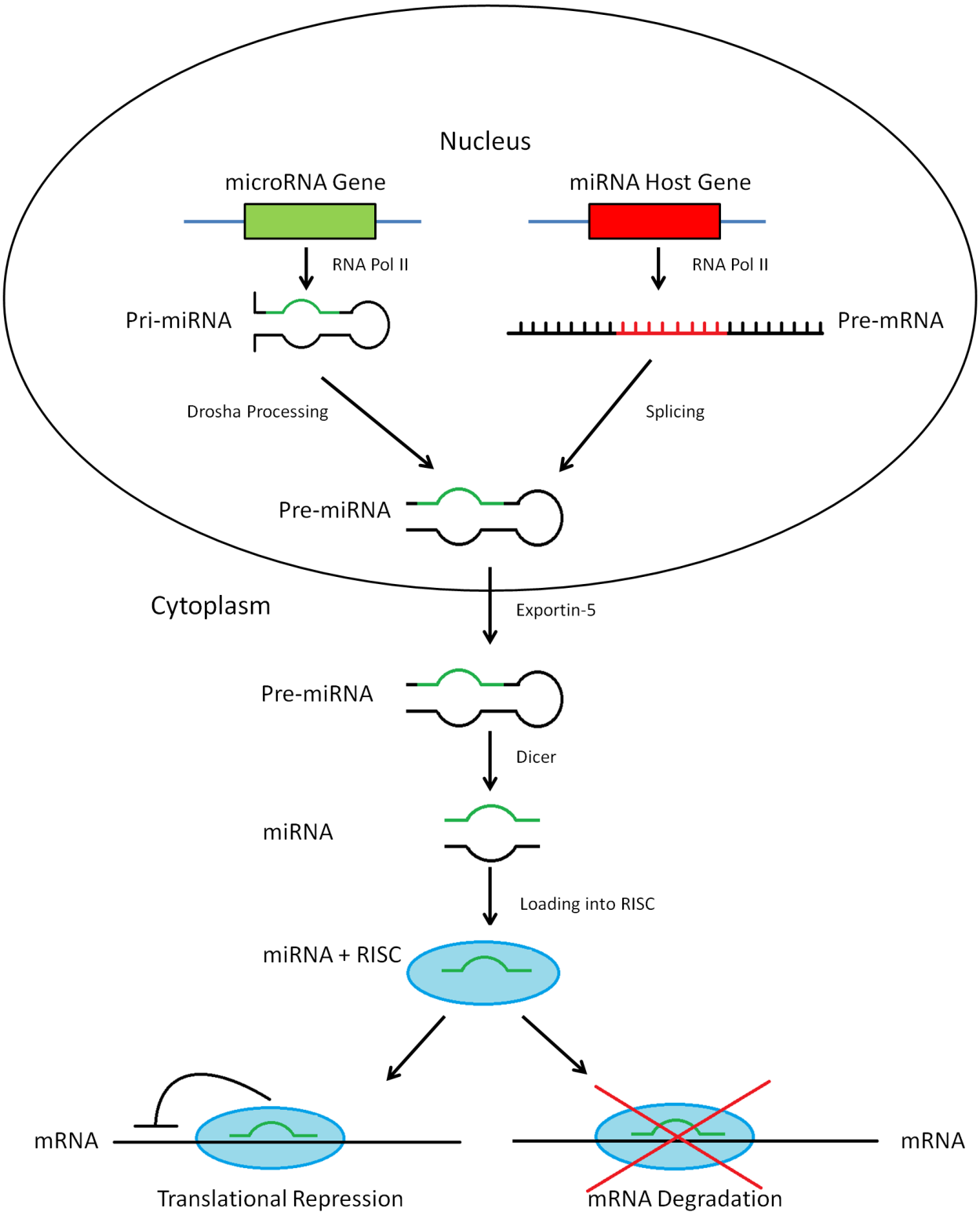

Figure 1.1 MiRNA biogenesis

1.5 Extracellular Vesicle Biogenesis and Packaging

Extracellular vesicles (EVs) are small membrane bound vesicles that are released from virtually all cell types. First discovered in the 1980's as "exosomes" the vesicles were found to be exfoliates from the cellular membranes[38]. However, further research has reclassified, the "exosomes" based on their size and origin.

EVs are secreted vesicles that include exosomes, microvesicles, oncosomes and apoptotic bodies. Exosomes originate from the endocytic pathway and are formed by budding into an early endosome forming a multivesicular body (MVBs) (Figure 1.2). The endocytic pathway is a highly studied process functioning in internalizing fluids, solutes, macromolecules and plasma membrane components through invagination of the plasma membrane[39]. Endocytosis is regulated by many different endocytotic pathways depending on the type of cargo being taken up. These pathways are divided into two main pathways: clathrin-dependent and clathrin-independent. Both pathways share a common first step, an inward curvature of the plasma membrane which changes the shape of the cells plasma membrane[40]. As the curvature increases, the invagination begins to take different shapes depending on the endocytotic pathway, where spherical, ellipsoid or tubular structures form and a narrow membrane neck is created. The narrow neck undergoes scission, which releases the vesicular structure into the intracellular milieu and enters the endosome.

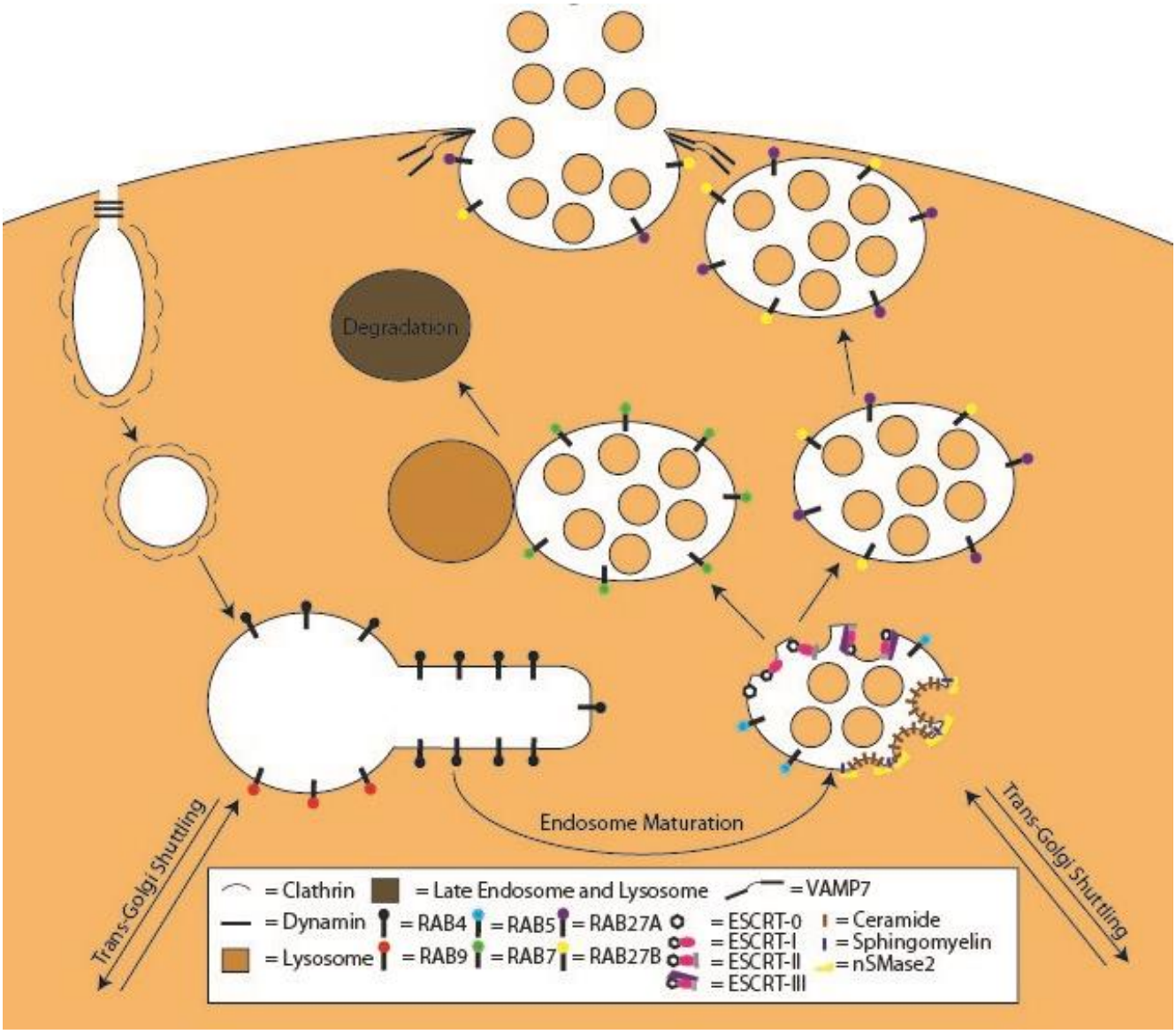

Figure 1.2 Exosome biogenesis.

An endosome is a persistent membranous structure which acts as the primary location for entering vesicles from the endocytic pathways. The early endosome is composed of regions of tubular extensions and large vesicles containing membrane invaginations giving rise to a multi-vesicular appearance[41]. It is thought that the different regions of the early endosome function as domains that have different functions, for instance, proteins targeted for recycling may cluster within primary tubular membranes[42]. Vesicles arising from different regions of the early endosome contain different acidic properties, changing from a pH of 6.2 to ~5.5 in the lumen of the multivesicular bodies[42,43]. While many ligands are degraded within the early endosome many receptors are recycled back to the surface of the cell[44]. The endosome is critical for recycling and degrading membrane components. In addition, the endosome can mature into lysosomes or into multivesicular bodies, which have differing functions. The fate of the endosome is dependent on markers on the endosome (Figure 1.2).

Ras-associated binding (Rab) proteins are small GTP-binding proteins that localize to intracellular membranes where they are able to interact and recruit Rab effector proteins[45]. Rab5 and Rab4 are primarily localized to the early endosome and regulate the early endocytotic events[46-49]. Other Rabs known to be localized in the early endosome include Rab10, Rab14, Rab21 and Rab22: however, their role is less characterized. Rab5 has been extensively researched due to its function in regulating the entry of cargo from the plasma membrane into the early endosome, in addition Rab5 recruits factors which contributes to specialized trafficking and sorting including regulating homotypic fusion[50]. Homotypic fusion increases the size of the early endosome, which is essential for endosomes to generate enough membrane surface to generate intraluminal vesicles (ILVs) and Rab5 mediated homotypic fusion is required for endosomal maturation[51,52]. Homotypic fusion of the early endosome is a fusion of two early endosomes

together; this is mediated by VAMP8, which acts as a R-SNARE to fuse the membranes together[53]. Rab proteins are not only important for early endosome function but they are also very important to regulate the traffic of vesicles within the early endosome (Figure 1.2).

The early endosome is responsible for sorting incoming vesicles to destinations (Figure 1.2). Sorting events occurring at this location determine the fate of internalized proteins and lipids marking them for recycling to the plasma membrane, degradation in the lysosome or delivery to the trans-Golgi network[43].

As the early endosome begins to mature it develops into a late endosome and becomes characterized by the formation of ILVs. These ILVs form inside the lumen of the late endosome and are formed by the inward budding of the endosomal membrane (Figure 1.2). The transformation of the early endosome into the late endosome is marked by a change of shape and location. Early endosome has a tube-like shape while the late endosome has a spherical shape, the endosome also moves from the periphery of the cell to the center of the cell towards the nucleus[54]. The late endosome containing ILVs is now considered a multivesicular body (MVB). The fate of the MVB can vary, it can be targeted for fusion to a lysosome as marked by a conversion of Rab5 to Rab7[55]. As an alternative to degradation the MVBs can fuse with the plasma membrane causing the release of the ILVs into the extracellular environment. The released ILVs are termed exosomes. There are several key Rabs that regulate the secretion of exosomes including: Rab27a, Rab27b, Rab35 and Rab11[5,56,57].

ILVs are formed through invagination and budding from the limiting membrane of the late endosome. This forms vesicles within the lumen of the late endosome containing cytosol and expose the extracellular domain of transferrin receptors at their surface. The most well described methods of ILV formation in late endosomes is driven by the endosomal sorting complex

required for transport (ESCRT) which is composed of approximately 30 proteins[58]. These proteins assemble into four complexes (ESCRT 0, -I, -II, -III) that act in succession to form ILVs. First ESCRT-0 recognizes and sequesters ubiquitinated proteins in the endosomal membrane, this is followed by membrane deformation by ESCRT-I and –II complexes causing buds with sequestered cargo; finally, ESCRT-III components drive vesicle scission[59,60]. ESCRT-0 is comprised of hepatocyte growth factor-regulated tyrosine kinase substrate that recognizes the mono-ubiquitylated cargo proteins and associates with STAM, Eps15 and clathrin to form a complex[61]. Hepatocyte growth factor-regulated tyrosine kinase substrate (HRS) recruits tumor suppressor gene 101 (TSG101) of the ESCRT-I complex which then recruits ESCRT-III, by ESCRT-II or ALIX (an ESCRT-accessory protein)[58]. Dissociation of ESCRT occurs through interactions with the AAA-ATPase Vps4[58].

ESCRT-III has recently been shown to be critical for ILV membrane scission. The ESCRT-III subunits assemble into large filamentous structures[62-64]. Snf7 an ESCRT-III subunit was shown to cause the formation of curved polymeric spirals on membranes *in vivo* when over expressed[65]. Snf7 spirals are able to induce a negative curvature to the underlying membrane, which gives rise to membrane tubules that extrude away from the cytoplasm. These ESCRT-III subunits all localize to the bud neck where they are able to cleave the bud to form ILVs[66].

Depleting ESCRT subunits does not completely impair ILV formation within late endosomes, which suggests that there are other methods for ILV formation[67]. ILV formation can occur using a type II sphingomyelinase that hydrolyses sphingomyelin to ceramide[68]. This pathway is dependent on raft-based microdomains for the lateral segregation of cargo within the endosomal membrane. The hydrolysis of sphingomyelin is conducted by the protein neutral sphingomyelinase (nSMase) and the product ceramide has a cone-shape structure which may induce spontaneous negative curvature[68]. Once ILVs are produced the MVB is shuttled to the cell membrane where the ILVs are released and are now considered exosomes (Figure 1.2).

The biogenesis of microvesicles (MVs) is not as well understood to that of exosomes. In general, MVs are formed through outward budding and fission of the cellular membrane. A combination of factors have been shown to induce formation of MVs. For example, redistribution of phosphatidylserine to the outer leaflet in addition to shrinking of actin-myosin machinery will cause ERK to be recruited to the membrane resulting in activation of myosin light chain kinase (MLCK) triggering the releases of MVs[69]. Another study has shown that recruitment of ESCRT-I subunit TSG101 to the plasma membrane within the Arrestin 1 domain-containing protein 1 (ARRDC1), causes the release of MVs containing TSG101[70]. MVs are unique compared to exosomes as the content of MVs generally reflects the process of its biogenesis. Oncosomes are large vesicles typically 1-10 μm in diameter and are produced through non-apoptotic blebbing from the plasma membrane[71].

1.5.1 Isolation of EVs

There has recently been a large surge of research into the function of miRNAs within EVs in communication; however, in LAC there is little information on precise mechanisms by which EVs function as communicators. Numerous methods can be used in the isolation of EVs and within certain protocols, many different fractions and purities of EVs can be isolated. Differential ultracentrifugation yields many different types of EVs including exosomes, oncosomes and microvesicles and in some cases has yielded protein aggregates[72]. To purify certain subtypes of EV or to purify EVs further, more steps or alternate methods are required. Inserting a sucrose gradient step into the centrifugation process has been shown to eliminate protein aggregate contamination from the EVs; however, high density lipoproteins have also been isolated using this method[73]. Another gradient used to separate EVs from apoptotic bodies and virus is iodixanol[74].

Additional methods of EV isolation include using microbeads, normally magnetic beads coated with an antibody recognizing EV surface markers. This technology is important for isolating specific subsets of EVs, however in *in vivo* settings different cell types can create EVs with overlapping surface marker types[75]. Due to the surface area of the beads, saturation of bindings can occur and a large population of EVs may be left out of the sample, resulting in low EVs and sometimes unusable yields. Other bead types for EV isolation include surfactant-free latex beads, that can be either hydrophilic or hydrophobic and covalently bind to EVs regardless of size or surface markers[76]. Size exclusion chromatography is another method of EV isolation that first removes large objects such as organelles through low-speed centrifugation, which is followed by filtration and finally size exclusion chromatography[77]. These EV isolation methods allow for the selection of a specific subset of EVs, however with many unknown EV subsets as well as overlapping markers it is difficult to confirm that one type of EV is isolated from a specific isolation technique.

1.5.2 EV markers and contents

EVs contain many of the same proteins that cellular compartments contain, thus there is no single marker that can separately distinguish EVs[78]. In addition, there are no currently accepted markers that can uniquely differentiate subsets of EVs from each other. Identification of EVs within supernatants is best performed using multiple techniques including determining size of EVs through nanoparticle tracking analysis (NTA) or electron microscopy and western blots for EV proteins. NTA allows visualization of particles in liquids in addition to quantification of particles[79]. The International Society of Extracellular Vesicles (ISEV) put forward a statement indicating the minimum requirements for the definition of extracellular vesicles and required

three markers to be present in EV preparations with an optional fourth[80]. The first marker suggests the presence of a membrane (CD63 or CD81), the second suggests enrichment of EVs (TSG101) and the third must be under-represented in the isolate due to its association with other compartments (H3)[80]. The fourth marker can be demonstrated as a membrane binding protein although association of these markers with EVs has been found to be variable. Characterization of EVs is necessary to indicate proper isolation of vesicles as contamination of lipoprotein complexes can lead to incorrect conclusions[81].

EVs contain a plethora of contents including proteins, RNAs and DNA. Sequencing of total RNA from serum derived EVs suggest that miRNAs and tRNAs make up approximately 15% of EV RNA[82]. Cancer EVs have also been shown to contain more total RNA compared to EVs from normal cells[83]. DNA within EVs can range in size from 100 base pairs to 2.5 kilobase pairs and can span across all chromosomes of genomic DNA[84,85]. The protein content of EVs varies depending on the method of EV biogenesis and cell type. Exosomes that arise from the late endosome compartment are generally more enriched with tetraspanins such as CD63 and CD81[86,87]. Microvesicle production through membrane budding involves the protein arrestin containing protein 1 (AARDC1) and contains both AARDC1 and TSG101[70]. The contents of EVs and microvesicles can overlap considerably with many of the same products found within them. However, there are some differences including microvesicles containing different repertoires of proteins compared to exosomes, such as the proteins glycoprotein Ib (GPIb) and P-selectin due to their plasma membrane origins[87]. The contents of EVs have recently been shown to be functional including miRNAs, proteins and mRNAs, even when transferred to other cells. In addition, processing of miRNAs within EVs has been shown to be independent of the cell and occurs with the necessary machinery inside the EVs[88].

1.5.3 miRNA incorporation into exosomes

MiRNAs have been demonstrated to have a higher proportion within exosomes when compared to the population of RNA in parental cells, and as profiling studies have shown, miRNAs are not randomly incorporated into exosomes[89]. For example, certain miRNAs such as miR-451a, miR-150-5p and miR-142-3p were demonstrated to be enriched within EVs from a variety of cell lines compared to their cellular levels[90]. Currently, miRNA sorting into exosomes is not well understood, however some methods of miRNA packaging have been elucidated. Proteins such as heterogeneous nuclear riboproteins (hnRNPs) hnRNPA2B1 and hnRNPA1 recognize specific miRNA binding motifs and were shown to selectively package miRNAs within exosomes[91]. Other methods of miRNAs packaging have been found at the ILV formation step of exosome biogenesis, including components of the ESCRT pathway which resulted in impaired miRNA activity within the EVs[92]. Another proposed mechanism utilizes the RISC complex which, captures miRNAs and transports them to early endosomes through the ESCRT pathway where the miRNAs are directed into ILVs[88]. Although this research demonstrates the enrichment of select miRNAs within exosomes, the mechanism as to how other miRNAs are selectively incorporated into exosomes remains unclear.

1.6 Detection and Diagnosis of Lung Cancer

As previously stated, lung cancer is generally asymptomatic before diagnosis. Many patients are unaware of their cancer until a symptom arises such as a cough, dyspnea, chest pain, bloody sputum or metastatic symptoms[93]. Lung cancer is diagnosed using numerous investigative methods, where a patient presenting with suspected lung cancer will first be taken

for chest imaging[94]. Generally, an X-ray, computed tomography (CT) scan, a positron emission tomography (PET) scan or magnetic resonance imaging is performed. The chest scans are then analyzed for unusual lesions or potentially cancerous masses and if warranted biopsies are taken. Biopsies are removed from sites in the lungs suspected of harboring the cancer, which can be guided by an ultrasound and/or endoscopy. Once obtained, the biopsies are taken to a pathologist for subtype and stage diagnosis, tests for this can include immunohistochemistry and genotyping[94,95]. Lung cancer is generally diagnosed in late stages of disease development, there are a number of research studies suggesting early detection of lung cancer improves overall survival outcomes and demonstrates the benefit of screening high risk patients[96,97].

1.6.1 Early detection of lung cancer

There are currently recommendations for screening of lung cancer in heavy smokers, although there are no current provincial or territorial screening programs in place[97]. However, it is recommended that heavy smokers are screened for lung cancer and pilot programs for early screening have started in some areas. The National Lung Screening Trail (NLST) showed that using low dose CT scanning for early detection of lung cancer could be achieved and would result in reduced lung cancer mortality[98]. The PanCan Early Detection of Lung Cancer taking place across Canada uses bronchoscopy screening, which has a better potential to detect early central lung cancers[96]. These methods may help in reducing lung cancer mortality through the use of active screening, however, due to time and limited hospital resources, other non-invasive and less time-consuming methods may need to be developed to accommodate high throughput screening.

1.6.2 Sputum as an early detector of lung cancer

Sputum is liquid that originates from your respiratory tract that contains mucus, bacteria and cells. The collection of sputum can be informative when diagnosing infections in the respiratory tract and has come under interest for use as an early indicator of lung cancer. Sputum cytology examines sputum microscopically to detect the presence of abnormal cells within the sputum however, this method was found to be neither additive in diagnostic value or in improving lung cancer survival[99]. However, more positive results have been found recently due to detection of mutations, DNA hypermethylation markers, miRNAs and tumor related proteins within the sputum, which have shown the potential for screening purposes[99].

Endogenous miRNAs were stably detected within sputum samples with miR-21 and miR-155 identified[100]. The overexpression of miR-21 within the sputum was significantly associated with NSCLC compared to cancer-free patients[100]. However, tumor stage was not associated with miRNA expression, which may suggest that miRNA signatures may only be used for detection. In another set of patients' sputum samples, miR-21, miR-31 and miR-210 were used as biomarkers to distinguish between lung cancer and solitary pulmonary nodules[101]. These markers can assist in indicating the presence of lung cancer through a non-invasive screening method.

1.6.3 Circulating miRNAs as biomarkers

There is significant interest in miRNAs circulating within the serum of patients as biomarkers for cancer detection[102]. Currently, there are a number of circulating miRNAs that are reported for non-invasive cancer detection, including the qRT-PCR analysis of miR-155 in the serum of breast cancer patients[103-105]. Numerous studies have investigated circulating miRNAs as biomarkers for early disease detection (Table 1.2)[106-137]. These studies applied numerous

methods, including miRNA sequencing, qRT-PCR and miRNA microarrays. Unfortunately, there was minimal overlap among their results in terms of identifying circulating miRNA biomarkers. While some miRNAs were consistently found elevated in NSCLC serum such as miR-21-5p, which was found elevated in six profiling studies, many of the other studies show no difference in miR-21-5p levels[109,128,131,134,135,138]. In addition, miR-155 was found to be elevated in NSCLC serum in four profiling studies; however, due to its common enrichment in breast cancer, this may not be suitable as a marker in women as it may generate false positives[109,128,133,137]. There are several factors that can explain the differences in miRNA profiling studies such as detection methods, sample preparation, sample size and demographics. Additionally, many studies do not consider the impact of hemolysis, which has consistently been found to alter miRNA levels[106,109,113,116-122,126,128-130,133-140]. While some studies do control for hemolysis through removing samples that contain high hemoglobin levels, the threshold for hemolysis is set at a high level and miRNA changes below this threshold can occur[141]. Finally, an important factor in determining biomarkers for screening of lung cancer is utilizing proper and clinically relevant controls. Many studies searching for circulating miRNA biomarkers utilize healthy individuals as controls rather than high risk heavy smokers, whom would more often be at risk for developing lung cancer and would undergo screening[124,125,127-129,132-134]. By utilizing healthy individuals who have never smoked, the differences in circulating miRNAs may be caused by smoking itself rather than the presence of cancer. The discrepancies between studies demonstrate the need for more strict guidelines and standardized methods for circulating miRNA biomarker discovery.

Lung Cancer Subtype	Altered miRNA in Circulation (↑ = increase in cancer, ↓ = decreased in cancer)	Method	Reference
NSCLC Diagnosis	↓miR-20b (plasma)	TaqMan miRNA Assay	Silva *et al.*, 2011[119]
NSCLC Diagnosis	↓let-7c, miR-152 (plasma)	qRT-PCR	Dou *et al.*, 2015[116]
NSCLC Diagnosis	↓miR-16-5p, miR-17b-5p, miR-19-3p, miR-20a-5p, miR-92-3p, ↑miR-15b-5p (serum)	TaqMan miRNA Assay	Fan *et al.*, 2015[117]
NSCLC Prognosis	↓miR-486, miR-30d, ↑miR-1, miR-499 (plasma)	Solexa Sequencing	Hu *et al.*, 2010[118]
Asymptomatic NSCLC Diagnosis	34 miRNA Signature (serum)	TaqMan miRNA Assay	Bianchi *et al.*, 2011[115]
NSCLC Diagnosis	↑ miR-125a-5p, miR-145-5p, miR-146a (Serum)	qRT-PCR	Wang *et al.* 2015[142]
NSCLC Diagnosis	24 miRNA Signature (plasma)	TaqMan miRNA Assay	Wozniak *et al.*, 2015[107]
NSCLC Diagnosis	8 miRNA Signature (exosomes)	qRT-PCR	Giallombardo *et al.*, 2016[123]
NSCLC Diagnosis	↑miR-429, miR-205, miR-200b, miR-203, miR-125b, miR-34b (serum)	TaqMan miRNA Assay	Halvorsen *et al.*, 2016[108]
NSCLC Diagnosis	↑miR-1254, miR-574-5p (serum)	qRT-PCR	Foss *et al.* 2011[122]
NSCLC Diagnosis	↑miR-20a, miR-24, miR-25, miR-145, miR-152, miR-199a-5p, miR-221, miR-222, miR-223, miR-230 (serum)	TaqMan miRNA Assay	Chen *et al.*, 2011[121]
NSCLC Diagnosis	miR-15b, miR-27b Signature (serum)	TaqMan miRNA Assay	Hennessey *et al.*, 2012[124]
NSCLC Diagnostic and Prognostic	↑miR-125b (serum)	qRT-PCR	Yuxia *et al.*, 2012[127]
NSCLC Diagnostic and Prognostic	↑miR-210 (serum)	qRT-PCR	Li *et al.*, 2013[125]

Lung Cancer Diagnosis	↓miR-125a-5p, miR-25, miR-126 (serum)	TaqMan miRNA Assay	Wang *et al.*, 2015[143]
NSCLC Diagnosis	↑miR-483-5p , miR-193a-3p, miR-25, miR-214, miR-7 (serum)	TLDA RT-qPCR Assay	Wang *et al.*, 2015[120]
NSCLC Diagnosis	↑miR-141 (plasma)	qRT-PCR	Arab *et al.*, 2017[129]
NSCLC Diagnosis	↑miR-141, miR-200b, miR-193b, miR-301 (serum)	TaqMan miRNA Assay	Nadal *et al.*, 2015[106]
Lung Cancer Diagnosis	↑miR-21, miR-210 ↓miR-486-5p (plasma)	qRT-PCR	Shen *et al.*, 2011[134]
Lung Cancer Diagnosis	↑miR-197, miR-155 (serum)	miRNA Microarray	Zheng *et al.*, 2011[137]
LA Diagnosis	↓miR-339-5p ↑miR-21 (plasma)	miRNA microarray	Sun *et al.*, 2017[138]
NSCLC Diagnosis	↑pri-miR-944, pri-miR-3662	TaqMan miRNA Assay	Powrózek *et al.*, 2017[132]
NSCLC Prognosis	↑miR-150 (serum)	qRT-PCR	Zhang *et al.*, 2017[136]
NSCLC Prognosis	↑miR-2, miR-24, miR-34a (plasma)	TaqMan miRNA Assay	Franchina *et al.*, 2014[130]
NSCLC Prognosis	↑miR-23b-3p, miR-10b-5p, miR-21-5p (exosomes)	qRT-PCR	Liu *et al.*, 2017[131]
Lung Cancer Diagnosis	↑miR-10b, miR-141, miR-155 (serum)	TaqMan miRNA Assay	Roth *et al.*, 2011[133]
Lung Cancer Diagnosis	↑miR-21, miR-155, miR-182, miR-197 (serum)	miRNA Microarray	Abd-El-Fattah *et al.*, 2013[128]
NSCLC Diagnosis	↑miR-21 ↓miR-152, miR-148a, miR-148b (serum)	TaqMan miRNA Assay	Yang *et al.*, 2015[135]
Lung Cancer	↑miR-21, miR-155 ↓miR-145 (plasma)	TaqMan miRNA Assay	Tang *et al.*, 2013[109]
NSCLC Prognosis	↑miR-1290	TaqMan miRNA Assay	Mo *et al.*, 2015[144]

Table 1.2 miRNAs published as potential circulating lung cancer biomarkers

Currently, new approaches for determining circulating miRNA biomarkers for NSCLC diagnosis are being developed including utilizing tumor-derived exosomal miRNAs[145]. In 2012 a study showed that the majority of miRNAs within the serum are concentrated within exosomes, which prompted many researchers to only examine exosomes as within the serum for miRNA markers for disease detection[146]. In LAC miR-181-5p, miR-30a-3p, miR-30e-3p and miR-361-5p were observed as verified diagnostic markers and are promising candidate in early detection of NSCLC[145]. With more selective methods of isolating tumor secreted miRNAs, effects from hemolysis may be eliminated and allow for lung cancer biomarkers to become more robust and selective.

1.6.4 Prognostic miRNA biomarkers in NSCLC

Producing tools to increase prognostic accuracy facilitates physicians in choosing treatment options. A number of studies have sought to identify markers that aid in predicting patient response to treatment and prognosis in NSCLC (Table 1.2). High levels of miR-1290 were found in NSCLC tissue and serum, which correlated with poor prognosis, lymph node metastasis and TMN staging[144]. In another study, elevation of serum miR-146a and a decrease in serum miR-19b predicated survival and response to chemotherapy in NSCLC[147]. Recently, examination of exosomal specific miRNAs has begun due to an increase in the number of tumor secreted exosomes present within the serum. High levels of exosomal miR-23b-3p, miR-10b-5p and miR-21-5p were associated with poor survival in the plasma of NSCLC patients[131]. Another lung exosomal miRNA study showed that miR-21 and miR-155 were upregulated in the serum of nude mice with recurrent H1299 cell line tumors compared to that of primary tumor bearing mice and non-tumor mice[148]. Taken together prognostic exosomal miRNAs biomarkers for NSCLC is still in its infancy, however with continued work and consistent, established protocols biomarkers may become clinically relevant and reproducible

1.7 Tumor Microenvironment

The tumor microenvironment consists of both cellular and non-cellular components, including the extracellular matrix, myofibroblasts, fibroblasts, neuroendocrine cells, adipose tissue, immune inflammatory cells, endothelial cells and the lymphatic system[149]. Non-malignant cells can make up more than 50% of the primary tumor as well as at metastatic sites[150]. The integration and communication of malignant cells and the supporting tumor microenvironment are critical to the development of tumors. For example, myofibroblasts can secrete factors that

can remodel the extracellular matrix causing increases in metastasis, angiogenesis and inflammation[151]. The tumor microenvironment has a large impact on the growth of cancer, and recently therapeutic strategies have been developed in order to combat target cells within the tumor microenvironment. Considering the important role the microenvironment plays in cancer development, communication to and from the tumor to the stroma is critical in remodeling the microenvironment and making it more favorable for tumor growth and development.

1.7.1 Lung EV miRNAs in tumor development

Tumor released EVs are mediators of intercellular communication between tumor cells and their surrounding environment, playing a role in both tumor growth and transforming the microenvironment[152]. In LAC, EVs are capable of increasing the metastatic potential of otherwise poorly metastatic cells. For examples in lung tissue and lymph nodes the transfer of EV miR-494-3p and miR-542-3p can enhance the metastatic potential of the stroma, while miR-21-5p may be capable of increasing resistance to cisplatin by transfer from resistant to non-resistant cells[153,154]. Additionally, LAC derived EV associated miR-21-5p and miR-29a-5p have been demonstrated to cause pro-inflammatory changes in immune cells through the toll-like receptor, TLR8[155]. This complements the work completed in other cancer types, where the tumor to stroma communication via miRNA cargo within EVs was examined and shown to promote angiogenesis, as well as activate the growth promoting properties of fibroblasts[3,156-159].

1.7.2 Extracellular communication to stromal cells in cancer

LAC cells are supported by a variety of non-cancer cells comprising the tumor stroma, including: fibroblasts which may provide growth factors, macrophages which may suppress an immune response, and endothelial cells which provide blood supply by creating new blood vessels through angiogenesis[160-162]. The two most abundant stromal cell types within the LAC tumor microenvironment are endothelial cells and fibroblasts.

Endothelial cells are critical for tumor growth, such that tumors cannot exceed 2-3 mm in diameter without sufficient formation of new blood vessels to support continued growth[163]. Angiogenesis establishes new blood vessels within the tumor, which then supplies nutrients and oxygen to the tumor promoting growth and metastasis[164,165]. Stimulation of angiogenesis is triggered by cancer cells through cell-to-cell communication occurring through soluble factors such as VEGF, cytokines, extracellular matrix modifications and secreted extracellular vesicles[166]. EVs are important mediators of angiogenesis as transfer of miR-126, miR-214, miR-296, miR-125a, miR-31 and miR-150 through extracellular vesicles have all been shown to stimulate angiogenesis[167-173]. Other mediators within EVs that can stimulate angiogenesis are proteins such as VEGF, FGF-2, PDGF and metalloproteases[174-178]. Promotion of angiogenesis leads to increased vascular formation within the tumor and allows continued growth an invasion.

The transformation of normal fibroblast to cancer-associated fibroblasts (CAFs) is highly affected by extracellular vesicle communication from the tumor[179-181]. Prostate cancer exosomes have previously been shown to induce TGFβ1 dependent fibroblast differentiation into the myofibroblast phenotype, through transfer of TGFβ1 within exosomes[182]. However, activation of fibroblasts through soluble TGFβ1 resulted in myofibroblasts that were not pro-tumorigenic or tumor-promoting[182]. Other cancers have implicated specific miRNAs in CAF transformation

including miR-155 in pancreatic cancer, where EVs targeting TP53INP1 in normal fibroblasts induced CAF formation[183]. In triple negative breast cancer miR-9 when transferred through EVs induces CAF formation and can enhance cell motility within the fibroblasts[158]. Activation of myofibroblast is critical in forming the tumor stroma and evidence suggests that EVs play a prominent role in promoting the CAF phenotype.

1.8 Thesis Themes, Rationale, Objectives and Hypothesis

The central theme of my thesis is the functional characterization of LAC secreted miRNAs. The majority of research effort has been focused on identifying miRNAs as biomarkers however, many have failed to address important selection factors, and little is known about the function of early LAC secreted miRNAs. LAC has a higher survival rate at earlier stages of disease therefore it is important to identify novel ways to diagnose this disease early and to better understand the mechanisms that drive LAC. A comprehensive analysis of circulating LAC miRNAs at early disease stages will allow for the development of LAC biomarkers to predict the presence of early LAC in a clinically relevant cohort of patients. Further, analyzing LAC secreted miRNAs contained in EVs will aid in understanding the mechanisms by which LAC communicates via miRNAs to its surrounding stroma, which may provide novel strategies for targeting early tumor development.

My overall objectives are to determine a miRNA signature in the serum of LAC patients to identify LAC in high risk patients as well as to characterize the function of LAC secreted EV miRNAs within the tumor stromal.

The hypotheses for the work presented are:

1. A miRNA signature in the serum of LAC patients will allow for identification of LAC in high risk patients.
2. LAC EV miRNAs communicate with stromal cells to modify the tumor microenvironment and promote tumorigenesis

1.9 Specific Aims and Thesis Outline

Aim 1: Profile LAC and non-cancer serum samples to identify a miRNA signature that can differentiate between tumor and normal cases

Chapter 2 describes the analysis of patient serum samples profiled for serum miRNAs. The chapter describes the methods taken to determine a set of miRNAs that can distinguish LAC from non-cancer.

Aim 2: Characterize early LAC EVs to determine specific miRNAs that are released from early LAC cell lines

Chapter 3 focuses on determining whether early LAC cell lines selectively package a select set of miRNAs for release from the cell. miRNA profiling is performed on both cell and EVs of five early LAC cell lines. Eight miRNAs are found to be selectively released from early LAC cell lines, which provides a basis for miRNAs to investigate in communication function. I correlate this finding with serum samples taken directly from LAC tumor vasculature beds during surgical resection to find miRNAs that are secreted from the tumor.

Aim 3: Determine the function of specific LAC EV miRNAs when transferred to normal stromal cells

Chapter 3 and 4 determine the function of miR-143-3p, miR-145-5p and miR-142-3p when transferred through EVs into endothelial cells and fibroblasts. EV incubation, western blots, wound healing assays and tube formation assays are performed on stromal cell lines. Targets are determined for miR-143-3p and miR-145-5p when transferred to endothelial cells. Chapter 4 further analyzes the function of miR-142-3p in fibroblasts cells and the role it plays in promoting the cancer associated fibroblast phenotype.

Chapter 2: Identification of serum miRNA biomarkers for early detection of lung adenocarcinoma

2.1 Introduction

Many patients with LAC remain without symptoms until later stage of disease progression. This makes it difficult to detect LAC at early stages as patients often have no reason to undergo lung cancer screening. Screening is generally conducted through sputum cytology, computed tomography (CT) scan, magnetic resonance imaging (MRI) scan and positron emission tomography (PET) scan. These tests show images of the lung and can return false positive results due to lung nodules in abundance within heavy smokers and are present in smaller amounts in virtually all people beyond young adulthood[184]. There are many advances coming forward in identifying benign lung nodules to remove them from analysis, however it remains a problem[185]. The national lung cancer screening trial in the United States demonstrated that 96.4% of positive results in low-dose CT screening were false positives while 94.5% of positive radiography screening results were false positives[98]. Patients who received treatment or biopsies for these false positives were put at risk of complications[98]. Once screened, patients suspected of lung cancer are sent for diagnosing either by; sputum cytology, thoracentesis, needle biopsy or bronchoscopy. The sampling of tissues through these methods is done to confirm diagnosis and the least invasive method is generally used to take a biopsy[186]. However, many of these methods are highly invasive and require surgery which can result in complications. In CT-guided transthoracic lung biopsy, pneumothorax occurs in 25.3% of patients and major complications (including hemothorax, air embolism, needle tract seeding and

death) occur in 5.7% of patients[187]. These methods are also performed on suspected lesions which can result in unnecessary invasive testing for benign lesions in the lung, as well false positives that can even lead to overtreatment. From these indications it is evident that a non-invasive screening and diagnostic method is required to reduce complications and reduce false positives.

Circulating biomarkers are a potential addition to the lung cancer screening process, as they may be used to reduce false positives in the screening process, limit the use of biopsies or be directly involved in diagnostics. One promising circulating biomarker, are miRNAs, due to their stability within the blood and during sample collection including storage[188]. All cell types, including tumor cells, secrete circulating miRNAs into the blood, which can be packaged within EVs or RNA-binding proteins, these packaging methods provide protection from RNases[3,92,189-191]. The secreted miRNAs are found within both the serum and the plasma of blood samples, however the plasma contains miRNAs associated with platelets, which can interfere with miRNA readings[126]. These aspects of serum miRNAs allow them to be robust non-invasive biomarkers.

Serum miRNAs were first discovered in 2007 in the serum of lymphoma patients, and shortly after they became useful as non-invasive biomarkers for detection of cancer[102,192,193]. Research has shown that circulating miRNAs can be used to not only detect the presence of cancer but other diseases as well including Alzheimer's, autism, schizophrenia, epilepsy and cardiovascular disease[194-198]. Utilizing serum miRNAs as diagnostic biomarkers can help provide non-invasive methods to diagnose disease early in development. miRNAs are comparably much more stable than mRNAs making them less prone to differences between samples and allowing for more consistent measurements[146]. Circulating serum miRNAs are found freely circulating, bound to Agronaut-2 protein and enclosed within EVs[199,200].

Exosomes are a subset of EVs produced through formation of intraluminal vesicles within endosomes, which are packaged with miRNAs in a selective manner[201]. Exosomes provide a protection for the miRNAs from degradation due to their lipid bilayer which separates the lumen of the exosomes from the serum[191]. Due the stability of miRNAs and the enrichment that exosomes provide for analysis, serum exosome miRNAs seem to be a promising biomarker for early cancer detection[202,203]. Research showed that the majority of miRNAs within the serum are located within exosomes, a subset of extracellular vesicles (EVs) 70-100nm in diameter[146]. However, contradicting studies showed that miRNAs are mainly bound to proteins within the serum and are free-floating[199,200]. Due to these contradicting studies we performed whole serum miRNA profiling to examine all potential sources for miRNA biomarkers.

Numerous studies have investigated circulating miRNAs as biomarkers for detection of NSCLC however, the results of these studies have largely been inconclusive and contradicting. The first use of a miRNA signature for NSCLC diagnosis was first conducted using Solexa sequencing and identified 91 miRNAs within the serum of healthy Chinese patients[114]. Two

NSCLC serum miRNAs (miR-25 and miR-223) were identified as upregulated in the serum and were validated in an independent trial of 75 healthy and 152 cancer patients using qRT-PCR[114]. This study resulted in numerous other researchers looking for unique miRNA signatures in cancer patient serum. The same researchers later used the same panel of 91 miRNAs across 400 NSCLC cases and 220 healthy control cases and found a panel of 10 miRNAs upregulated in NSCLC serum (miR-145-5p, miR-152, miR-199a-5p, miR-20a, miR-221, miR-222, miR-223, miR-24, miR-25 and miR-320)[121]. The healthy donors in both these cases however, were not heavy smokers and therefore were not likely mimicking the conditions of high risk individuals that clinical testing would examine[114,121]. Other miRNA panels for NSCLC detection have also been conducted, however the candidate miRNAs in each case vary significantly (Table 2.1). This may be caused by numerous issues including factors relating to sample collection, method of miRNA detection and type of analysis. Our research eliminates the effects of hemolysis through removal of miRNAs related to hemolysis and utilizes heavy smoker patients at high risk of developing LAC as controls. This will allow for us to create a clinically relevant reproducible circulating miRNA biomarker for discrimination between LAC and non-cancer.

In this chapter I examine circulating serum miRNAs in LAC patients compared to high risk non-cancer controls, to determine a subset of miRNAs that are able to identify LAC in high-risk patient serum based on the detection of miRNAs.

2.2 Materials and Methods

2.2.1 Sample collection

To examine the utility of differentially expressed miRNAs as NSCLC biomarkers, we collected serum samples from patients with early LAC and heavy smoker non-cancer volunteers using a peripheral blood draw. 50 samples of early LAC serum samples were collected and compared to 51 non-cancer samples collected from demographically matched, high risk smokers without cancer. Our results were validated in an independent set of samples consisting of 35 patients with LAC and 28 demographically matched high risk non-cancer controls. All patient samples are listed in Table 2.1. (Ethics Number)

	Lung Adenocarcinoma Patients	Non-cancer Controls	*P*-value (Adenocarcinoma vs Control)	Validation Lung Adenocarcinoma Samples	Validation Non-Cancer Samples
Total patients	50	51		35	28
Mean age	67	63	0.0129[b]	70	65
Age range	48-83	50-75		44-85	53-78
# of males	26	29	0.46[c]	13	9
Former Smokers	26	30	0.14[c]	24	13
Current Smokers	24	21		10	15
Never Smokers	0	0		0	0
Mean pack years	43.6	46.5	0.88[b]	49.7	46.8
Pack year range	16.5-82	31-80		10-150	17-66
	Stage (%)			**Stage (%)**	
1A	8 (30.7)			9 (25.7)	
1B	5 (19.2)			4 (11.4)	
2A	3 (11.5)			5 (14.3)	
2B	2 (7.6)			3 (8.6)	
3A	6 (23)			11 (31.4)	
Unknown	2 (7.6)			3 (8.6)	
Caucasian	26	43			

[a] Data missing data for some cases
[b] Student's t-test
[c] Fisher's exact test

Table 2.1 Patient demographics

2.2.2 Blood processing

Samples were collected in SST vacutainer tubes and allowed to clot at room temperature for 30 minutes. After clotting samples were centrifuged for 15 minutes at room temperature at 1500g. Aliquots of serum samples were collected and frozen at -80^{o}C for storage.

2.2.3 RNA isolation

RNA was extracted by miRNeasy Mini Kit (Qiagen) from 200 µL of serum according to instructions from manufacturer. MS2, an RNA carrier (Roche Applied Science), was added to QIAzol Lysis Reagent prior to isolation as it improves RNA purification, MS2 was added at 1.25 µL per 200 µL of serum[204]. Once isolated, RNA was re-suspended in 50 µL of nuclease-free water and immediately frozen at -80^{o}C.

2.2.4 qRT-PCR of serum miRNAs

Serum miRNAs were unable to be reliably measured due to low yields, so fixed volumes of eluted RNA was utilized for profiling[205,206]. Reverse transcription was conducted using miRCURY LNA Universal RT miRNA PCR, Polyadenylation and cDNA synthesis kit (Exiqon Inc.). Quantitative real-time polymerase chain reaction (qRT-PCR) was conducted on cDNA using miRNA Read-to-Use PCR, Human panel I and panel II with miRCURY LNA Universal RT miRNA PCR, SYBR Green master mix. ROX reference dye normalization was conducted using Viia7 software (Applied Biosystems). miRNAs measured having more than 1 melting curve were excluded from analysis along with miRNAs within 5 Ct's of the negative control (Ct > 35).

Validation set qRT-PCR was conducted using Thermo Fisher TaqMan custom pre-spotted plates with each miRNA run in triplicates. Validation samples were profiled for miR-197-3p, miR-23a, miR-23b, miR-142-3p, miR-582-5p, miR-92b-3p, miR-200a-3p and miR-497-5p. RNA was run utilizing TaqMan miRNA reverse transcription kit and TaqMan Master Mix II, no UNG was used for qRT-PCR, according to manufacturer's recommendations.

2.2.5 Data analysis

Raw serum miRNA profiles from human panel I+II were entered into GenEx (MultiD) for compilation and interplate calibration (n=101). Once calibrated, raw miRNA qRT-PCR data was exported for analysis. MiRNAs that were detected at less than 35 Ct's in fewer than 50% of samples were eliminated from further analysis to ensure reliable detection in the majority of patients. MiRNAs affected by hemolysis, which have previously been determined by MacLellan *et al*. (2014), were then further removed from analysis (Table 2.2)[139]. Remaining miRNAs were normalized to the best miRNA normalizer as determined by geNorm and NormFinder. Normalized data was then loaded into Statistica for further analysis. Mann Whitney U tests were conducted using Statistica Software requiring a p-value < 0.05 for significance, data was then entered into an excel file for a Benjamini-Hochberg correction to account for multiple testing[207]. For best subset analysis, Logit model was utilized, and a forward stepwise model was built for each normalized data set, p-values to enter and to be removed were set at 0.05. miRNAs with variable status "In" were selected for use in the Logit model best subset analysis. Using a best subset analysis, we selected the smallest number of miRNAs that were able to maintain an AUC above 0.8000, to reduce the odds of overfitting of models. Equations for LAC and non-cancer identification, were formed using parameter estimates with p-values < 0.05.

MiRNA	MiRNA	MiRNA	MiRNA
hsa-let-7a	hsa-miR-16-2*	hsa-miR-26a	hsa-miR-454
hsa-let-7a*	hsa-miR-17	hsa-miR-26b	hsa-miR-484
hsa-let-7b	hsa-miR-17*	hsa-miR-27a	hsa-miR-486-3p
hsa-let-7c	hsa-miR-181a	hsa-miR-296-5p	hsa-miR-486-5p
hsa-let-7d	hsa-miR-181b	hsa-miR-29a	hsa-miR-496
hsa-let-7d*	hsa-miR-181d	hsa-miR-29a*	hsa-miR-500a
hsa-let-7f-1*	hsa-miR-182	hsa-miR-29b	hsa-miR-501-3p
hsa-let-7f-2*	hsa-miR-183	hsa-miR-29b-2*	hsa-miR-501-5p
hsa-let-7g	hsa-miR-185	hsa-miR-29c	hsa-miR-502-3p
hsa-let-7i	hsa-miR-186	hsa-miR-301a	hsa-miR-502-5p
hsa-miR-101	hsa-miR-188-5p	hsa-miR-30b	hsa-miR-503
hsa-miR-103	hsa-miR-18a	hsa-miR-30c	hsa-miR-532-3p
hsa-miR-103-2*	hsa-miR-18b	hsa-miR-30d	hsa-miR-532-5p
hsa-miR-106a	hsa-miR-190	hsa-miR-30e	hsa-miR-545
hsa-miR-106b	hsa-miR-1908	hsa-miR-30e*	hsa-miR-550a
hsa-miR-107	hsa-miR-191	hsa-miR-32	hsa-miR-574-3p
hsa-miR-126	hsa-miR-192	hsa-miR-320a	hsa-miR-576-3p
hsa-miR-126*	hsa-miR-194	hsa-miR-320b	hsa-miR-576-5p
hsa-miR-130a	hsa-miR-195	hsa-miR-324-3p	hsa-miR-584
hsa-miR-130b	hsa-miR-196b	hsa-miR-324-5p	hsa-miR-590-5p
hsa-miR-132	hsa-miR-1974	hsa-miR-328	hsa-miR-598
hsa-miR-133b	hsa-miR-1979	hsa-miR-331-3p	hsa-miR-624*
hsa-miR-135a	hsa-miR-199a-3p	hsa-miR-335	hsa-miR-625*
hsa-miR-140-3p	hsa-miR-19a	hsa-miR-338-3p	hsa-miR-627
hsa-miR-140-5p	hsa-miR-19b	hsa-miR-33b	hsa-miR-628-3p
hsa-miR-142-5p	hsa-miR-20a	hsa-miR-342-5p	hsa-miR-629
hsa-miR-143	hsa-miR-20a*	hsa-miR-345	hsa-miR-636
hsa-miR-144	hsa-miR-20b	hsa-miR-361-3p	hsa-miR-651
hsa-miR-144*	hsa-miR-21	hsa-miR-361-5p	hsa-miR-652
hsa-miR-146a	hsa-miR-210	hsa-miR-363	hsa-miR-660
hsa-miR-146b-5p	hsa-miR-2110	hsa-miR-374a	hsa-miR-7
hsa-miR-148a	hsa-miR-215	hsa-miR-374b	hsa-miR-886-5p
hsa-miR-148b	hsa-miR-22	hsa-miR-376c	hsa-miR-92a
hsa-miR-150	hsa-miR-221	hsa-miR-378	hsa-miR-93
hsa-miR-151-3p	hsa-miR-222	hsa-miR-378*	hsa-miR-93*
hsa-miR-151-5p	hsa-miR-223	hsa-miR-421	hsa-miR-941
hsa-miR-152	hsa-miR-223*	hsa-miR-423-3p	hsa-miR-942
hsa-miR-15a	hsa-miR-24	hsa-miR-423-5p	hsa-miR-96
hsa-miR-15b	hsa-miR-25	hsa-miR-424	hsa-miR-98
hsa-miR-15b*	hsa-miR-25*	hsa-miR-425	
hsa-miR-15b*	hsa-miR-26a	hsa-miR-425*	
hsa-miR-16	hsa-miR-26b	hsa-miR-451	

Table 2.2 MiRNAs affected by hemolysis as published by MacLellan *et al*. (2014)[139]

2.3 Results

2.3.1 Identification of a circulating miRNA for use as a normalizer

Normalization of serum miRNAs aims to remove differences due to sample collection and quality of profiled miRNA. MiRNAs normally used as housekeeping and endogenous controls in tissue are generally unsuitable as circulating miRNA normalizers due to their abundance within red blood cells, and so appropriate miRNA normalizers within the serum are difficult to determine. For example, miR-16-5p is the most expressed miRNA in red blood cells, and hemolysis leads to substantial increase of that miRNA in serum concentration[141,208]. Therefore, lysis of red blood cells will cause contamination of serum miRNA content resulting in different standardization based on amount of hemolysis. Another example, is RNU6B (U6) a common miRNA used for tissue normalization, however in the serum it has seen high variability even in healthy patients indicating its unsuitability[209]. Currently, no miRNA has been shown to be a consistent normalizer in the serum of patients, although if detecting more than 100 miRNAs global normalization is often referred to as the gold standard[210]. However, we were only able to detect 11 miRNAs not affected by hemolysis and detected in each sample, so global mean could not be an effective method (Table 2.3). To achieve normalization within our sample set, we sought to determine an endogenous miRNA within our serum samples that could be utilized as a normalizer. To select miRNAs candidates to act as normalizers in our serum samples, I eliminated any miRNAs detected above 35 Ct's in every sample. After elimination 69 miRNAs remained, miRNAs affected by hemolysis (Table 2.2) were then removed leaving 11 miRNA candidates remaining (Table 2.3)[139]. Remaining miRNAs for normalizations were analyzed for their potential as normalizers using both geNorm and NormFinder software[211,212].

miRNAs
miR-23a
miR-23b
miR-197
miR-145
miR-505
miR-99a
miR-125a-5p
miR-342-3p
miR-125b
miR-142-3p
miR-122

Table 2.3 miRNAs detected in every sample and not affected by hemolysis

NormFinder estimates the standard deviation (SD) of each miRNA, and then compares it against the expression of the other genes. The miRNA which has the lowest intra- and inter-group variation is considered the most stable miRNA[212]. The program geNorm analyses the stability of each miRNAs and associates an expression stability value (M-value) for each miRNA and identifies the best miRNA as a reference gene. The M-value is based on mean pairwise variation between genes across all samples, the miRNA with the lowest M-value is considered to be the most stable[211].

Scores for each miRNA candidate and analysis are reported in Table 2.4 and Table 2.5. Three miRNAs showed consistently strong scores for miRNAs as normalizers miR-197, miR-23a and miR-23b (Figure 2.1). We selected three miRNA normalizers to use, to be highly robust in our selection of miRNAs and to ensure that validation of at least one miRNA normalizer would occur. MiR-197 and miR-23a have both previously been reported as useful miRNAs for normalization, however this is the first time miR-23b has been demonstrated as a miRNA normalizer for serum miRNAs. We had previously reported that miR-122-5p was a suitable normalizer for serum samples, however within our LAC serum analysis miR-122-5p had the highest variability between samples[139]. This may be caused by differing platforms as the previously published data was utilizing an older platform with differing products and for certain miRNAs primer design was altered.

Gene Name	M-Value
miR-23a	0.501929434
miR-23b	0.501929434
miR-197	0.583430471
miR-145	0.62397506
miR-505	0.684115404
miR-99a	0.724214161
miR-125a-5p	0.75853554
miR-342-3p	0.791727679
miR-125b	0.812377637
miR-142-3p	0.837827795
miR-122	0.952339571

*Average expression stability (M-Value)

Table 2.4 geNorm analysis of 11 candidate miRNAs for serum normalization

Gene Name	SD	Acc. SD
miR-197	0.0113	0.0113
miR-23a	0.0113	0.008
miR-23b	0.0134	0.007
miR-125b	0.0148	0.0058
miR-99a	0.0148	0.0055
miR-505	0.0158	0.0052
miR-145	0.0165	0.005
miR-342-3p	0.0174	0.0048
miR-125a-5p	0.0194	0.0048
miR-142-3p	0.0209	0.0047
miR-122	0.0272	0.0049

*Acc. SD (accumulated standard deviation)
*SD (Standard Deviation)

Table 2.5 NormFinder analysis of 11 candidate miRNAs for serum normalization.

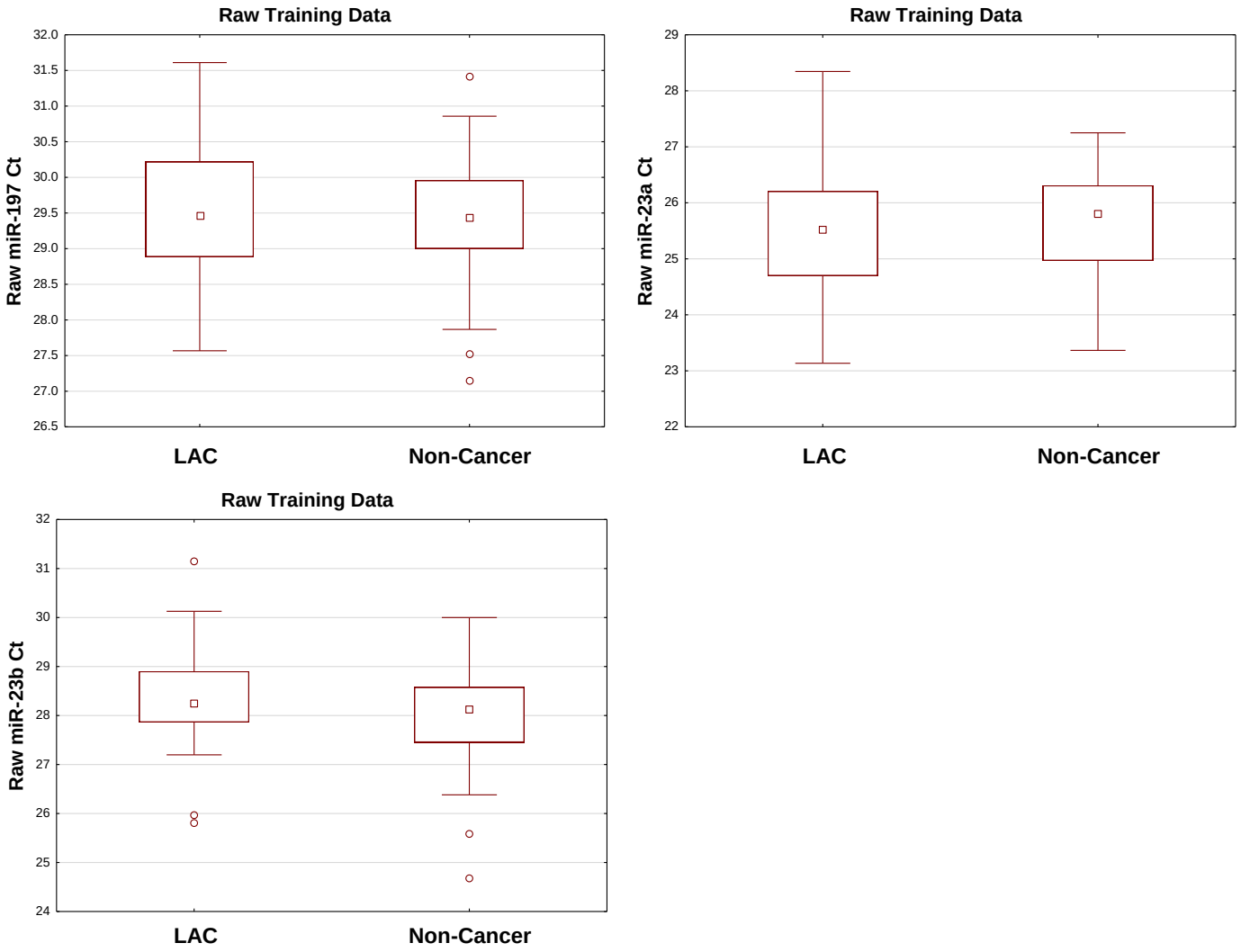

Figure 2.1 Box plot of training data raw Ct values of A) miR-197, B) miR-23a and C) miR-23b from both LAC serum and non-cancer controls. (n = 50 LAC, n=51 Non-Cancer)

2.3.2 Validation of endogenous miRNA normalizers

To confirm that our miRNAs would be normalizers across platforms we utilized individual TaqMan qRT-PCR primers on a separate subset of samples to determine if expression of normalizers was consistent (Figure 2.2). Using raw qRT-PCR data we entered the data into both geNorm and NormFinder and found that miR-197 showed a much higher standard deviation between LAC and non-cancer indicating that a shift had occurred between platforms and that miR-197 was no longer suitable for use as a normalizer (Table 2.6). Indicated by NormFinder analysis, miR-23a and miR-23b remained suitable as normalizers due to low M-values < 0.15 (Table 2.7). However, miR-23b had a higher standard deviation in geNorm analysis compared to miR-23a which indicated miR-23a is the more suitable normalizer for LAC and non-cancer serum (Table 2.4 and Table 2.5). Thus miR-197 and miR-23b have been removed as normalizers for analysis.

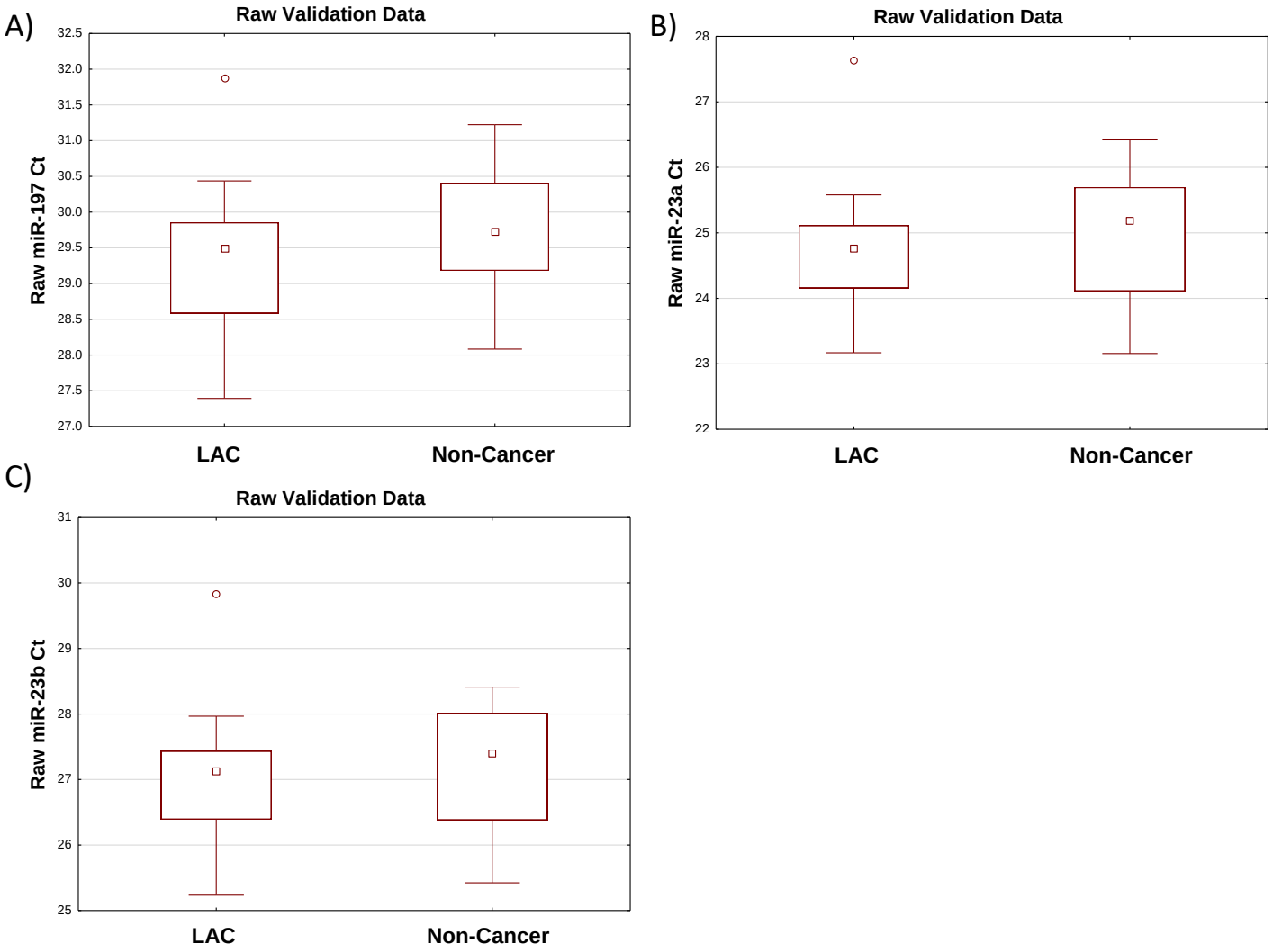

Figure 2.2 Box plot of candidate miRNA normalizers between lung adenocarcinoma and non-cancer in validation sample sets A) miR-197 B) miR-23a C) miR-23b. (n = 35 LAC, n=28 Non-Cancer)

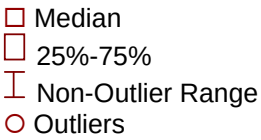

Gene Name	SD	Acc. SD
miR-23a	0.1086	0.1086
miR-23b	0.1253	0.0829
miR-197	0.3384	0.1256

*Acc. SD (accumulated standard deviation)
*SD (Standard Deviation)

Table 2.6 geNorm analysis of normalization candidates for validation data

Gene Name	M-Value
miR-197	0.281448704
miR-23a	0.127979299
miR-23b	0.127979299

*Average expression stability (M-Value)

Table 2.7 NormFinder analysis of normalization candidates for validation data

2.3.3 Identification of miRNAs differentially detected in lung adenocarcinoma and healthy controls

To identify potential microRNA candidates as biomarkers for early LAC detection, microRNAs in LAC sera and non-cancer control sera had to meet three criteria: (1) Ct values <35 to ensure reliable consistent detection, (2) microRNAs must not be affected by hemolysis to ensure serum microRNAs cannot be affected by blood drawing technique and storage and (3) microRNAs must be present in >50% of all samples. These criteria were utilized to ensure that the miRNAs indicated as biomarkers are reliably detected, not affected by hemolysis and would be useful as indicators of LAC in a majority of patients. A total of 86 microRNAs met these criteria (Table 2.8).

miRNAs Detected <35Ct's and Not Affected by Hemolysis		
hsa-let-7b*	hsa-miR-28-3p	hsa-miR-95
hsa-let-7e	hsa-miR-28-5p	hsa-miR-99a
hsa-miR-1	hsa-miR-29b-1*	hsa-miR-99b
hsa-miR-106b*	hsa-miR-301b	
hsa-miR-10a	hsa-miR-30a	
hsa-miR-10b	hsa-miR-30a*	
hsa-miR-122	hsa-miR-326	
hsa-miR-1249	hsa-miR-339-3p	
hsa-miR-125a-5p	hsa-miR-339-5p	
hsa-miR-125b	hsa-miR-33a	
hsa-miR-1266	hsa-miR-342-3p	
hsa-miR-127-3p	hsa-miR-34a	
hsa-miR-128	hsa-miR-365	
hsa-miR-130b*	hsa-miR-373*	
hsa-miR-133a	hsa-miR-375	
hsa-miR-134	hsa-miR-376a	
hsa-miR-136	hsa-miR-382	
hsa-miR-139-5p	hsa-miR-409-3p	
hsa-miR-141	hsa-miR-490-3p	
hsa-miR-142-3p	hsa-miR-491-5p	
hsa-miR-145	hsa-miR-495	
hsa-miR-1537	hsa-miR-497	
hsa-miR-1538	hsa-miR-543	
hsa-miR-154	hsa-miR-550a*	
hsa-miR-181c*	hsa-miR-551a	
hsa-miR-1909	hsa-miR-551b	
hsa-miR-1913	hsa-miR-582-5p	
hsa-miR-193a-5p	hsa-miR-632	
hsa-miR-193b	hsa-miR-638	
hsa-miR-197	hsa-miR-654-3p	
hsa-miR-199a-5p	hsa-miR-663	
hsa-miR-199b-5p	hsa-miR-664	
hsa-miR-200a	hsa-miR-671-5p	
hsa-miR-200c	hsa-miR-744	
hsa-miR-205	hsa-miR-766	
hsa-miR-22*	hsa-miR-769-5p	
hsa-miR-23a	hsa-miR-885-5p	
hsa-miR-23b	hsa-miR-888	
hsa-miR-24-2*	hsa-miR-92b	
hsa-miR-26b*	hsa-miR-934	
hsa-miR-27b	hsa-miR-940	

Table 2.8 List of miRNAs not affected by hemolysis and detected in more than 50% of all samples

A Mann-Whitney U test was conducted on miRNA detected in >50% of all serum samples and normalized to miR-23a. After correcting for multiple testing using the Benjamini-Hochberg correction 22 miRNAs were significantly enriched in LAC serum while one miRNA was enriched in non-cancer serum (Table 2.9). MiR-142-3p was the most significantly different miRNA, being enriched in LAC serum compared to non-cancer. MiR-142-3p when enriched in the serum of LAC patients has previously been associated with, patients suffering from recurrence within 24 months of tumor excision[213].

miRNAs (miR-23a Normalized)	Uncorrected p-value	Benjamini-Hochberg Significance (FDR 0.10)	Benjamini-Hochberg p-value
Enriched in LAC Serum			
hsa-miR-142-3p	0.000102	significant	0.00548686
hsa-miR-551b	0.000187	significant	0.00548686
hsa-miR-199a-5p	0.000191	significant	0.00548686
hsa-miR-27b	0.000487	significant	0.010471255
hsa-miR-766	0.000927	significant	0.015942803
hsa-miR-33a	0.001522	significant	0.018709302
hsa-miR-497	0.001853	significant	0.018709302
hsa-miR-23b	0.002429	significant	0.018709302
hsa-miR-139-5p	0.002573	significant	0.018709302
hsa-miR-28-5p	0.002622	significant	0.018709302
hsa-miR-127-3p	0.002828	significant	0.018709302
hsa-miR-376a	0.002828	significant	0.018709302
hsa-miR-136	0.004654	significant	0.02816332
hsa-miR-24-2*	0.004912	significant	0.02816332
hsa-miR-495	0.005665	significant	0.030448303
hsa-let-7e	0.015876	significant	0.080314886
hsa-miR-339-5p	0.017312	significant	0.082713469
hsa-miR-22*	0.021492	significant	0.095267448
hsa-miR-154	0.022155	significant	0.095267448
hsa-miR-1	0.024991	significant	0.096273199
hsa-miR-34a	0.025747	significant	0.096273199
Enriched in Non-Cancer Serum			
hsa-miR-582-5p	0.001946	significant	0.018709302

Table 2.9 miRNAs significantly enriched within lung adenocarcinoma serum compared to non-cancer control serum as analyzed by Mann Whitney U test with a Benjamini-Hochberg correction

2.3.4 Identification of miRNAs able to differentially distinguish between LAC and non-cancer

In order to identify miRNAs that could be utilized to differentiate between LAC and non-cancer we conducted a logistic regression model. We began by setting minimums for selecting miRNAs first an AUC of 0.8000 must be met to ensure specificity and sensitivity and the minimum number of miRNAs that fit above 0.8000 AUC would be used, to prevent overfitting. Next miRNAs were entered into Statistica for a forward stepwise logit regression to identify miRNAs that were suitable for inclusion in best subset analysis. Certain miRNAs were removed from analysis due to recent findings, including miR-720 which was discovered to be a fragment of tRNA[214]. MiR-155 was also removed from analysis due to its correlation with smoking-associated diseases including coronary artery disease and type 2 diabetes[215-217]. This miRNA was therefore removed, as coronary artery disease and type 2 diabetes were not recorded in patient data and may lead to discriminating of smoking-associated diseases rather than LAC[218]. miRNAs that were found to have a variable status of "In" in the forward stepwise analysis were then placed into the logit regression to determine best subsets for discriminating between LAC and non-cancer.

Using miR-23a normalized serum data ten miRNAs were selected for inclusion in the model (miR-142-3p, miR-497, miR-582-5p, miR-27b, miR-92b, miR-200c, miR-638, miR-29b-1-3p, miR-1909 and miR-940) (Table 2.10). Included miRNAs were then entered into a logit regression best subset analysis which examines which miRNAs are best at discriminating between LAC and non-cancer in combination. The ROC curve for all ten miRNAs was found to have an AUC of 0.8877, while a four-miRNA signature of miR-582-5p, miR-497, miR-27b and miR-92b was found to have an AUC of 0.8045 (Table 2.11) (Figure 2.3). To prevent overfitting, we utilized the four-miRNA signature in discriminating between LAC and non-cancer. A discriminate score equation was derived from the miRNA signature utilizing parameter estimates (Table 2.12).

Logit Modeled Probability miR-23a Normalized LAC vs Non-Cancer Serum				
Effect	Degree of Freedom	Wald Stat.	Wald p	Var. Status
hsa-miR-142-3p	1	5.217141	0.022365	In
hsa-miR-582-5p	1	8.734898	0.003122	In
hsa-miR-638	1	9.545789	0.002004	In
hsa-miR-497	1	9.226806	0.002385	In
hsa-miR-29b-1*	1	4.750941	0.029282	In
hsa-miR-92b	1	4.379165	0.036381	In
hsa-miR-27b	1	5.628781	0.017668	In
hsa-miR-200c	1	6.202137	0.012760	In
hsa-miR-940	1	4.694019	0.030268	In
hsa-miR-1909	1	5.047135	0.024667	In

Table 2.10 miRNAs from forward stepwise logit regression for entrance into best subset analysis

Number of miRNAs Included in Logit Regression	AUC Score
10	0.8877
9	0.8564
8	0.8440
7	0.8194
6	0.8156
5	0.8127
4	0.8045
3	0.7694
2	0.7549

Table 2.11 MiRNAs included in logit regression and their associated AUC score

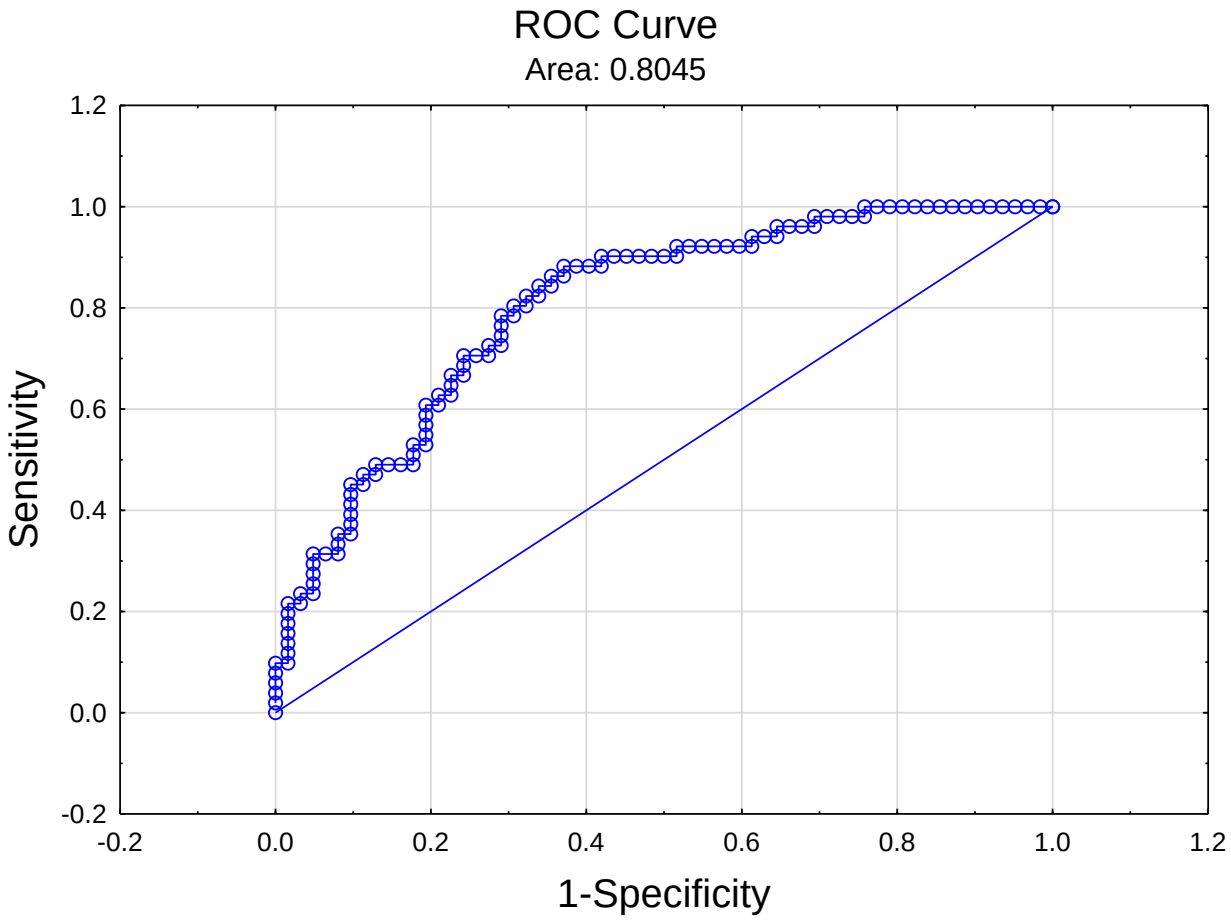

Figure 2.3 ROC curve of LAC miRNA classifiers normalized to miR-23a

	Formula (Score if score < 0, LAC Predicted)
Discriminate Score	$= -3.7122 - 1.3276(CT\ miR - 27b) - 0.6026(CT\ miR - 497) + 0.5841(CT\ miR - 582 - 5p) + 0.8318(CT\ miR - 92b)$

Table 2.12 Formulas for discrimination of patient serum

2.3.5 Validation of serum miRNA signatures in separate serum sample cohort

To validate miRNA linear regression models in predicting LAC presence in serum, 64 new patient serum samples were run on a custom TaqMan designed panel of miRNAs including miR-23a, miR-92b, miR-582-5p, miR-27b and miR-497. Samples were normalized to miR-23a and entered the linear regression model equation described in Table 2.12. A score of less than 0 indicated LAC prediction while a score more than 0 indicated non-cancer prediction. In a collection of 63 validation samples LAC was correctly predicted 68.6% of the time and non-cancer 67.9% of the time (Table 2.13). Patient samples that were misclassified ranged from stage I to stage III and were evenly distributed between the groups, which may suggest that the discriminate score is not biased towards the tumor stage (Table 2.14). Given the changes in sensitivity and specificity between our training and validation data we sought to improve our accuracy by looking for demographic differences between training and validation. Our validation samples had a large difference between male and female samples (~35% of validation samples, compared to 50% of training samples), so we sought to determine if sex may play a role in the detection of serum miRNAs (Table 2.1).

	Predicted LAC	**Predicted Non-Cancer**	**Percent Correct**
Observed LAC	24	11	0.686
Observed Non-Cancer	9	19	0.679

Table 2.13 Predicted cases using independent validation data normalized to miR-23a

Tumour Stages	Misclassified Cases/Total Cases
I	3/9
II	4/13
III	5/14

Table 2.14 Misclassified tumour stages in validation cohort

2.3.6 Serum miRNAs are differentially detected in male and female samples

Previously researchers have shown sex associated differences in male and female serum miRNAs[126,219,220]. These differences in miRNAs by sex may impact miRNAs as biomarkers and to account for this effect we separated LAC and non-cancer samples based on sex.We conducted a Mann Whitney U test on male patient samples between LAC and non-cancer serum, and on female patient samples between LAC and non-cancer serum. In males nineteen miRNAs were significantly differentially enriched between LAC and non-cancer serum after a Benjamini-Hochberg correction when normalized to miR-23a (Table 2.15). In females only six miRNAs were found to be differentially enriched between LAC and non-cancer serum, but no miRNAs remained significant after correction for multiple testing. These results indicate that LAC serum miRNAs may have a higher probability for detecting the presence of LAC in males compared to females.

miRNAs (miR-23a Normalized)	Uncorrected p-value	Benjamini-Hochberg Significance (FDR 0.10)	Benjamini-Hochberg p-value
Enriched in LAC Serum			
hsa-miR-142-3p	0.000065	significant	0.005978015
hsa-miR-139-5p	0.000325	significant	0.014946457
hsa-miR-27b	0.001024	significant	0.02753425
hsa-miR-551b	0.001628	significant	0.029035395
hsa-miR-199a-5p	0.001894	significant	0.029035395
hsa-miR-28-5p	0.003243	significant	0.042622181
hsa-miR-136	0.005177	significant	0.059538833
hsa-miR-339-5p	0.007097	significant	0.064363034
hsa-miR-376a	0.007418	significant	0.064363034
hsa-miR-23b	0.008462	significant	0.064363034
hsa-miR-495	0.008462	significant	0.064363034
hsa-let-7f	0.010494	significant	0.064363034
hsa-miR-33a	0.010494	significant	0.064363034
hsa-miR-155	0.015267	significant	0.087785674
hsa-miR-766	0.016893	significant	0.088102476
hsa-let-7e	0.017237	significant	0.088102476
Enriched Non-Cancer Serum			
hsa-miR-582-5p	0.001197	significant	0.02753425
hsa-miR-505	0.010494	significant	0.064363034

Table 2.15 miRNAs significantly enriched within male lung adenocarcinoma serum compared to male non-cancer control serum as analyzed by Mann Whitney U test with a Benjamini-Hochberg correction.

Due to the differences caused by sex in miRNAs significantly enriched within LAC serum and non-cancer controls, I further examined the best subset of miRNAs for classification of LAC by sex. We performed linear regression best subset analysis on training data separated by sex. In males a two-miRNA signature was derived for normalization to miR-23a using miR-142-3p and miR-582-5p as classifiers with an AUC of 0.8309 (Figure 2.4A) (Table 2.16). In females a two-miRNA signature of miR-497 and miR-200a was derived for miR-23a normalized data and with an AUC of 0.7903 (Figure 2.4B) (Table 2.16).

A)

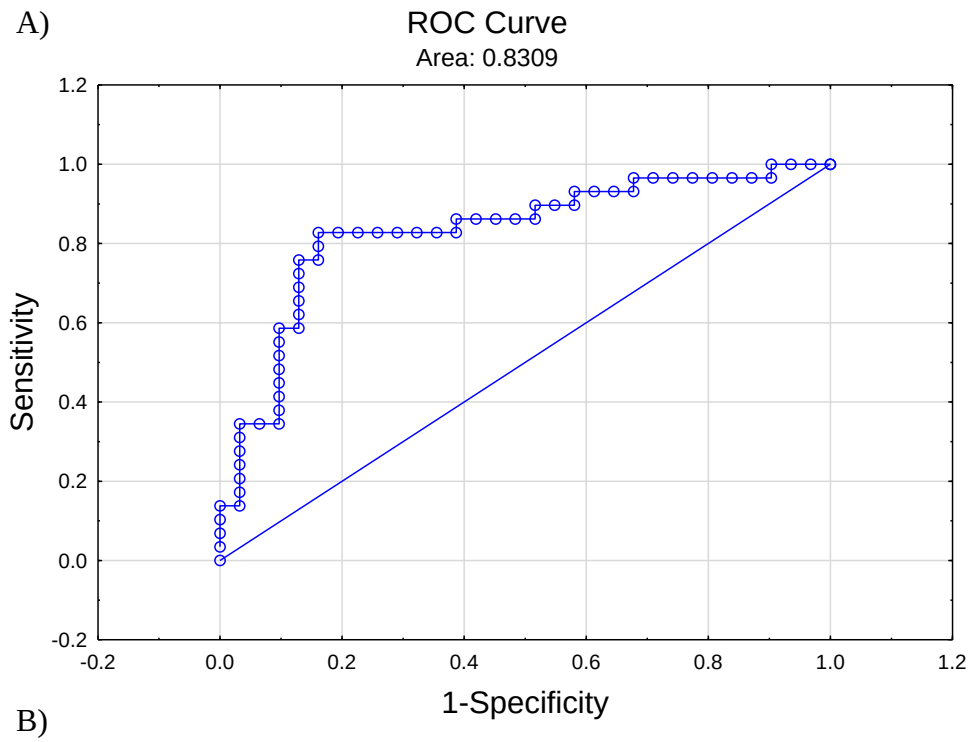

B)

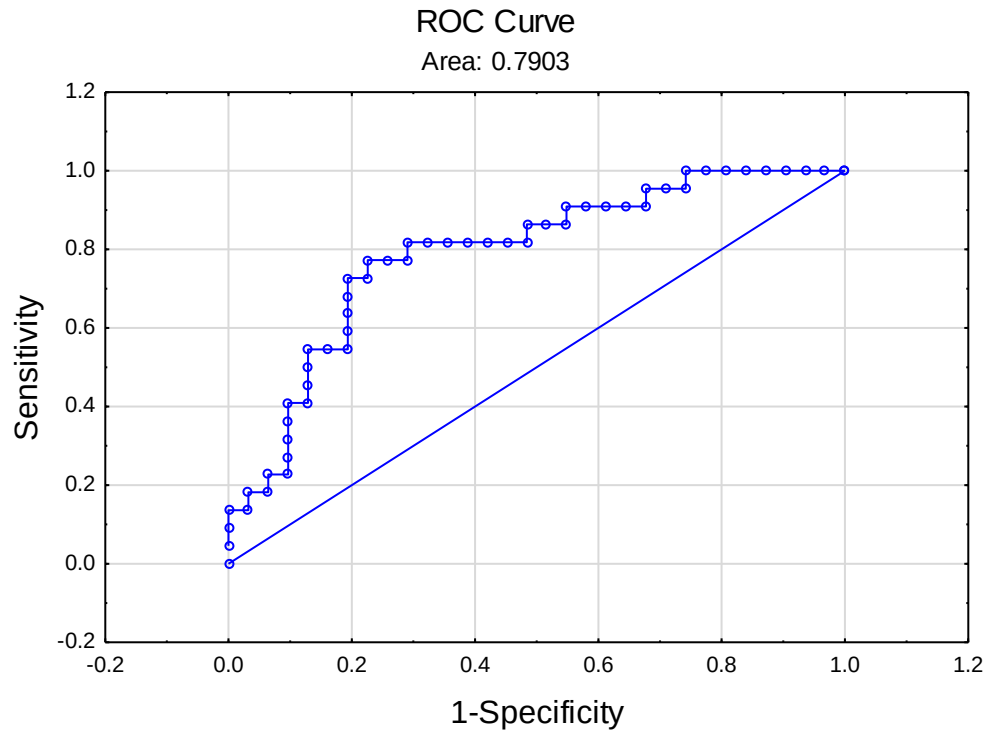

Figure 2.4 ROC curve of A) miR-23a normalized male serum data for derived miRNA signature B) miR-23a normalized female serum data for derived miRNA signature

	Formula (Score if score < 0, LAC Predicted)
Male Discrimination Score	$= -3.9161 - 1.3184(Ct\ miR-142-3p) + 0.7065(Ct\ miR-582-5p)$
Female Discrimination Score	$= 1.1027 - 1.0421(Ct\ miR-497) - 0.7623(Ct\ miR-200a)$

Table 2.16 : Table of sex specific discriminate score analysis for identification of LAC serum.

2.3.7 Validation of sex-specific serum miRNA signatures in separate serum sample cohort

We next sought to validate our sex specific miRNA signatures on a separate sample cohort. Utilizing the same validation samples to profile miR-142-3p, miR-200a, miR-497, miR-582-5p and miR-92b using TaqMan primers and the serum discrimination equations derived previously in table 2.11, it was found that female specific discrimination equations poorly predicted LAC serum with around a 35% accuracy, while predicting non-cancer serum accurately around 75% of the time (Table 2.17). In female discrimination equations we found that non-cancer tended to be predicted. In males LAC was predicted in all but one sample, suggesting that the derived formula tends to predict LAC (Table 2.18). We sought to determine if a specific miRNA may be causing these tendencies by examining normalized Ct values for each sex specific miRNAs between validation and training (Figure 2.5). In figure 2.5 and figure 2.6 we see that most miRNA normalized Ct values show the same trend between training and validation, except for miR-142-3p which shows a deviation in trend from differentially expressed in training data to non-differentially expressed in validation data. In addition, we examined identical serum samples run on the different platforms to ensure the trends we were seeing were

validated. We found a significant difference between training miR-142-3p and validation miR-142-3p in identical samples using a T-test (Figure 2.7). We sought to remove miR-142-3p from male analysis to determine if a different subset of miRNAs could be used to differentiate between LAC and non-cancer, using only previously used miRNAs on validation panels.

	Predicted LAC	Predicted Non-Cancer	Percent Correct
Observed LAC	8	15	0.348
Observed Non-Cancer	4	14	0.778

Table 2.17 Female predicted cases using independent validation data normalized to miR-23a

	Predicted LAC	Predicted Non-Cancer	Percent Correct
Observed LAC	12	0	1.000
Observed Non-Cancer	8	1	0.111

Table 2.18 Male predicted cases using independent validation data normalized to miR-23a

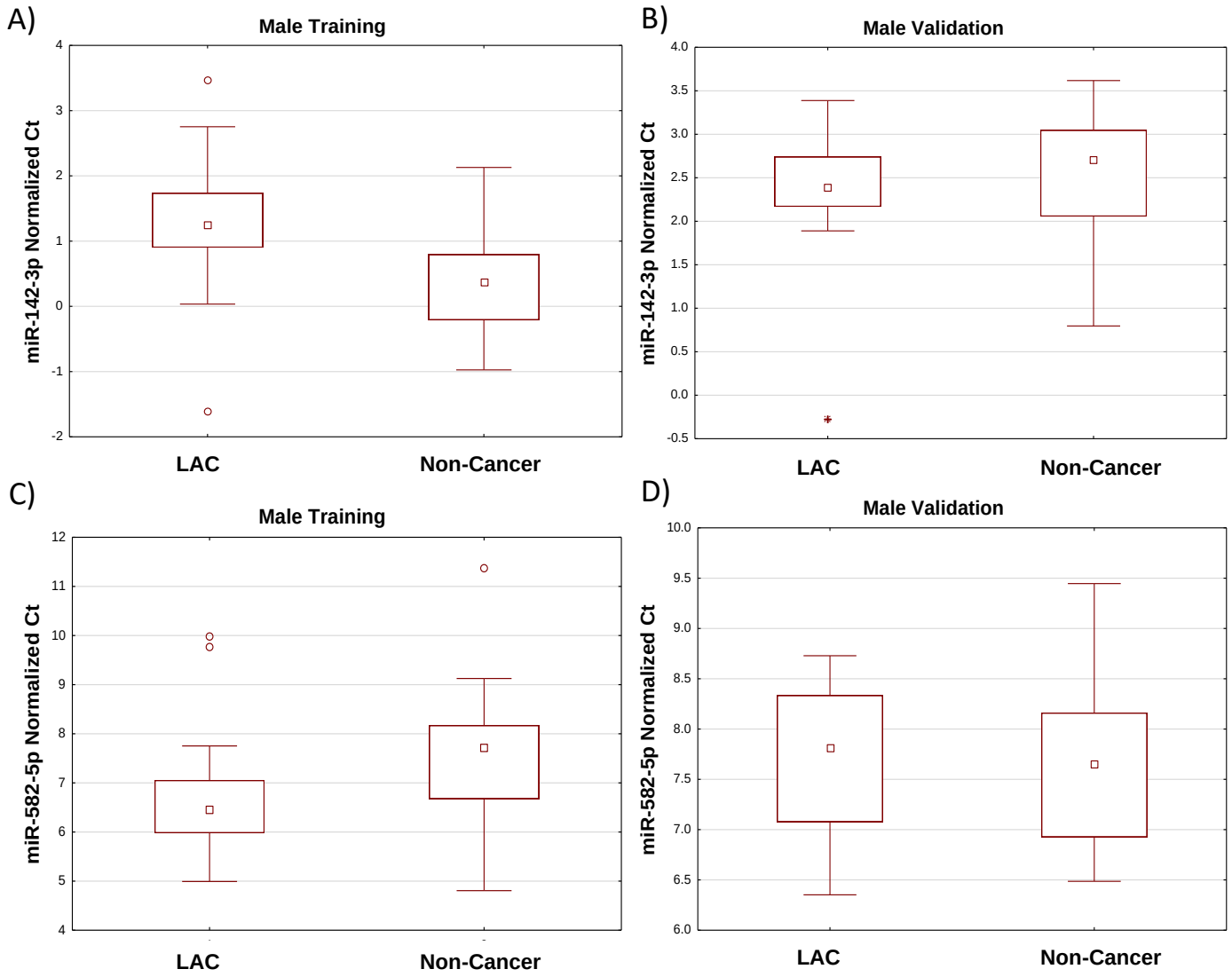

Figure 2.5 Box plots of male miRNA candidates normalized to miR-23a a) miR-142-3p training data LAC vs Non-Cancer b) miR-142-3p validation data lung adenocarcinoma vs Non-Cancer c) miR-582-5p training data LAC vs Non-Cancer d) miR-582-5p validation data lung adenocarcinoma vs Non-Cancer. (Training Male: n = 26 LAC, n= 29 Non-Cancer, Validation Male: n = 13 LAC, n = 9 Non-Cancer)

☐ Median
☐ 25%-75%
I Non-Outlier Range
✳ Extremes
○ Outliers

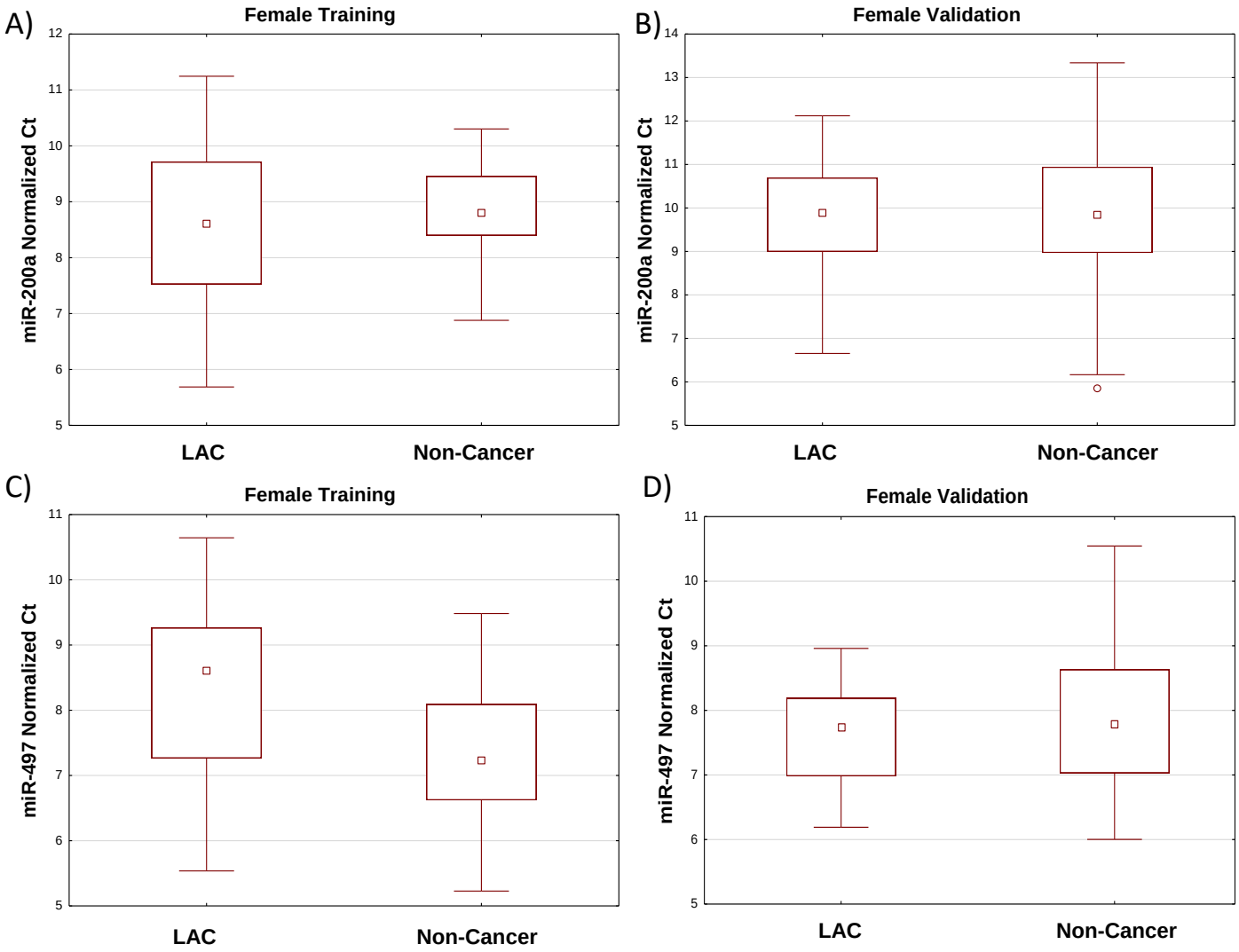

Figure 2.6 Box plots of female miRNA candidates normalized to miR-23a a) miR-200a training data LAC vs Non-Cancer b) miR-200a validation data LAC vs Non-Cancer c) miR-497 training data LAC vs Non-Cancer d) miR-497 validation data LAC vs Non-Cancer. (Training Female: n = 24 LAC, n= 22 Non-Cancer, Validation Male: n = 23 LAC, n = 19 Non-Cancer)

□ Median
□ 25%-75%
I Non-Outlier Range
○ Outliers

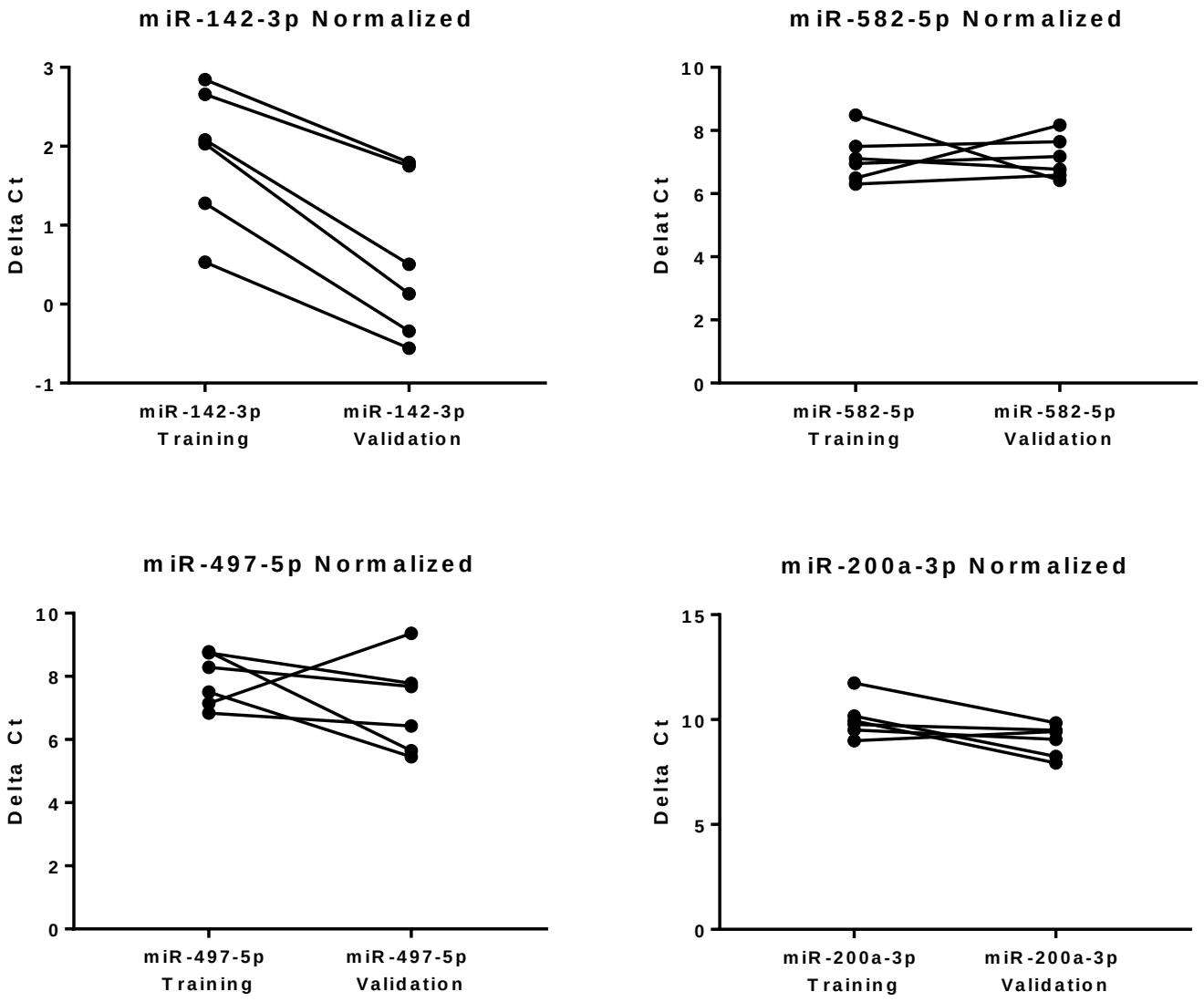

Figure 2.7 Delta Ct values of examined miRNAs between identical serum samples analyzed using SYBR (Training) green and TaqMan (Validation).

After removal of miR-142-3p from male training data analysis, and using miRNAs previously validated on panels in our best subset analysis, we found a three-miRNA signature able to differentiate LAC from non-cancer in males (miR-27b, miR-582-5p and miR-92b), it had an ROC curve of 0.8464 (Figure 2.8) (Table 2.16). Using the male sex specific formula lacking miR-142-3p we found that LAC was correctly predicted 83% of the time and non-cancer was correctly predicted 67% of the time (Table 2.17). This male sex specific formula shows the highest accuracy of all derived formulas and shows the greatest promise for use as a clinical biomarker panel. The two tumor samples misclassified by the discriminate score were stage III LAC patients, which could indicate that the discriminate score is more useful for discriminating between stage I and II LAC patients than later stages, however further validation with a larger sample size would be required (Table 2.21).

	Formula (Score if score < 0, LAC Predicted)
Male Discrimination Formula	$= -7.1458 - 3.0974(Ct\ miR - 27b) + 0.8773(Ct\ miR - 582 - 5p) + 0.9141(Ct\ miR - 92b)$

Table 2.19 Male sex-specific formula for prediction of LAC normalized to miR-23a

	Predicted LAC	**Predicted Non-Cancer**	**Percent Correct**
Observed LAC	10	2	0.833
Observed Non-Cancer	3	6	0.666

Table 2.20 Prediction of lung adenocarcinoma or non-cancer in validation samples normalized to miR-23a

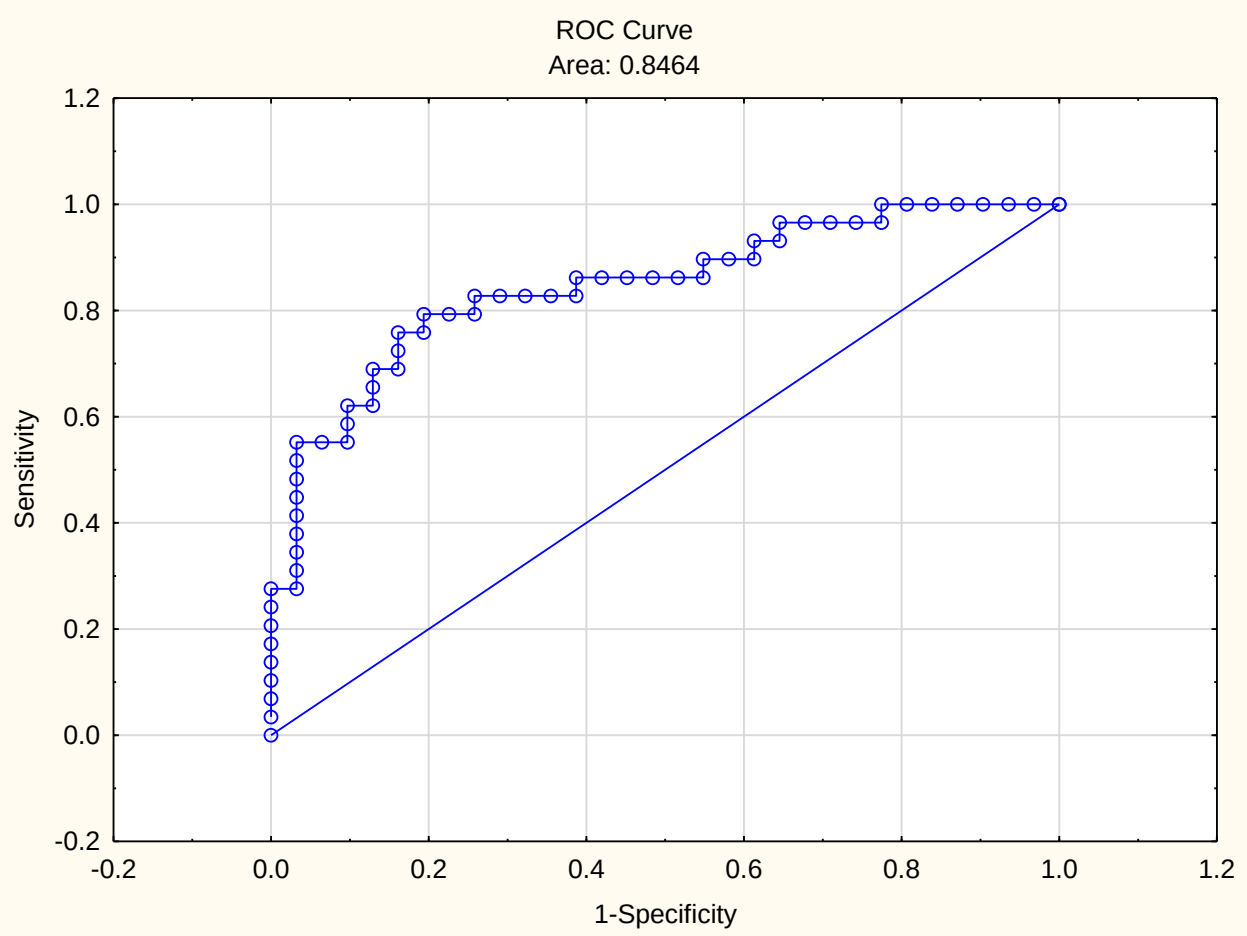

Figure 2.8 ROC curve of miR-23a normalized male serum data without miR-142-3p

Tumour Stages	Misclassified Cases/Total Cases
I	0/3
II	0/3
III	2/7

Table 2.21 Tumour stages misclassified by male discriminative score in male validation patient cohort

Taken together the data demonstrates that discriminating between LAC serum and non-cancer serum may be more easily distinguishable through analyzing male and female serum separately. The ability of miRNAs to distinguish between LAC and non-cancer serum was increased when female patient serum was eliminated. However, with an inability to classify female serum successfully we may want to expand the search for miRNAs in female patients either through profiling for an increased number of miRNAs or increasing the number of samples profiled. In male samples however normalizing to miR-23a and examining differentially expressed miR-27b, miR-582-5p and miR-92b presents itself as a promising biomarker for use in LAC detection in high risk patients.

2.4 Discussion

Our results demonstrate that while there is an abundance of miRNAs differentially enriched in LAC serum compared to non-cancer controls, the construction of a sensitive and specific panel of microRNA biomarkers may be possible in male patients. While attempting to validate the results of the Human Panel I +II SYBR Green product, we changed platforms to reflect the more accurate and specific TaqMan assays. We took six samples from our training set and ran them on the TaqMan assays (Figure 2.7). The result of changing platforms resulted in changes within our miRNA sequences and the efficiency of their detection which was demonstrated in Figure 2.7. We chose to continue with our analysis and validate our serum candidate miRNAs using TaqMan as it is considered to have a higher specificity for miRNA analysis[221]. One difference to note is our normalization candidate miR-197 which, can most likely be attributed to the change in platform (Figure 2.1 and Figure 2.2). In the case of miR-197 the change in trend from being evenly expressed in all serum samples to having higher expression in LAC, indicates that changing of platforms caused a shift in miR-197 detection through either detection method or primer sequence. This aspect of our research demonstrates the need for a consistent platform that researchers can utilize to conduct analysis, and for a normalization method to be found which can be utilized across platforms.

NSCLC has been extensively profiled for miRNA biomarkers in both the sputum and the serum of patients to predict the presence of NSCLC in patients. Profiling of NSCLC sputum showed that detection of miR-21 was significantly higher in patients with NSCLC[100]. An important caveat to this study was that samples have a significant change in average pack years between NSCLC and non-cancer controls[100]. In further sputum analysis for miRNA biomarkers a panel of miRNAs including miR-21, miR-486-5p, miR-375 and miR-200b, was capable of

distinguishing LAC patients from normal subjects, this research showed no significant differences in pack years between non-cancer and LAC sputum[222]. Sputum miRNA biomarkers are able to avoid the issues of hemolysis in serum studies, which may make them a more robust model in determining miRNA biomarkers as you are not limited by miRNAs affected by hemolysis. For example, in lung cancer plasma miR-21 and miR-210 were shown to be elevated while miR-486-5p had lower enrichment in lung cancer serum[134]. However, miR-21 is associated with hemolysis and therefor proper controls will be required if miR-21 is to be utilized as a biomarker within the serum[139]. Within our analysis we excluded miR-21 as a potential biomarker due to its significant effects from hemolysis. This may indicate that miR-21 is acceptable as a diagnostic sputum biomarker but not as a serum, again indicating that sputum biomarkers may be more robust due to not relying on non-hemolysis affected miRNAs. However, for NSCLC located in the periphery of the lung, well away from the major airways, sputum miRNAs may not be relevant as secreted miRNAs may not be able to enter the sputum efficiently for detection. For LAC and lung cancers located at distant sites in the lung periphery serum miRNAs may become a more accurate method for detection.

In two meta-analyses conducted by He *et al.* (2015) and Wang *et al.* (2015) it was found that panels consisting of multiple miRNAs offered a higher sensitivity and specificity for disease detection compared to single miRNAs[113,223]. Both studies showed that panels consisting of several miRNAs had a much higher diagnostic potential as biomarkers for NSCLC. In trials using multiple miRNAs as biomarkers positive results have been found. One group of investigators utilized a 13 miRNAs signature on 1115 participants all heavy smokers and above 50 years old participating in the COSMOS lung cancer screening trial, they found a sensitivity and specificity of 79.2% and 75.5% respectively[113]. The reported miRNA signature may be

useful as a first-line screening tool in high-risk heavy smoker individuals. While the miRNAs are useful in diagnosis, they may also have use in discriminating between benign lesions and NSCLC. A four-miRNA signature (miR-378a, miR-379, miR-139-5p and miR-200b-5p) was identified as being able to discriminate between LAC patients and granuloma patients within a cohort of healthy former smokers[224]. These studies confirm that serum miRNAs are useful in identifying and diagnosing lung cancers, however due to their distinct signature compared to our derived signatures obvious differences are found. The method used within their study does utilize some miRNAs we found affected by hemolysis (miR-378a), as well as only former smokers as controls.

The usage of clinically relevant controls is essential when determining biomarkers for LAC detection. Within many lung cancer miRNA biomarker studies, healthy non-smokers are utilized to differentiate between smoking-related LAC and non-cancer[124,125,127-129,132-134]. However, in the clinic high-risk individuals who are likely to be screened for LAC presence would be individuals with heavy smoking backgrounds. Our non-cancer samples mirror clinical patients that would be actively screened for LAC presence and these types of non-cancer patient samples are rare, thus our study offers a unique investigation into LAC circulating miRNA biomarkers. These results demonstrate the need for defined guidelines for both miRNA exclusions and proper controls for miRNA biomarker discovery.

Circulating miRNAs as biomarkers are still in its infancy, despite being highly researched for many diseases no current clinical trials are being conducted. There are many factors that can affect serum miRNA levels including amount of hemolysis, presence of virus/infection, age, sex and ethnicity[219,225-227]. With the number of factors influencing the amount of miRNAs within the serum and specific levels of certain miRNAs, a more stringent selection process may need to be

conducted with patients grouped into age, sex and ethnic cohorts for analysis. Through grouping of samples into more specific categories for analysis we may be able to determine clinical markers for detection of disease. Another factor contributing to challenges in using miRNAs as biomarkers is the lack of a standard endogenous control. In our research using the SYBR platform miR-197 was found to be a strong endogenous control, however when switching platforms miR-197 became an unusable endogenous miRNA (Figure 2.2 and Figure 2.3). This can also be seen in meningioma serum as miR-197 has been shown to decrease by 2-fold in the serum, suggesting its use as a endogenous control is situational and platform specific[220]. It is critical that a miRNA standard for normalization of serum biomarkers is created as common miRNAs used as endogenous controls like U6 and miR-16, which are highly influenced by the level of hemolysis within the serum sample, are unsuitable[139,228]. By creating a highly reproducible cross-platform normalizer for serum analysis it will accelerate and allow for comparative analysis of serum miRNAs as biomarkers.

Chapter 3: Selective secretion of microRNAs from lung cancer cells via extracellular vesicles promotes CAMK1D-mediated tube formation in endothelial cells

3.1 Introduction

Lung cancer remains the leading cause of cancer death worldwide, and LAC, the most common histological subtype, has a dismal 5-year survival rate of ~16%[229,230]. While advances have been made in treatments, survival rates remain poor[231]. With a greater understanding of the molecular mechanisms driving LAC, development of innovative treatment options to better combat this disease may become possible.

Recently, there has been increased interest in the role of extracellular vesicles (EVs) in tumorigenesis. EVs are a heterogeneous group of secreted small membrane bound vesicles. They are known to play a variety of roles in cancers, including establishing a pre-metastatic niche, conferring drug resistance, and promoting angiogenesis through cell-cell communication [232,233]. EVs contain a variety of cargo that determine EV function, such as mRNAs, miRNAs, and proteins[234]. MiRNAs are small non-coding RNAs that post-transcriptionally regulate expression of protein coding genes[235,236]. MiRNAs are known to be involved in numerous biological processes, in disease development, and are highly deregulated in cancer[237]. In breast cancer, EVs containing miR-181c promote metastases to the brain through destruction of the blood brain barrier[238]. Other roles for EV miRNA include promoting chemotherapy resistance. For example, in breast cancer, the transfer of EVs containing miR-100, miR-122 and miR-30a from resistant MCF-7 breast cancer cells are known to promote chemotherapy resistance to MCF-7 drugs

sensitive cells[239]. Finally, the role of tumor derived EVs in promoting angiogenesis has been well established, Liu *et al*. found that EVs containing miR-21 was able to increase VEGF levels in recipient cells through targeting of STAT3[240-242]. These roles of EVs play are critical to the developing tumor, allowing for communication to surrounding cells and for the tumor to influence the stroma to support its growth.

The loading of miRNAs into EVs is not a passive process and can differ depending on cell type and disease state[237]. Certain miRNAs are selected for EV loading and exclusion from cells, while others are selectively retained by cells, suggesting a biological role for these miRNAs in cancer[243]. Sorting of miRNAs into EVs has been previously reported through hnRNPA2B1, a RNA binding protein regulated by SUMOylation and able to bind the RNA motif GGAG, however it does not fully explain all miRNA sorting into EVs[91]. The ability of cells to selectively secrete specific miRNAs within EVs to use as communicators is of great interest as they transform the cells they enter and can even be used as potential biomarkers. Herein, we report on miRNAs that are selectively enriched within EVs of LAC cells and show that EVs enriched for specific miRNAs enter endothelial cells and promote blood vessel formation by altering the activity of CAMK1D, an anti-angiogenic kinase.

3.2 Materials and Methods

3.2.1 Cell culture

All LAC cell lines and 293T cells were obtained from ATCC. LAC cell lines H1395, H1437, H2073, H2228 and H2347 were cultured in RPMI 1640 media supplemented with 10% fetal bovine serum (FBS). HMEC-1 cells were generously donated by the Aly Karson Lab and, HPL1D cells were donated by the Will Lockwood lab. Cell lines HMEC-1 and 293T were

cultured in DMEM supplemented with 10% FBS. For EV collection, cells were grown in media supplemented with 1% depleted FBS (dFBS), which is FBS that has been depleted of EVs through overnight centrifugation at 110,000g and at 4ºC. Cell counting was performed using a hemocytometer.

3.2.2 EV collection

To collect EVs, "donor" LAC cells were grown in ten plates (15 cm), under normal conditions. Forty-eight hours prior to reaching 85% confluence, media was replaced with RPMI 1640 containing 1% dFBS. Cells were allowed to secrete EVs into dFBS media for 48 hours, after which the conditioned media was collected. Our EV isolation protocol is based on a differential ultracentrifugation protocol described by Rani *et al*. [244]. Conditioned media was centrifuged at 300g for 10 min, then at 2,000g's for 20 min and at 10,000g's for 30 min at 4ºC. Supernatant was collected at each stage of centrifugation and transferred to fresh 50 mL tubes for continued centrifugation. When completed, conditioned media was placed into open top ultracentrifuge tubes (Seton) and, using an ultracentrifuge set at 4ºC, media was spun for 70 min at 110,000g. Supernatant was discarded, and the EV pellet was rinsed with PBS to reduce protein contamination before a second round of ultracentrifugation. The EV pellet was either processed to collect RNA (using a miRCURY RNA Isolation Kit [Exiqon]) or protein (using RIPA buffer) or re-suspended in 0.02 µm-filtered PBS to perform NanoSight analysis or re-suspended in un-supplemented DMEM media to perform EV transfer assays.

3.2.3 qRT-PCR

Cell line RNA and EV RNA was collected using miRCURY RNA Isolation Kit (Exiqon). Seven hundred and forty-two miRNAs were measured using microRNA Ready-to-Use PCR, Human panel I+II (Exiqon) on a Viia 7 Real-Time PCR System (Thermo Fisher). Cell line and EV profiles were normalized to global mean and fold-change analysis was used to compare matched cellular and EV miRNA profiles[245]. We subsequently validated EV miRNA candidates using a TaqMan Assay normalized to input and cel-miR-39-3p miRNA spike in to account for PCR efficiencies.

3.2.4 Vectors

Over-expression (OE) cell lines were created using the FIV lenti-vectors HmiR0085-MR01 for miR-145, HmiR0084-MR01 for miR-143, or CmiR0001-MR01 (miR-Scramble) for a scramble sequence control (GeneCopoeia), vectors express both 3p and 5p miRNAs. Vectors were packaged using 293T cells and a Lenti-Pac FIV Expression Packaging Kit (GeneCopoeia). For knockdown assays, we used SMPD3 shRNA vectors TRCN0000048944, TRCN0000048945, TRCN000004896 and TRCN0000048947 (GE Dharmacon). Empty vector pLKO.1 was used as a control. The shRNA vectors were packaged using 293T cells and the plasmids VSVG and d8.91 using TransIT-LT1 transfection reagent (Mirus). Cells were infected over a 24-hour period, after which miRNA over-expression lines were selected using G418 for ten days, and shRNA lines were selected using puromycin for four days.

3.2.5 Serum analysis

Serum samples were collected from patients undergoing LAC resection with curative intent (Table 3.1). All blood was collected in SST vacutainer tubes. For each patient, blood draws were taken from pulmonary venous effluent draining the tumor vascular bed, and from the systemic arterial blood of the same patient during surgery. Serum was isolated by centrifugation at 1500g for 15 min, and then frozen and stored at -80°C. RNA was isolated from 200 µl of serum using a Qiagen miRNeasy kit. MiRNAs were profiled for 742 miRNAs as described above. We removed miRNAs that are known to be affected by hemolysis by a fold change of greater than four[139]. Samples were normalized to miR-122-5p, which we have previously reported as an appropriate miRNA for normalizing patient matched samples on the SYBR Green Human Panel I+II, as it is not affected by hemolysis and shows little inter-patient variability[139].

Table 3.1: Patient demographics

Patient Demographics:		**Patients:**
Variable:	Patients:	10
Age (Years):		
	Mean:	71.55555556
	Median:	73
	Range:	62 - 79
Sex:		
	Females:	5
	Male:	4
	N/A:	1
Smoking History:		
	Current/Former:	7
	Never:	1
	N/A:	2
Stage:		
	I:	4
	II:	2
	III:	0
	IV:	0
	NA:	4

Table 3.1 Patient demographics

3.2.6 EV incubation

Previously collected EVs were suspended in 100 µl DMEM media with no added supplements. The media was added to 50% confluent HMEC-1 cells in a 96 well plate and incubated for 24 hours, after which protein and RNA were collected.

3.2.7 Tube formation assays

In triplicate for each treatment, $1.2x10^5$ HMEC-1 cells were added onto 24-well plates containing 200 µl of 10mg/ml Matrigel (Corning). EVs suspended in un-supplemented DMEM were incubated with the HMEC-1 cells for 16 hours. DIC images were taken using an Axiovert S1000 microscope under the 10X objective, with an image being taken at the center of each well. Tube length was quantified using ImageJ with the 'Angiogenesis Analyzer' plugin, and triplicates were averaged.

3.2.8 Western blot

1:100 diluted phosphatase inhibitor cocktails I&II (Millipore Sigma) and 1:100 protease inhibitors (Thermo Fisher) were added to RIPA buffer to decrease sample degradation. Protein was quantified using a Pierce BCA kit and 10 µg of each sample was separated with a 12% SDS-PAGE gel and transferred onto PVDF membranes. Membranes were blocked in 5% BSA, 1X TBS and 0.1% Tween-20 for 1 hour. Membranes were incubated overnight at 4°C with primary antibodies diluted in blocking buffer. We used anti-CD63 (1:1000 dilution, EXOAB-Cd63A-1, System Biosciences), anti-TSG101 (1:1000 dilution, ab83, Abcam), anti-CAMK1D (1:800 dilution, #3365, Cell Signaling) and loading control anti-Histone H3 (1:4000, # 4499 Cell Signaling) followed by HRP conjugated anti-rabbit (1:2000, #7074, Cell Signaling). Detection was done using an Amersham ECL kit and hyperfilm (General Electric). Western images were quantified using the 'gel analysis' function in ImageJ (http://imagej.nih.gov).

3.3 Results

3.3.1 Identification of miRNAs enriched in the EVs of LAC cells

EVs from early stage LAC cell lines H1395, H1437, H2073, H2228, and H2347 were collected by differential ultracentrifugation (Table 3.2)[244]. Analysis by nanoparticle tracking analysis (NTA) revealed the majority of EVs were ~110 nm in size (Figure 3.1A-F). This size range is consistent with the size of exosomes, a subset of EVs. Furthermore, EV presence was confirmed by western blot for common EV markers CD63 and TSG101 (Figure 3.1H). RNA from both donor cells and isolated EVs was extracted using the miRCURY™ RNA Isolation (Exiqon) kit and profiled for miRNA expression using microRNA Ready-to-Use PCR, Human panel I+II, V4.M (Exiqon).

Cell Line	Stage	Mutations and Features
H1395	II	15 pack years, BRAF mutation c.1406G>C
H1437	I	70 pack years, TP53 mutation c.800G>C, CDKN2A mutation c.1_471del471, MET mutation c.970R>C[246]
H2073	IIIa	30 pack years
H2228	-	Non-smoker, RB1 mutation c.610delG, CDKN2A mutation c.1_471del471, TP53 mutation c.991C>T, EML-ALK fusion[247]
H2347	I	Non-smoker, NRAS mutation c.182A>G

Table 3.2 Tumour stages, mutation profile and characteristics of early LAC cell lines according to ATCC[248].

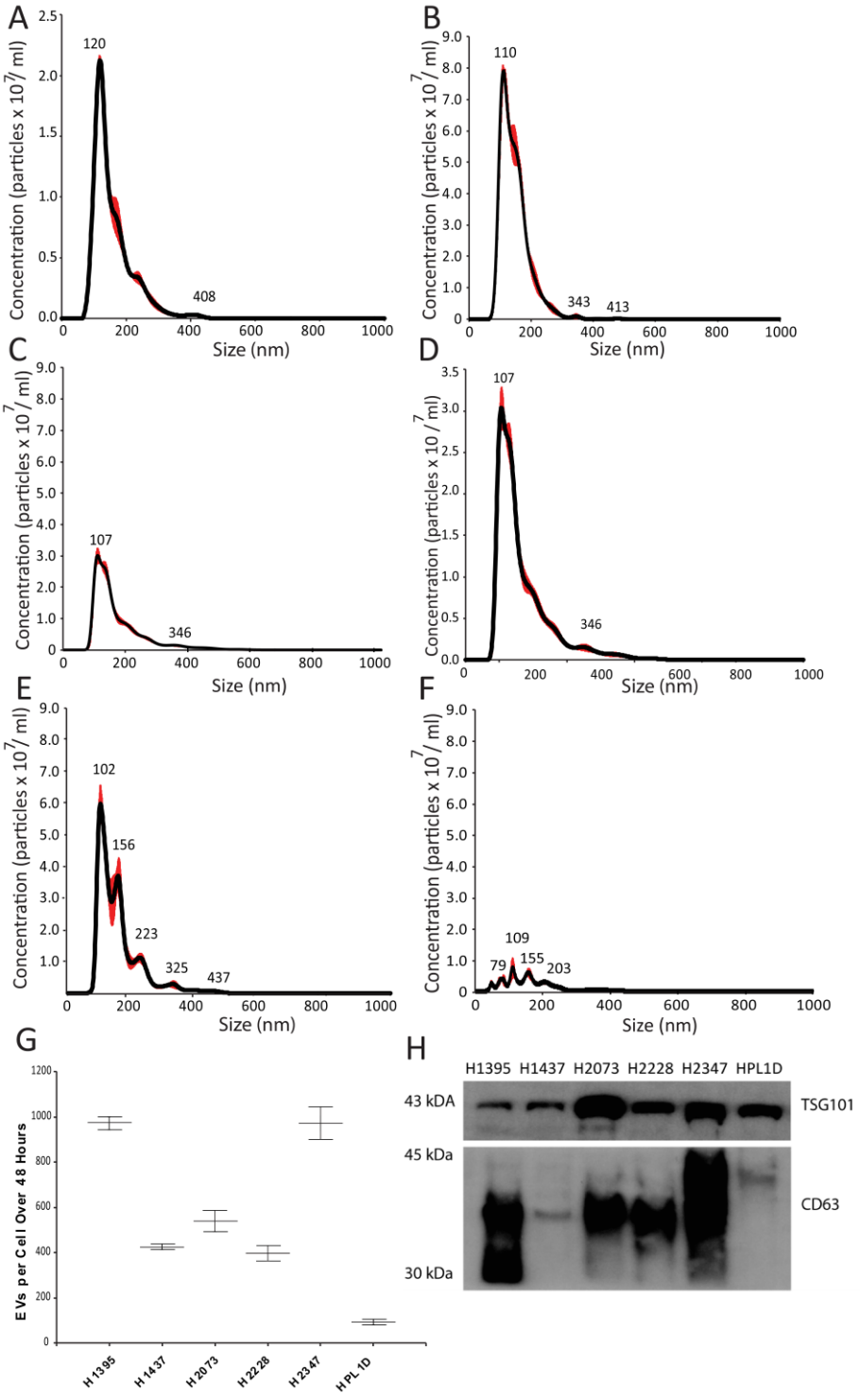

Figure 3.1 EV identification. A-C) Nanoparticle Tracking Analysis of EVs, quantifying size and concentration using NanoSight: A) H1395 B) H1437 C) H2073 D) H2228 E) H2347 F) HPL1D cell line G) Comparison of number of EVs produced per cell over 48 hours F) Western blot confirmation of EV associated proteins CD63 and TSG101. Error bars represent standard deviation. Red shaded area is standard deviation between triplicates for each vesicle size.

Of the 742 miRNAs examined, an average of 264 miRNAs were detected in the EV fractions and 258 miRNAs in the donor cell fractions. For each donor cell-EV pair on average, four miRNAs were uniquely detected in the donor cell fraction and 12 miRNAs were uniquely detected in the EV fraction. We used a 4-fold detection cut-off between the EV and donor cell miRNA profiles to identify miRNAs that were selectively enriched in EVs. A 4-fold cut off was utilized to be highly stringent on candidate miRNA selection and allow for high reproducibility. On average 11 miRNAs were selectively enriched within EVs per cell line (Table 3.3). On average, 14 miRNAs were selectively retained in each donor cell line as compared with associated EVs (Table 3.4). Nine miRNAs were recurrently enriched in the EVs of ≥3 of the five cell lines profiled (Table 3.5). However, none of these donor cell-enriched miRNAs were commonly enriched across the entire panel of cell lines. Recurrent miRNAs were validated in the matched donor cell and EV RNA samples using individual qRT-PCR reactions. A 4-fold difference was observed for all candidate miRNAs, except for miR-144-3p, which was eliminated from further analysis.

To determine whether the EV-enriched miRNAs were tumor cell specific, we isolated EVs from a normal epithelial lung cell line (HPL1D). RNA was extracted from donor cells and EVs were isolated as above. Using qRT-PCR, we determined the expression of our eight candidate miRNAs in the two RNA isolates. We found four of our eight miRNA candidates were also enriched within the EVs of HPL1Ds (miR-142-3p, miR-150-5p, miR-223-3p, and miR-451a); however, the extent of the enrichment observed in the tumor EV fraction was at least double that observed within the HPL1D EVs (Figure 3.2). This difference cannot be attributed to differences in miRNA expression in donor cells, as cellular expression of these miRNAs is similar between HPL1Ds and the tumor cell lines (Figure 3.3). Additionally, NTA analysis

revealed that EV production from HPL1D cells was less than 25% of what was observed in LAC cells: while HPL1D cells produced ~92 EVs per cell over 48 hours, H1395, H1437, H2073, H2228 and H2347 cells produced ~972, ~425, ~540, ~396 and ~972 EVs per cell over 48 hours, respectively (Figure 3.1G). In addition, while some miRNAs are commonly selected for EV export between tumor and normal cells, the enrichment in the tumor EVs is far greater (Figure 3.2) and EV production from the tumor cells is on average ten times higher than normal lung cell production (Figure 3.1G).

miRNAs Enriched in LAC Cell Lines				
H1395	**H1437**	**H2073**	**H2228**	**H2347**
hsa-let-7a	hsa-miR-1908	hsa-miR-1248	hsa-let-7a	hsa-let-7a-2*
hsa-let-7b	hsa-miR-1974	hsa-miR-181a*	hsa-miR-149	hsa-miR-1201
hsa-let-7c	hsa-miR-326	hsa-miR-193b*	hsa-miR-181d	hsa-miR-128
hsa-let-7d	hsa-miR-502-5p	hsa-miR-1974	hsa-miR-1974	hsa-miR-193b*
hsa-let-7e	hsa-miR-671-5p	hsa-miR-24-1*	hsa-miR-24-1*	hsa-miR-551b
hsa-miR-106b*		hsa-miR-490-3p	hsa-miR-299-5p	hsa-miR-671-5p
hsa-miR-1201		hsa-miR-671-3p	hsa-miR-342-3p	hsa-miR-766
hsa-miR-128			hsa-miR-423-3p	
hsa-miR-181b			hsa-miR-489	
hsa-miR-181d			hsa-miR-500a	
hsa-miR-18a*			hsa-miR-501-3p	
hsa-miR-1908			hsa-miR-502-5p	
hsa-miR-196a			hsa-miR-542-5p	
hsa-miR-197			hsa-miR-93*	
hsa-miR-29b-2*				
hsa-miR-324-3p				
hsa-miR-331-3p				
hsa-miR-423-3p				

Table 3.3 MiRNAs enriched in cell fraction compared to EVs by at least 4-fold

miRNAs Enriched in Exosomes				
H1395	**H1437**	**H2073**	**H2228**	**H2347**
hsa-miR-126	hsa-miR-103-2*	hsa-let-7d*	hsa-miR-142-3p	hsa-miR-142-3p
hsa-miR-142-3p	hsa-miR-126*	hsa-miR-142-3p	hsa-miR-143	hsa-miR-144
hsa-miR-144	hsa-miR-1260	hsa-miR-143	hsa-miR-144	hsa-miR-145
hsa-miR-145	hsa-miR-128	hsa-miR-144	hsa-miR-150	hsa-miR-150
hsa-miR-150	hsa-miR-142-3p	hsa-miR-145	hsa-miR-223	hsa-miR-20a*
hsa-miR-223	hsa-miR-143	hsa-miR-150	hsa-miR-451	hsa-miR-223
hsa-miR-31*	hsa-miR-144	hsa-miR-223	hsa-miR-486-5p	hsa-miR-451
hsa-miR-32	hsa-miR-145	hsa-miR-30a*	hsa-miR-502-3p	hsa-miR-502-5p
hsa-miR-451	hsa-miR-150	hsa-miR-330-5p	hsa-miR-605	hsa-miR-605
hsa-miR-486-5p	hsa-miR-199a-3p	hsa-miR-451	hsa-miR-638	hsa-miR-99b*
hsa-miR-720	hsa-miR-199a-5p	hsa-miR-486-5p	hsa-miR-720	
hsa-miR-886-3p	hsa-miR-223	hsa-miR-501-3p		
hsa-miR-888	hsa-miR-451	hsa-miR-502-5p		
	hsa-miR-486-5p	hsa-miR-605		
	hsa-miR-542-5p	hsa-miR-720		
	hsa-miR-545	hsa-miR-766		
	hsa-miR-605			
	hsa-miR-616*			
	hsa-miR-663			
	hsa-miR-720			
	hsa-miR-886-3p			

Table 3.4 MiRNAs enriched in LAC cell line EVs compared to cell fraction by at least 4-fold

miRNAs	Number of Cells Lines with miRNA Enriched in EVs >4-Fold (n=5)	H1395 Fold Change	H1437 Fold Change	H2073 Fold Change	H2228 Fold Change	H2347 Fold Change
miR-451a	5	273.22*	214.29*	50.42*	458.11*	83.26*
miR-142-3p	5	30.93	71.08*	17.70*	95.84*	18.68
miR-223-3p	5	179.01*	41.20*	12.10*	55.89*	20.46*
miR-144-3p	5	51.05*	32.55*	6.38*	59.16*	8.49*
miR-605-5p	4	0.92	17.11*	5.20*	54.51*	8.90*
miR-150-5p	4	79.45*	5.35	2.93*	21.15*	8.73*
miR-145-5p	4	31.25*	9.19*	7.39*	3.10*	4.15
miR-486-5p	3	38.42	9.62*	3.07*	6.88*	3.52*
miR-143-3p	3	20.07*	13.13*	1.76*	11.24*	1.23

*: indicates EV miRNA fold change where no miRNA was detected intracellularly, and intracellular Ct levels was set to threshold cut off, of 35 Cts for fold change analysis

Table 3.5 Profiling fold change of miRNAs enriched by 4-fold in the EVs of at least 3 lung adenocarcinoma cell lines using microRNA qRT-PCR

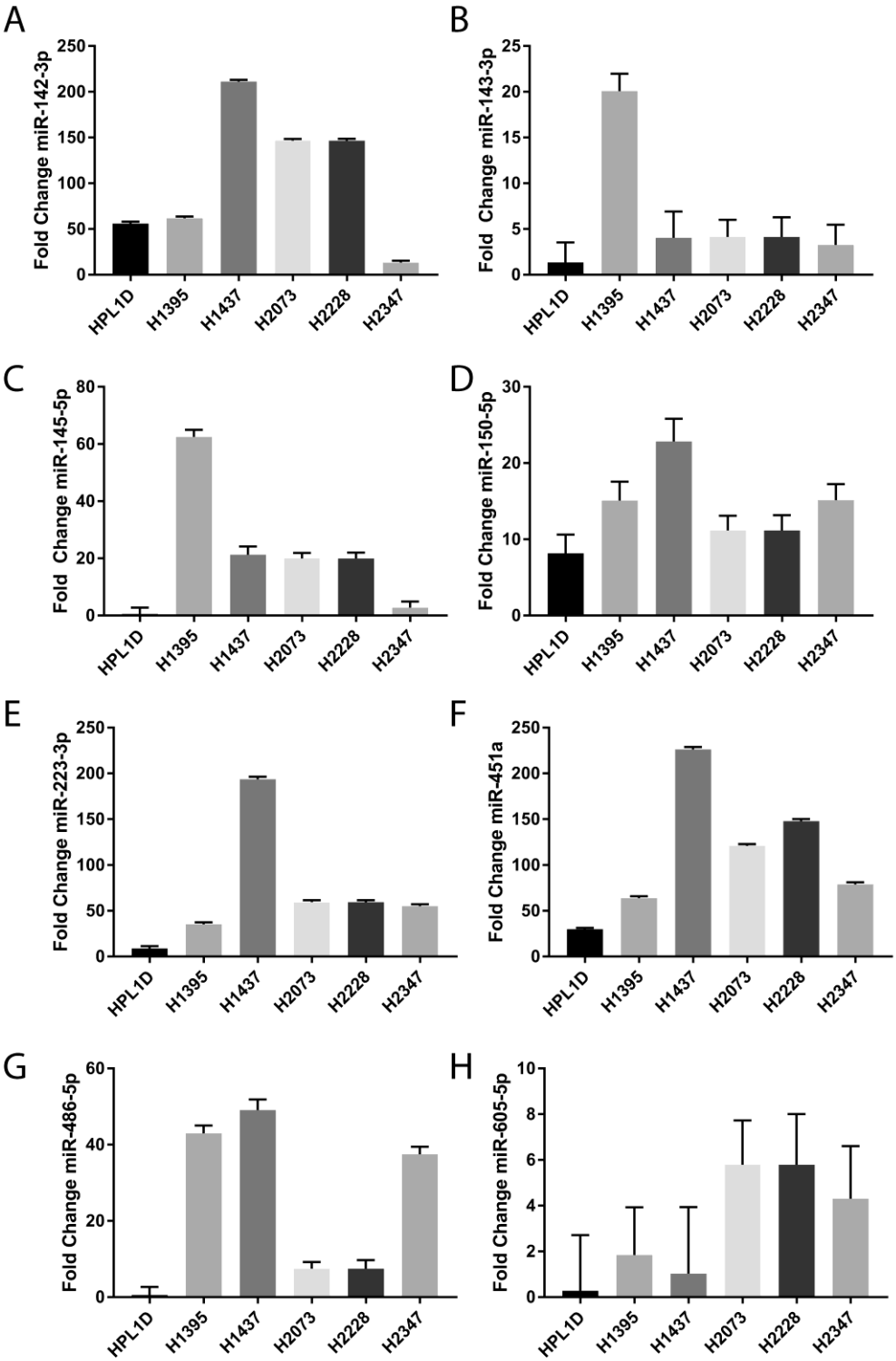

Figure 3.2 Fold Change of EV candidate miRNAs in LAC cell lines H1395, H1437, H2073, H2228, H2347 and normal lung line HPL1D in triplicate using TaqMan qRT-PCR for miRNAs: A) miR-142-3p B) miR-143-3p C) miR-145-5p D) miR-150-5p E) miR-223-3p F) miR-451a G) miR-486-5p H) miR-605-5p. Error bars represent standard deviation.

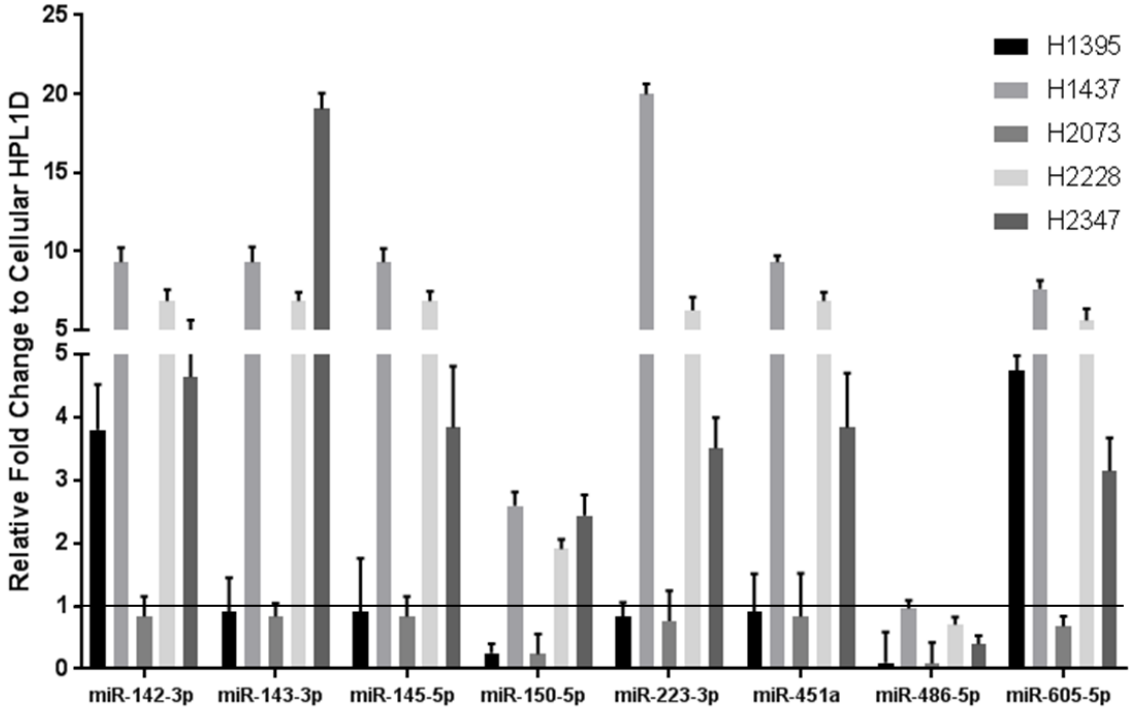

Figure 3.3 Fold change of LAC cell lines intracellular candidate miRNAs compared to HPL1D intracellular miRNAs normalized to U6. Error bars represent standard deviation.

3.3.2 Inhibition of EV release increases the levels of candidate miRNAs within LAC cells

To confirm that the detected candidate miRNAs were isolated from EVs, as opposed to co-precipitating factors, we inhibited the release of EVs by silencing SMPD3, a critical protein in ceramide-dependent exosome biogenesis[156]. We would expect the miRNA cargo within the EVs to remain in the cell and therefore show increased cellular expression. SMPD3 was inhibited using shRNAs and a ~75% knockdown was observed in both H2073 and H1437 cell lines (Figure 3.4A). When SMPD3 was inhibited in H1437 cells EV production decreased 83%, in H2073 cells we observed a ~60% decrease in EV production (Figure 3.4B) and a cellular increase in all candidate miRNAs was noted in both cell lines (Figure 3.4C).

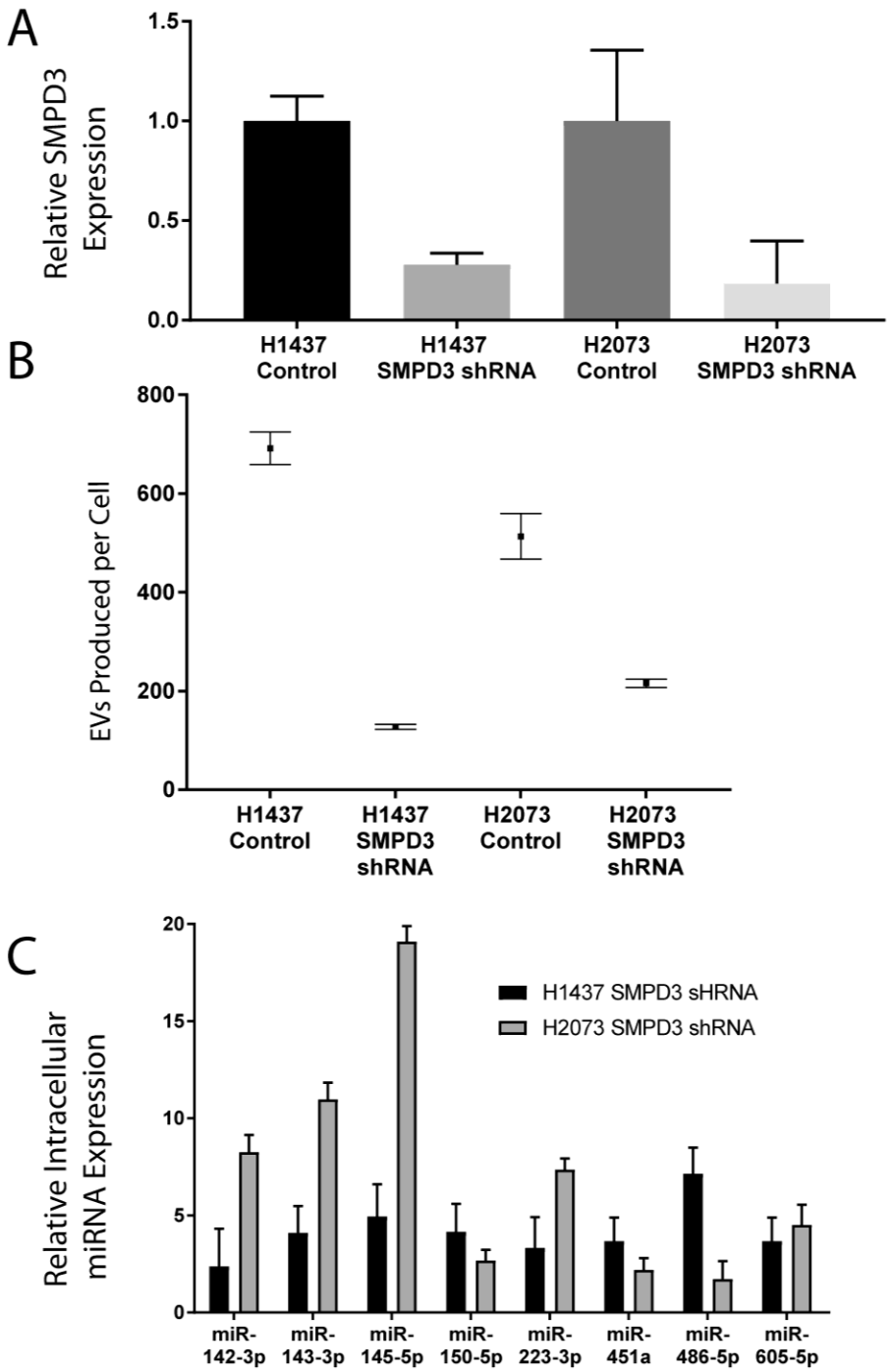

Figure 3.4 Analysis of EV inhibition using SMPD3. A) Cellular inhibition of SMPD3 in H1437 and H2073 cell lines using shRNA against SMPD3 confirmed using qRT-PCR B) EV secretion analysis measuring EVs produced per cell over 48 hours of H1437 and H2073 cells lines using SMPD3 shRNA inhibition using NanoSight C) Fold change analysis of candidate miRNAs from H1437 and H2073 intracellular RNA with SMPD3 shRNA inhibition. Error bars represent standard deviation.

3.3.3 MiR-143-3p and miR-145-5p are enriched within serum draining directly from LAC tumors

We next undertook qRT-PCR profiling of miRNAs in serum samples obtained from the pulmonary venous effluent draining directly from the tumor vascular bed. These serum samples were collected during surgical resection of LAC, as were matched samples from peripheral blood vessels. MiRNAs known to be influenced by hemolysis were removed from analysis[139]. On average, 169 miRNAs were detected in each sample, 52 miRNAs were expressed in all samples, 72 miRNAs were enriched in each tumor effluent sample by at least 4-fold, and only 12 miRNAs were enriched in peripheral samples by at least 4-fold. Twenty-two miRNAs were consistently enriched by at least 4-fold in the tumor effluent samples in at least half of the ten paired samples, while no miRNAs were recurrently down-regulated in tumor effluent samples (Table 3.6). Five of our eight EV miRNA candidates (miR-142-3p, miR-150-5p, miR-223-3p, miR-451a, miR-486-5p) were shown to be increased by hemolysis and were thus excluded from analysis. Of the remaining EV miRNA candidates, miR-143-3p and miR-145-5p were enriched in tumor draining effluent samples. These miRNAs both exhibited effluent sample enrichment in six of ten cases and exhibited 9.1-fold and 13.8-fold average over-expression in tumor effluent samples as compared to peripheral samples. Given their increased EV expression in LAC cell lines and increased serum abundance in LAC patient serum samples, we reasoned that EV-mediated miR-145-5p and miR-143-3p activity might promote in lung tumorigenesis.

miRNA	Mean Fold Change	Up Regulated by 4-Fold in Tumor Draining Serum (n =10)
hsa-miR-375	18.16	9
hsa-miR-200c-3p	36.86	9
hsa-miR-125b-5p	18.76	9
hsa-miR-200b-3p	20.97	8
hsa-miR-141-3p	64.67	8
hsa-miR-10a-5p	9.88	8
hsa-miR-34a-5p	12.95	7
hsa-miR-204-5p	9.30	7
hsa-miR-99a-5p	8.63	6
hsa-miR-95-5p	5.30	6
hsa-miR-497-5p	10.57	6
hsa-miR-30a-3p	8.69	6
hsa-miR-145-5p	9.14	6
hsa-miR-143-3p	13.78	6
hsa-miR-99b-5p	7.16	5
hsa-miR-99a-3p	8.73	5
hsa-miR-365a-3p	5.35	5
hsa-miR-30a-5p	11.71	5
hsa-miR-199b-5p	7.78	5
hsa-miR-193b-3p	7.88	5
hsa-miR-18a-3p	4.32	5
hsa-miR-133a-5p	6.01	5

Table 3.6 Mean fold change of miRNAs enriched in at least 5 of the 10 tumor draining samples

3.3.4 MiR-145-5p and miR-143-3p promote tube formation in endothelial cells

Recent work in LAC demonstrated that miR-145-5p and miR-143-3p can promote neoangiogenesis by direct targeting of CAMK1D in endothelial cells, and that loss of the miR-145/miR-143 cluster in these cells led to decreases in neoangiogenesis via CAMK1D[249]. It was suggested that miR-143/145 was not expressed by the tumor cells, but rather was produced by a subset of endothelial cells driving neoangiogenesis. We show that miR-145-5p and miR-143-3p are in fact produced by LAC cells; however, no expression is observed in the tumor cells, as these miRNAs are efficiently packaged into EVs and exported from the cell.

To interrogate the impact of EV-associated miR-143-3p and miR-145-5p, the levels of these miRNAs within EVs must be manipulated. We over-expressed miR-143, miR-145 and a miR-Scramble (SCR/C) individually in H1437 cells and H2073 cells which resulted in >90-fold over-expression of these miRNAs in the EVs derived from these cells (Figure 3.5). EVs from cells over-expressing miR-143 and miR-145, as well as miR-Scramble EVs (using a miRNA scramble, but still expressing normal levels of miR-143-3p and miR-145-5p in the EVs) were collected and incubated with HMEC-1 cells for 24 hours, along with HMEC-1 cells receiving no EVs. Following this, EVs were removed, the cells were washed and cellular RNA from HMEC-1 cells was extracted. MiR-145-5p and miR-143-3p increased by ~14-fold and ~6-fold in HMEC-1 cells incubated with EVs over-expressing miR-143 and miR-145 respectively when compared to HMEC-1 cells that were not incubated with EVs (Figure 3.6). HMEC-1 cells incubated with miR-Scramble over-expressing EVs (with normal miR-145-5p and miR-143-3p levels within EVs) showed an increase in miR-145-5p >5 fold and a slight increase in mR-143-3p by >2 fold (Figure 3.6). On the other hand, HMEC-1 cells showed no significant changes in intracellular levels of a miRNA (miR-346) that was not found in EVs from H1437 cells (Figure 3.6).

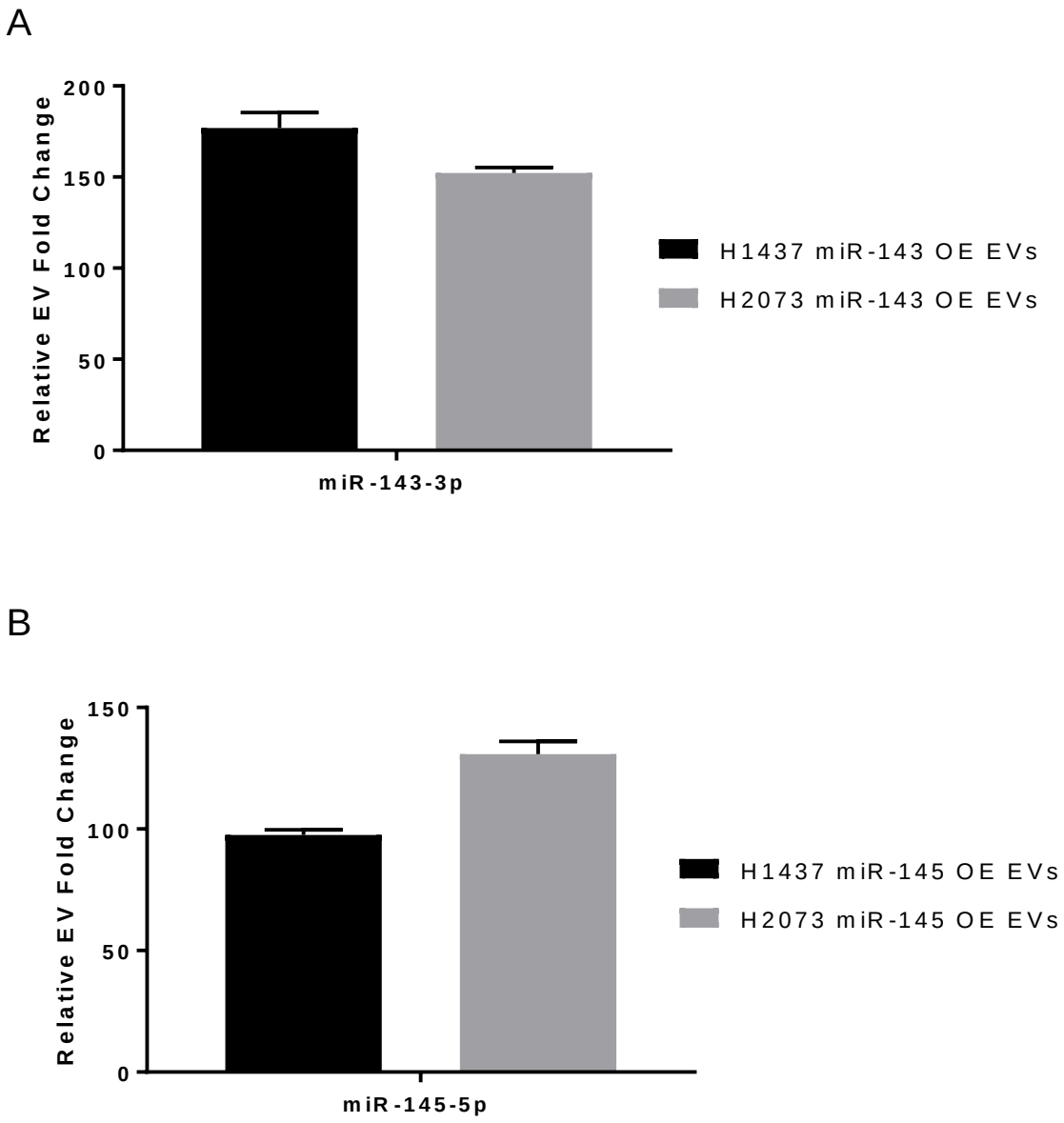

Figure 3.5 Relative fold change within the EVs of LAC miRNA overexpression cell lines H1437 and H2073 compared to miR-Scramble EVs for A) miR-143 OE EVs and B) miR-145 OE EVs. Error bars represent standard deviation

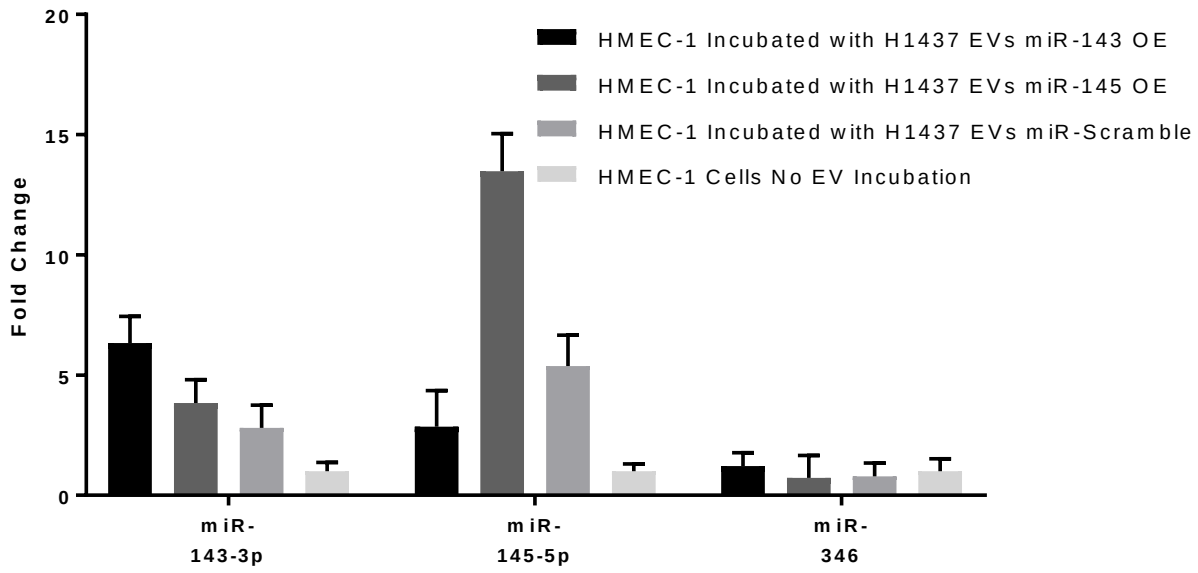

Figure 3.6 Lung adenocarcinoma cell extracellular vesicle miRNAs are taken up by HMEC-1 cells. Intracellular fold change analysis of miR-143-3p, miR-145-5p and miR-346 in HMEC-1 cells incubated with EVs from H1437 cells over expressing miR-143, miR-145 and miR-Scramble, compared to HMEC-1 cells receiving no extracellular vesicle incubation. Error bars represent standard deviation.

We next sought to determine if the transfer of EVs, and in particular miR-143-3p and miR-145-5p, within the EVs is capable of inducing tube formation changes in endothelial cells. HMEC-1 cells were grown without EVs or in the presence of EVs enriched with miR-143, EVs enriched with miR-145 or control EVs (endogenous EV levels of miR-143 and miR-145). All HMEC-1 cells exposed to EV incubation treatments formed tubes after 16 hours (Figure 3.7B). The addition of EVs from H1437 miR-Scramble over-expressing cells (with normal miR-145-5p and miR-143-3p levels within EVs) significantly increased the ability of HMEC-1 cells to form tubes compared to the HMEC-1 cells receiving no EVs ($p<0.01$) (Figure 3.6B). The addition of EVs over-expressing miR-145-5p or miR-143-3p further increased the length of tubes formed compared to miR-Scramble over-expressing EVs (Figure 3.7B). Significance was reached for miR-145 ($p<0.05$) but not for miR-143 ($p>0.05$) (Figure 3.7B).

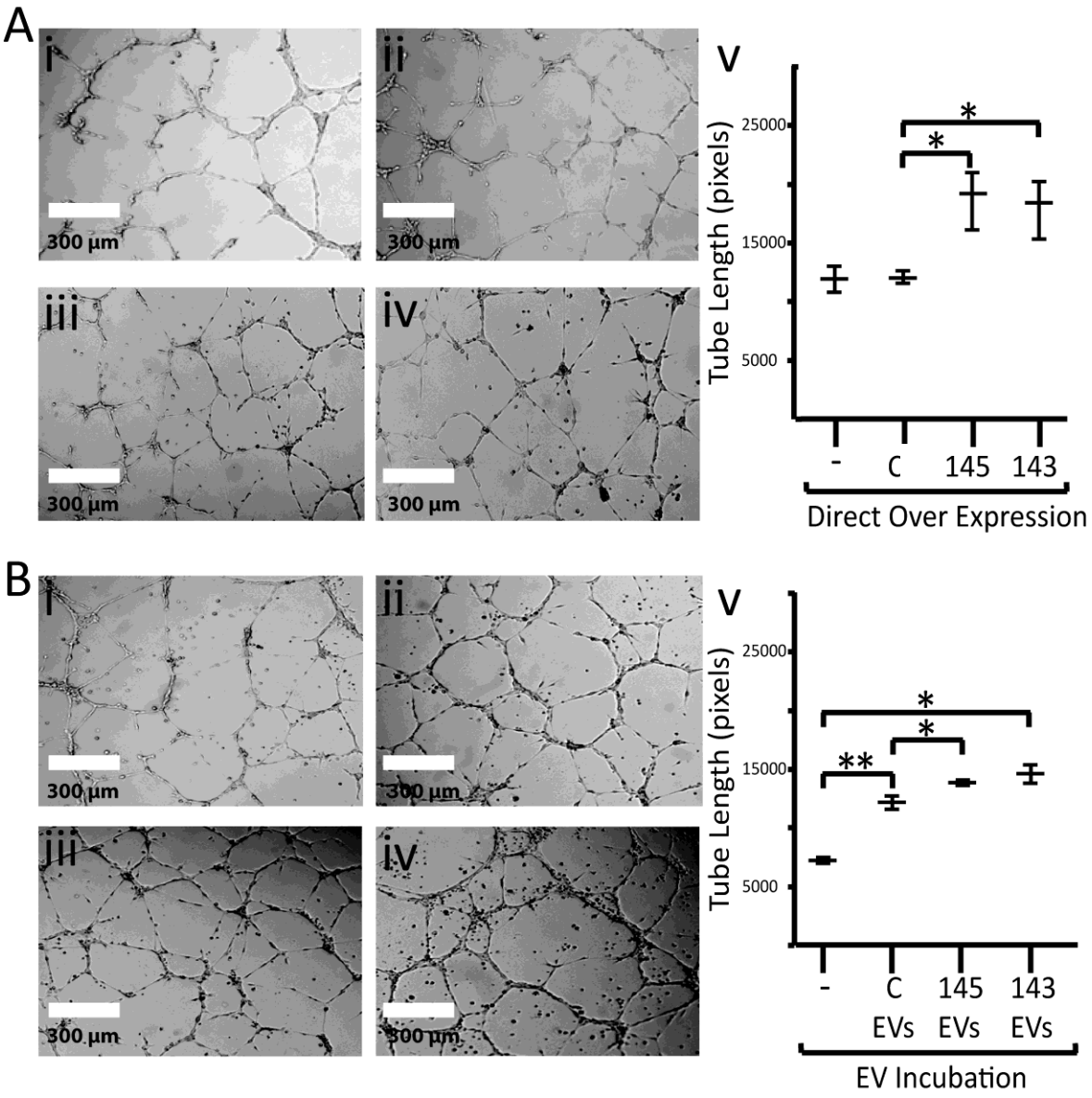

* = p-value < 0.05
** = p-value < 0.01

Figure 3.7 Impact of miR-143 and miR-145 on tube formation. A) Tube formation photos of HMEC-1 cells at 10x magnification with i) no vector ii) control vector iii) miR-143-3p over-expression vector or iv) miR-145-5p over-expression vector v) graph of tube formation on HMEC-1 endothelial cells with no direct over expression (-) and direct over expression of miR-Scramble (C), miR-143 (143) and miR-145 (145) B) Tube formation photos of HMEC-1 cells at 10x magnification incubated with EVs from H1437 cells i) No extracellular vesicles, ii) miR-Scramble over-expressing extracellular vesicles iii) miR-143-3p over-expressing extracellular vesicles or iv) miR-145-5p over-expressing extracellular vesicles v) graph of tube formation for HMEC-1 cells incubated with no EVs (-), H1437 miR-Scramble overexpressing extracellular vesicles (C EVs), H1437 miR-143 overexpressing extracellular vesicles (143) and H1437 miR-145 overexpressing extracellular vesicles (145). Error bars represent standard deviation.

To determine if the EV-transferred miRNAs target CAMK1D in HMEC-1 cells, protein lysates from HMEC-1 cells were collected after incubation with EVs or with the negative control (incubation with no EVs). All HMEC-1 cells that received EVs containing miR-143-3p or miR-145-5p showed a decrease in CAMK1D protein by western blot (Figure 3.8A). The addition of miR-Scramble over-expressing EVs from H1437 cell lines caused a decrease in the cellular quantity of CAMK1D by 53% compared to the negative control (Figure 3.8A). A greater decrease was observed in HMEC-1 cells incubated with EVs over-expressing miR-145 or miR-143, showing a 79% and 83% decrease respectively compared to HMEC-1 cells receiving no EVs (Figure 3.8A).

To confirm that the observed increases in tube formation were at least in part caused by the presence of miR-145-5p or miR-143-3p, we examined the tube forming ability of HMEC-1 cells that directly over-expressed miR-145 and miR-143 (as opposed to being over-expressed via EVs). Figure 3.7A demonstrates that direct over-expression was capable of increasing tube formation by 36% and 34% for miR-145 and miR-143, respectively ($p<0.05$ for both). No changes in tube formation were noted in cells transfected with a miR-Scramble vector or in cells that were not exposed to infection. HMEC-1 cells over-expressing miR-143 and miR-145 had decreased CAMK1D protein levels (87% and 96%, respectively) compared to HMEC-1 cells over-expressing the miR-Scramble (Figure 3.7A,B).

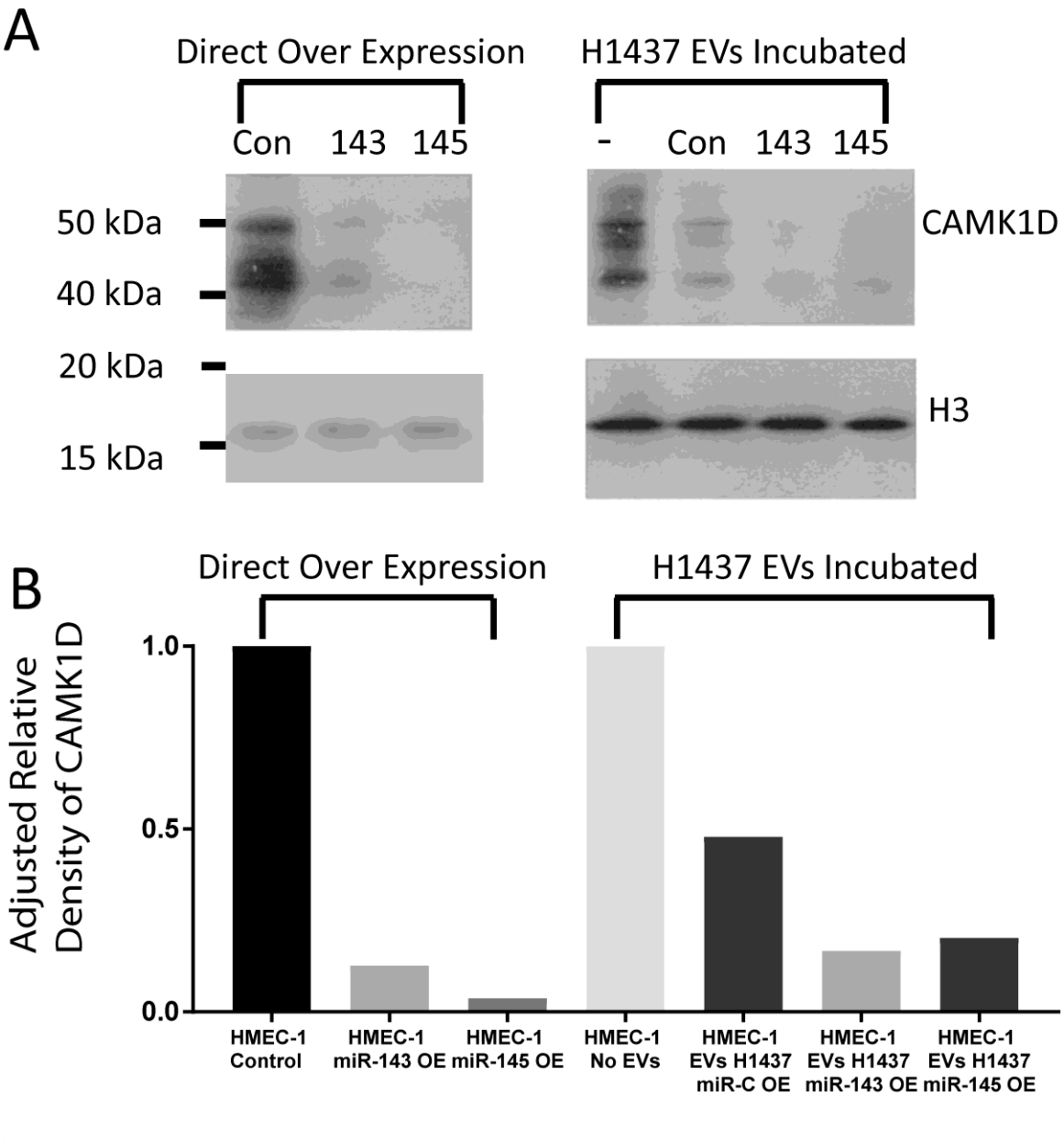

Figure 3.8 Analysis of CAMK1D targeting by miR-143 and miR-145. A) Western blot of CAMK1D and Histone 3 in HMEC-1 cells after direct over expression of miR-143, miR-145 and miR-Scramble within HMEC-1 cells and after incubation with EVs isolated from H1437 over expressing miR-143, miR-145, miR-Scramble and unmodified cell B) Densitometry analysis of CAMK1D western blot in Figure 3.8A.

We identified a set of miRNAs that are selectively packaged into EVs and released from LAC cell lines. Cross referencing with miRNA profiles obtained from serum collected from blood directly draining from the tumor suggests a biological role for miR-143-3p and miR-145-5p in lung tumorigenesis. These miRNAs were shown to be produced by LAC cells and packaged into EVs. Once packaged the EVs are capable of shuttling miRNA cargo to endothelial cells *in vitro* where EVs containing miR-143-3p and miR-145-5p down-regulate CAMK1D, promoting angiogenesis.

3.4 Discussion

In the present study, to determine early events in EV miRNA communication, we used early stage LAC cell lines and identified several miRNAs (miR-142-3p, miR-143-3p, miR-145-5p, miR-150-5p, miR-223-3p, miR-451a, miR-486-5p, and miR-605-5p) that are selectively packaged into EVs and released into the culture media. The function of tumor-derived EVs is dictated by EV cargo and it is now appreciated that EV cargo differs between cell types and disease state. Therefore, it is imperative to evaluate the function of EVs in LAC in order to understand their role in this disease.

Profiling of a panel of LAC cell line EVs revealed that eight miRNAs were frequently enriched within EVs and absent within the donor cells that gave rise to these EVs. These results suggest the enriched miRNA candidates are sorted and packaged efficiently into EVs, so much so that their intracellular detection in donor cells is difficult with standard molecular techniques. The mechanisms by which miRNAs are packaged into EVs are not well understood. Previous studies have proposed miRNA uptake into EVs occurs through specific miRNA sequences and hydrophobic modifications such as methylation[91,243]. These mechanisms may explain some

miRNA selection, but they do not fully account for the specific cohort of candidate miRNAs that we observe here. For example, miR-451a (which we observe to be enriched in the EVs) also contains a CL (cellular) motif, which has been suggested to mediate exclusion from EVs[91]. Four of our miRNA candidates (miR-142-3p, miR-150-5p, miR-451a, and miR-486-5p) are found within EVs of many cell types including HEK 293T cells, breast cancer cells, and oral cancer cells[90,250]. These miRNAs are known tumor suppressors that alter activity of many genes involved in tumorigenesis including TGFβR1, MUC4, ARHGAP, and RAB14[251-254]. Selection of these miRNAs for export would then promote tumor growth by eliminating intracellular tumor suppressive activity of the miRNAs[251-254].

Our remaining miRNA candidates (miR-143-3p, miR-145-5p, miR-223-3p, and miR-605-5p) appear to be more specific to LAC. These miRNAs are generally considered tumor suppressive miRNAs in many cancer types. MiR-143-3p has been shown to target KRAS and IGF1R in colorectal cancer[255,256]. MiR-145-5p is also known to target IGF1R in colorectal cancer, as well as EGFR in LAC[256,257]. Over-expression of miR-223 in ovarian cancer cell lines reduces proliferation and colony formation, also by targeting of IGF1R[258]. MiR-605-5p has not been widely studied; however, it may function as a tumor suppressor given some indication that it can enhance transactivation of p53 by inhibiting MDM2 in lung and breast cancer cell lines[259].

There is limited information on the function of these candidate miRNAs in cells of the tumor microenvironment. Continued research into stromal function of EV miRNAs will allow for a greater understanding of tumor-stromal EV signaling in cancer. To the best of our knowledge, this is the first time miR-143-3p and miR-145-5p are reported as enriched within EVs released directly from LAC cells. MiR-143-3p and miR-145-5p are important tumor suppressors in many cancer types including lung, bladder, colon, and breast[260-263].

The data presented suggests the function of selective packaging and release of certain miRNAs is two-fold. The tumor cells selectively package tumor suppressive miRNAs within EVs to eliminate their function intracellularly and, in doing so, end up transporting miRNAs to endothelial cells (and possibly other stromal cells), which creates a more favorable tumor microenvironment.

Herein, we also demonstrated that miR-143-3p and miR-145-5p derived from LAC cell EVs can target the endothelial cell function of CAMK1D, a negative regulator of angiogenesis. Dimitrova *et al.* (2016) first showed that stromal expression of miR-143/miR-145 promotes neoangiogenesis by targeting CAMK1D[249]. They also reported that expression of miR-143/miR-145 occurs in a small population of endothelial cells, but not lung epithelial cells[249]. Our results show that miR-143-3p and miR-145-5p are in fact expressed by LAC cells; however, they are packaged into EVs so efficiently that expression of these miRNAs in the donor cells is typically not detected. Once in the EVs, miR-143/miR-145 can enter endothelial cells and down-regulate CAMK1D protein levels. The depletion of CAMK1D mediated by LAC EVs results in increased tube formation in the endothelial cells. These two results are compatible with Dimitrova *et al.* (2016) findings and may be happening in combination, which may further promote neoangiogenesis.

It is evident that miRNAs within EVs play a significant role in tumorigenesis. We report that 8 miRNAs are frequently enriched within EVs released from LAC cells. MiR-143-3p and miR-145-5p, two miRNAs enriched within LAC EVs, were also found enriched within serum obtained from blood draining directly from LAC tumor bearing lungs which suggests that LAC tumors secreted miR-143-3p and miR-145-5p into the serum. Both miRNAs have been previously implicated as mediators of neo-angiogenesis and our analysis shows that when

transferred through tumor derived EVs miR-143-3p and miR-145-5p promote tube formation through down-regulation of CAMK1D in endothelial cells. Our work highlights how certain miRNAs considered to be down-regulated (or absent) in LAC are efficiently selectively packaged and released from the tumour cells via EVs and play a role in altering the tumor microenvironment. Further research into the role of additional miRNAs that are selectively packaged into EVs is required to better understand cell-cell communication between the tumor and its microenvironment.

Chapter 4: Extracellular vesicle secretion of miR-142-3p from lung adenocarcinoma cells promote tumorigenesis through cell-cell communication with the stroma

4.1 Introduction

Extracellular communication between tumor cells and cells within the adjacent stroma is a strong promoter in creating a favorable tumor microenvironment[264]. EVs represent a group of secreted vesicles released by virtually all cell types, the EVs along with their content can be transferred from one cell to another, allowing cancer cells to communicate with cells in their microenvironment[156-159]. This type of communication has been shown to promote angiogenesis, and activate growth promoting properties of fibroblasts in several tumor types[3,156-159]. EV cargo is dependent on the type of donor cell and its disease state, with differences in miRNA profiles being used to differentiate between cancerous and non-cancerous cells[265-267]. Certain miRNAs are enriched in EVs compared to the donor cell from which they originated, indicating that a subset of miRNAs are selectively packaged into EVs[268]. In Chapter 3, I described how I was able to determine miRNAs enriched within LAC derived EVs. We found a number of miRNAs enriched within LAC EVs with miR-142-3p being the most abundant (Table 3.5). It was also found enriched in normal HPL1D lung cell line EVs, however not to the extent of LAC line enrichment. MiR-142-3p has previously been found to be enriched within oral cancer cell line EVs and when transferred to endothelial cells promoted angiogenesis through repression of TGFβR1[269]. MiR-142-3p has also been found enriched in the exosomes of patients during cardiac allograft rejection, which compromised the endothelial barrier and resulted in increased

vascular endothelial permeability[270]. These studies indicate the importance of EV associated miRNAs and that their contents can be used to signal adjacent cells into transforming and altering the microenvironment.

Within LAC tissue miR-142-3p is reported to be down regulated by 2-fold in 52% of LAC cases[271]. Re-expression of miR-142 has been shown to silence TGFβR1[251,272]. TGFβR1 increase in expression is associated with invasion and metastasis in tumor development[273]. In addition, overexpression of miR-142-3p was shown to induce apoptosis in select LAC cell lines[272]. Cellular elimination of miR-142-3p via EVs may be a mechanism to eliminate tumor suppressive miRNAs but may also be promoting tumorigenesis through cell-cell communication via EVs as we have previously shown in oral cancer[269]. Herein we examine the impact of LAC EV secreted miR-142-3p on both endothelial cells and fibroblasts and demonstrate the pro-tumorigenic influence on the tumor stroma.

4.2 Materials and Methods

4.2.1 Cell lines

Cell lines were obtained from ATCC, the LAC cell lines H1437 and H2073 were cultured in RPMI 1640 media with 10% FBS, according to the supplier's guidelines. HMEC-1 and 293T cells were cultured in DMEM media supplemented with 10% FBS.

4.2.2 Vectors

Over-expression (OE) of miR-142-3p was achieved using the lenti vector: miR-142 OE (HmiR02082-MR01), a miR-Scramble OE (miR-C) sequence was used as a control (CmiR0001-MR01). Virus was produced in 293T cells using the Lenti-Pac FIV Expression Packaging Kit

(FPK-LvTR, GeneCopoeia) according to the supplied protocol. Infected cells were selected using G418 at 200 μg/mL. TGFβR1 open reading frame (ORF) clone (TRCN0000488036) within a pLX_TRC317 vector as well as an empty vector control were purchased from Sigma Aldrich (hereafter TGFβR1 ORF and Empty ORF) and used for rescue experiments. ORF vectors were packaged in 293T cells using the packaging vectors VSVG and d8.91 using the transfection reagent TransIT-LT1. Cells were selected using puromycin over 4 days.

4.2.3 EV isolation

EVs were isolated as described previously [244]. Briefly, cells were seeded onto 10, 15 cm plates. 48 hours prior to reaching 90% confluency standard media was replaced with RPMI media, supplemented with 1% FBS depleted of bovine EVs by ultracentrifugation. Upon cells reaching 90% confluency EV containing media was removed. To remove non-EV debris, at 4°C EV containing media was centrifuged at 200g for 10 minutes, 2000g for 20 minutes and 10,000g for 60 minutes and then at 110,000g for 90 minutes to pellet EVs. The pellet was rinsed and re-suspended with PBS and then pelleted again at 110,000g for 90 minutes, in order to separate out possible impurities.

4.2.4 Quantitative PCR

RNA was extracted using the miRCURY RNA Isolation Kit (Exiqon) according to the manufacturer's protocol. RT-PCR was performed on 100ng of RNA using TaqMan miRNA reverse transcription kits and TaqMan Universal Master Mix II and MicroRNA assays (Life Technologies). All assays were performed according to the manufacturer's protocol in triplicate. U6 RNA was used as a reference gene when examining cellular miRNA, EV miRNA was normalized to input and cel-miR-39 spike-in (Qiagen) as there is yet no established endogenous controls for EVs.

4.2.5 Proliferation assay

H2073 and H1437 cell lines stably overexpressing miR-142 or miR-C were plated in 6 wells of five 96 well plates at a density of 1000 cells per well. Cell viability was measured over five days using Colorimetric thiazolyl blue tetrazolium bromide (Sigma-Aldrich) as described previously, with two outliers (highest and lowest) values from each treatment removed from analysis. Statistical significance was determined using a student T-test. A p-value cut off < 0.05 being used for significance.

4.2.6 Tube formation assay

Coated plates were created by the addition of 300µl of growth factor reduced Matrigel (Corning) to 12 well plates. HMEC-1 cells grown to 80% confluency were seeded at $2.0x10^5$ cells per well. EVs diluted in DMEM were collected from 1, 15cm plate of either miR-C or miR-142 OE H1437 cells and incubated with the HMEC-1 cells before seeding on Matrigel plates. No EV incubation controls that had the addition of unaltered media was also included. This was

performed in triplicate. To isolate the effect of miR-142-3p HMEC-1 cells with miR-142 or miR-C OE were also analyzed. After 16 hours the center of each well was imaged at 10x objective magnification using differential interference contrast Axiovert S1000 microscope. The ImageJ macro 'Angiogenesis Analyzer' (http://imagej.nih.gov) was used to quantify the average tube length.

4.2.7 Fibroblast activation

WI-38 and IMR90 cells were seeded in 96 well plates after reaching 30% confluence. EVs isolated from one 15cm plate of H1437 miR-C OE and H2073 miR-C OE cells and miR-142 OE H1437 and H2073 lines were added to the culture media per well. The media was replaced with EV supplemented media at 24 hours, and again at 48 hours after the first EV incubation. Protein and RNA were extracted 72 hours post initial EV incubation. To determine whether EV signaling activated the TGFβ signaling pathway, WI-38 and IMR90 cells were incubated in DMEM with 10% dFBS with a treatment consisting of either: No Treatment, H1437 miR-C EVs, H1437 miR-142 EVs, H2073 miR-C EVs, H2073 miR-142 EV or 10ng/mL TGFβ. Protein was harvested at 0 hour, 24 hours, 48 hours, 72 hours and 96 hours.

4.2.8 Wound healing assay

WI-38 and IMR90 cells were seeded in 12 well plates, upon reaching 80% confluency, a 1mm scratch from a P1000 pipette tip was made. The cells were rinsed with DMEM containing 10% FBS twice, and then the treatment was added. Treatments were conducted within DMEM with 10% dFBS and were: H1437 miR-C OE EVs, H1437 miR-142 OE EVs, H2073 miR-C OE EVs, H2073 miR-142 OE EVs, TGFβ 10ng/mL and no treatment. Experiment was conducted in triplicate and photos were taken at HR0, HR18, HR24 and H48. Analysis of wound healing assay was conducted on tScratch (https://github.com/cselab/TScratch.git)[274]. Statistical analysis of wound closure was conducted using a one-way ANOVA followed by post hoc analysis.

4.2.9 Western blotting

RIPA buffer with 1:100 phosphatase inhibitor cocktail I & II (Sigma-Aldrich) and protease inhibitor (Thermo Fisher Scientific) was used to lyse EVs and cells. Protein was quantified using a Pierce BCA kit (Thermo Fisher Scientific). 10μg of protein was run on a NuPage 4-12% Bis-Tris Gels (Thermo Fisher Scientific) and then transferred to PVDF membranes (Millipore). Membranes were blocked in 5% BSA, 1x TBS, and 0.1% Tween-20 for 1 hour at room temperature. Primary antibodies 1:1000 anti-TGFβR1 (AF3025, R&D Systems), 1:1000 anti-PDGFRβ (SC-432, Santa Cruz), 1:2000 anti-Desmin, 1:1000 anti-αSMA (14968, Cell Signaling Tehcnology), 1:4000 anit-H3 (C1H2, Cell Signaling Technology), 1:1000 pSMAD2/3 (8828, Cell Signaling Technology) and 1:8000 anti-GAPDH (2118, Cell Signaling Technology) were applied for 16 hours at 4°C diluted in blocking buffer. Horseradish peroxides conjugated secondary antibodies 1:2000 anti-mouse (NXA931, GE Healthcare) or 1:2000 anti-rabbit (7074, Cell Signaling Technology) were applied for 1 hour at room temperature. Quantification was performed with normalization of TGFβR1 to GAPDH using the ImageJ 'gel analysis' function.

4.3 Results

4.3.1 MiR-142-3p is transferred from LAC cells to endothelial cells and fibroblasts through EVs

Previously we have demonstrated that miR-142-3p is selectively enriched by > 4-fold in the EVs derived from LAC cells compared to the donor cell[275]. Three of the five cell lines analyzed (H1437, H2073, H2228) did not have detectable quantities of miR-142-3p in the cellular RNA fraction, indicating a very efficient EV packaging mechanism. MiR-142-3p was

detectable in the remaining intracellular fraction of cell lines (H1395 and H2347), but still showed a >18-fold increase in the corresponding EVs[275]. In order to generate EVs that secrete miR-142-3p at an elevated level, we constructed LAC cell lines over expressing either a miRNA scramble (miR-C) or miR-142. The miR-142 over-expressing cell lines showed an increase in miR-142-3p within the EVs by 3.4-fold in H1437 cells and a 5.1-fold in H2073 cells compared to miR-C paired lines. Levels of miR-142-3p within miR-C cell line EVs showed no significant changes compared to non-transformed cell lines. Thus, we created LAC EVs with an enrichment of miR-142-3p within them.

I sought to determine if overexpression of miR-142 within LAC cell lines affected proliferation. Considering its previously established role in targeting of TGFβR1 in LAC, we expected to see a decrease in proliferation due to silencing of TGFβR1[251]. Instead, we found that miR-142 when overexpressed did not affect proliferation of H1437 or H2073 cell lines (Figure 4.1). This is a little surprising as A549, H23 and H838 cell lines have previously been shown to have decreased proliferation when miR-142 is overexpressed[272,276]. However, the effect of miR-142-3p expression has yet to be determined in both of the cell lines used here (H1437 and H2073). This difference may be due to the variable origins and mutational status of each of these lines compared to the early LAC cell lines we utilize (Table 3.2 and Table 4.1).

Cell Line	Stage	Mutations and Features
A549	-	Hypotriploid in 24% of cells, der(6)t(1;6) (q11;q27); ?del(6) (p23); del(11) (q21), del(2) (q11), M4 and M5, Y chromosome lost in 40% of cells, produce lecithin, KRAS mutation c.34G>A, CDKN2A mutation c.1_471del471
H23	-	Derived prior to therapy, TP53 mutation c.738G>C, KRAS mutation c.34G>T
H838	3B	80 pack years, CDKN2A mutation c.1_471del471, TP53 mutation c.184G>T

Table 4.1 Tumour stage of LAC cell lines, mutation profiles and characteristics of A549, H23 and H838 according to ATCC[248]

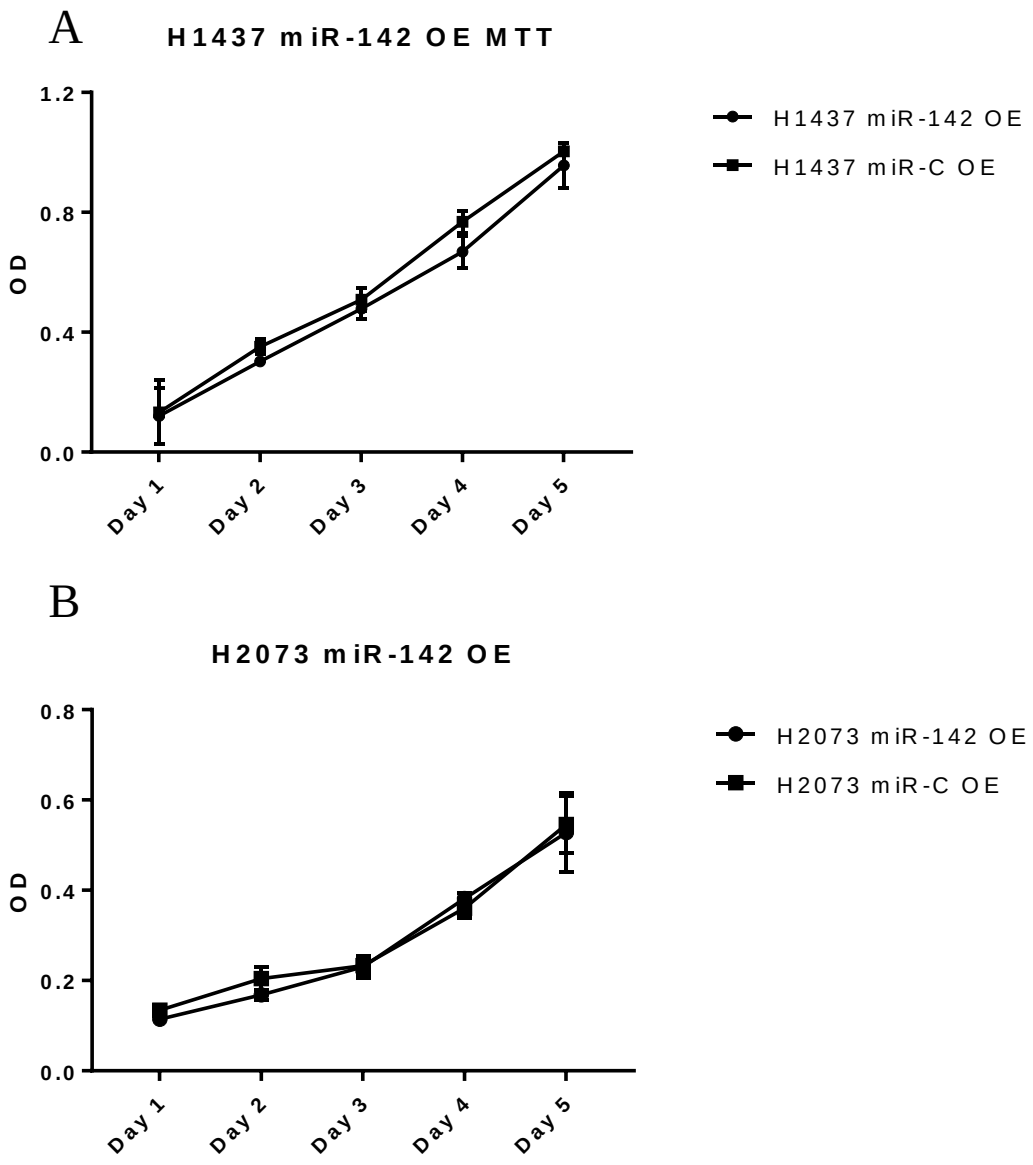

Figure 4.1 MTT of direct overexpression of miR-C or miR-142 in A) H1437 B) H2073. Error bars represent standard deviation.

To determine if miR-142-3p in EVs from LAC cells can communicate with cells in the tumor microenvironment we asked whether miR-142-3p can be transferred to endothelial and/or fibroblast cells. EVs from LAC cell lines H1437 and H2073 over-expressing miR-C or miR-142 were collected and incubated with either endothelial HMEC-1 cells or lung fibroblast WI-38 and IMR90 cells. After 48 hours of incubation the cells were washed to eliminate remaining EVs. Intracellular RNA was collected, and miR-142-3p was quantified by qRT-PCR. HMEC-1 cells receiving miR-C EVs (expressing endogenous miR-142-3p levels within the EVs) had a 2.4 (H1437) and 2.3 (H2073) fold greater level of intracellular miR-142-3p then those receiving none (Figure 4.2). We observed a 2.5 and a 2.0-fold increase in intracellular miR-142-3p levels in WI-38 cells and a 1.9 and 2.1fold increase in IMR90 cells incubated with miR-C H1437 EVs and H2073 EVs respectively (which contain endogenous levels of miR-142-3p in their EVs) (Figure 4.2). To ensure that this effect was caused by miRNA transfer and not an induction of local miRNA expression by way of some other EV contained factor, this experiment was also performed using EVs collected from miR-142 OE H1437 and H2073 cells. The addition of miR-142 OE EVs increased concentration of miR-142-3p in HMEC-1 receiver cells by 8.7 and 9.5-fold for EVs from H1437 and H2073 respectively (Figure 4.2). While an 11.1-fold and an 8.4-fold increase in intracellular miR-142-3p levels was seen in WI-38 cells and 7.9-fold and 8.2-fold in IMR90 cells when incubated with miR-142 OE EVs from H1437 and H2073 cell lines respectively compared to WI-38 and IMR90 cells receiving no EVs. Indicating that both H1437 and H2073 EVs enter HMEC-1 cells, WI-38 and IMR90 cells and increase intracellular miRNAs, which we have previously demonstrated[275].

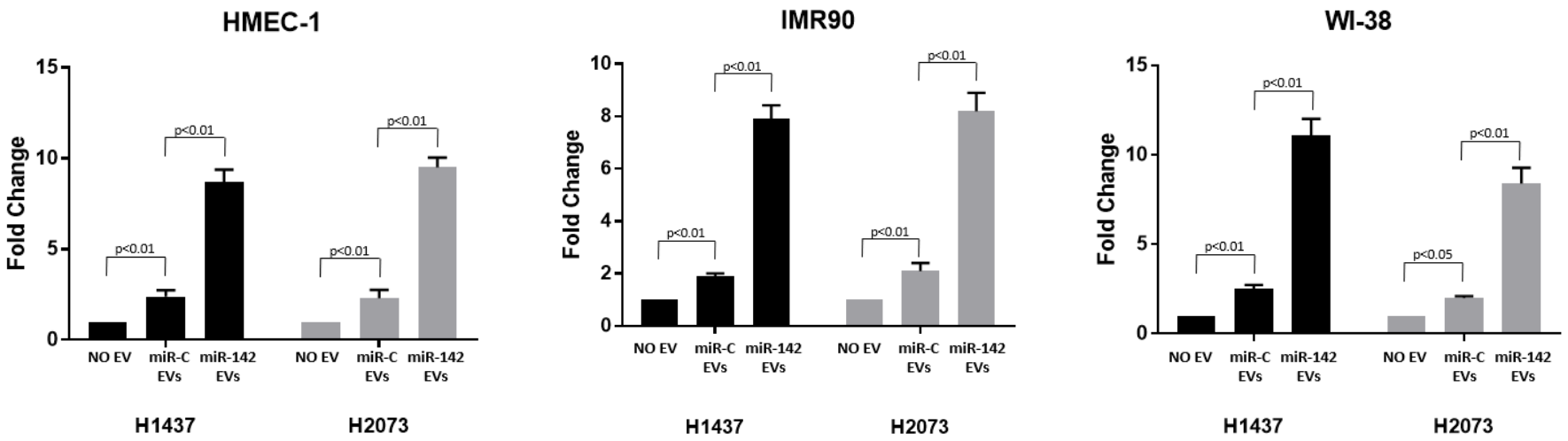

Figure 4.2 Lung adenocarcinoma cell extracellular vesicle miRNAs are taken up by HMEC-1, WI-38 and IMR90 cells. Intracellular fold change analysis of miR-142-3p in HMEC-1, WI-38 and IMR90 cells run in triplicate incubated with extracellular vesicles from H1437 and H2073 cells over expressing miR-142 and miR-C, compared to HMEC-1 cells receiving no extracellular vesicle incubation. Error bars represent standard error mean.

4.3.2 Secreted miR-142-3p targets TGFβR1 in HMEC-1 cells

TGFβR1 has been shown to be a target of miR-142-3p in LAC cells and has also been shown to be a target in HMEC-1 endothelial cells[251,277]. To determine if the TGFβR1 pathway is involved in attenuation of angiogenesis via LAC secreted miR-142-3p, EVs from H1437 cells or H2073 cells that OE miR-142 or miR-C were incubated with HMEC-1 cells. 48 hours after EV incubation, protein was extracted from the cells and compared to HMEC-1 cells grown without the addition of EVs. There was an observed decrease of TGFβR1 in HMEC-1 cells receiving miR-C EVs (containing endogenous levels of miR-142) from H1437 cells of 66% and a decrease of 37% with miR-C EVs from H2073 cells (Figure 4.3). The decrease in TGFβR1 was enhanced when HMEC-1 cells were incubated with miR-142 OE EVs from donor cells. A decrease of 83% in TGFβR1 was observed when HMEC-1 cells were incubated with H1437 miR-142 OE EVs and 55% when incubated with H2073 miR-142 OE EVs compared to HMEC-1 cells incubated with no EVs (Figure 4.3). To confirm that TGFβR1 was inhibited by miR-142-3p, HMEC-1 cells were directly infected with stable OE of miR-142 and a 91% decrease in TGFβR1 was observed (Figure 4.3).

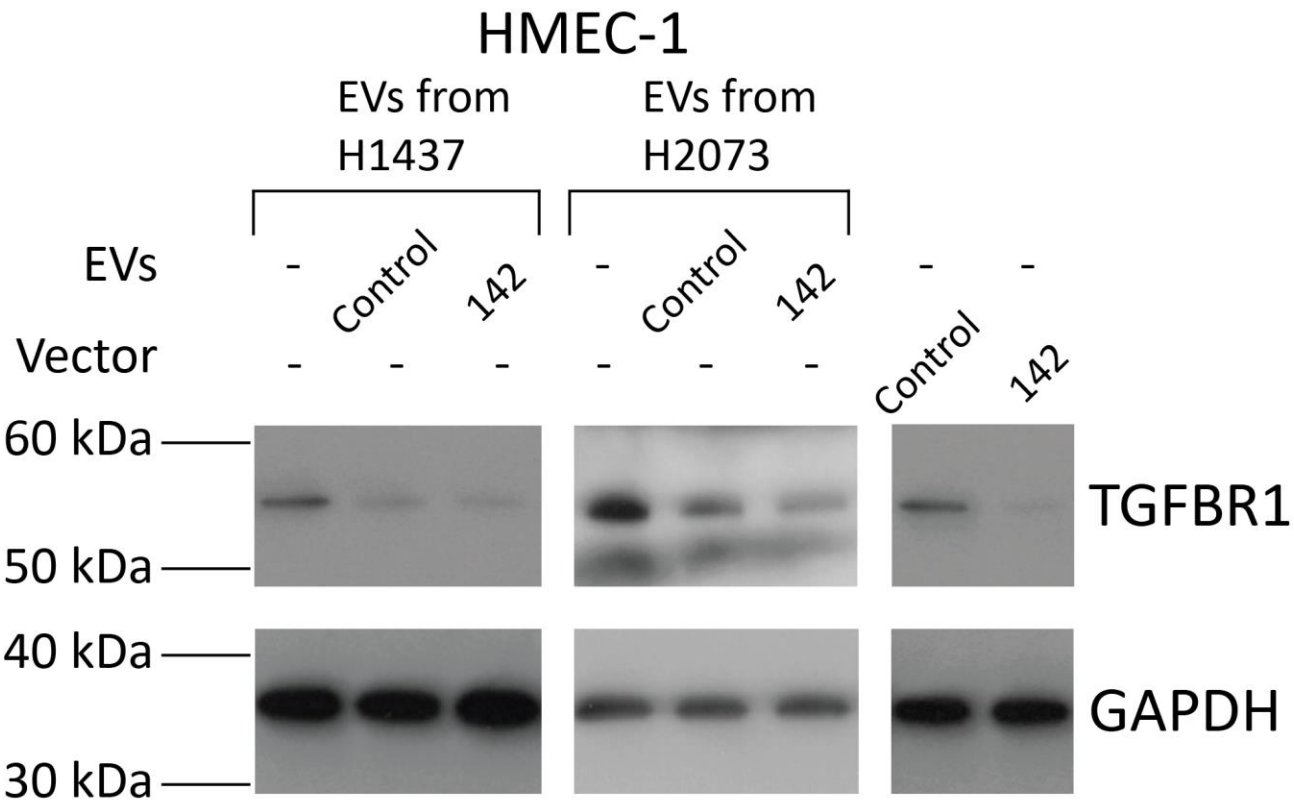

Figure 4.3 Analysis of TGFβR1 protein expression by western blot in HMEC-1 cells after direct over expression of miR-142 and miR-C within HMEC-1 cells and after incubation with EVs isolated from H1437 and H2073 over expressing miR-142, miR-C and untreated cell.

To determine if LAC secreted miR-142-3p can promote angiogenesis we performed a tube formation assay on HMEC1 endothelial cells. Endothelial cells were in three treatment groups, those that did not receive EVs, those receiving EVs from miR-C cells (containing endogenous levels of miR-142-3p) and those receiving EVs from miR-142 OE cells (resulting in an increase of miR-142-3p in the EVs). This was performed with EVs derived from both H1437 and H2073 cells. All treatments were capable of forming tubes (Figure 4.4 A-F, I). The addition of miR-C EVs increased tube formation by 9% ($p<0.05$, H1437) and 23% ($p<0.05$, H0273). The addition of miR-142-3p OE EVs increased tube formation by 37%, ($p<0.05$ H1437) and 40% ($p<0.05$ H2073) when compared to the HMEC-1 cells with no EVs added. To confirm alterations in tube formation were a result of miR-142-3p, the tube formation assays were repeated with direct OE of miR-142 (Figure 4.4 G-I). This caused an increase in tube formation by 40% ($p<0.05$) compared to HMEC-1 cells with miR-C OE.

To address the possibility that the interaction between miR-142-3p and TGFβR1 is incidental to the finding of an alteration in tube formation we performed a phenotypic rescue experiment in HMEC-1 cells. HMEC-1 cells were infected with a TGFβR1 ORF clone, an open reading frame (ORF) is a construct expressing the mRNA of the target gene, in this case TGFβR1 that lacks the binding site for miR-142-3p and becomes insensitive to inhibition from miR-142-3p (Figure 4.5 A). This experiment showed that tube formation was decreased upon OE of TGFβR1 even with the addition of miR-142 OE EVs, from H1437 or H2073. This caused a decrease in tube formation of 34 and 35% respectively (Figure 4.5 B-E).

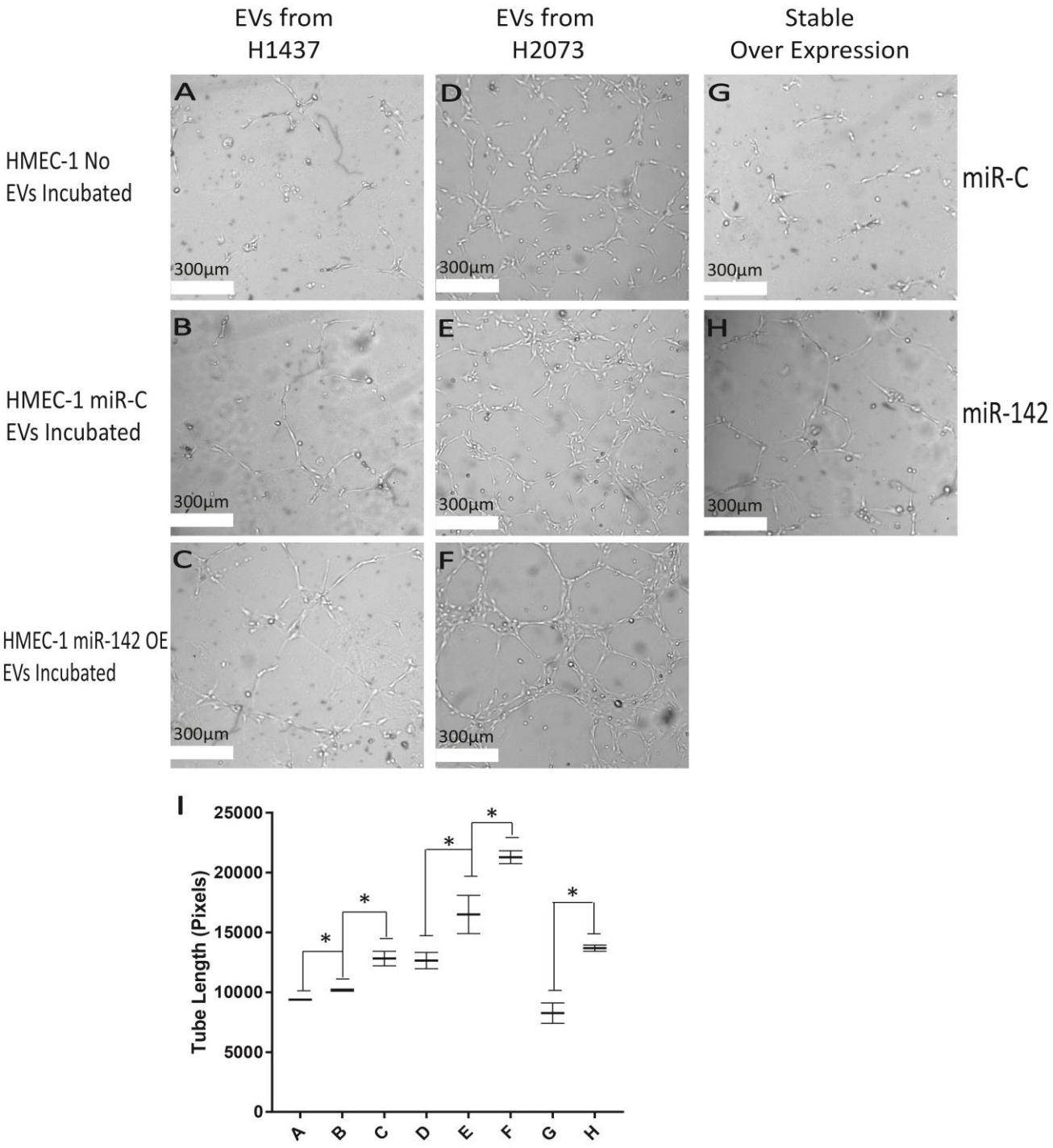

Figure 4.4 Tube formation assay of HMEC-1 cells run in triplicate A) no extracellular vesicle incubation B) incubated with H1437 miR-C extracellular vesicles C) incubated with H1437 miR-142 EVs D) no extracellular vesicle incubation E) incubated with H2073 miR-C extracellular vesicles F) incubated with H2073 miR-142 extracellular vesicles G) direct overexpression of miR-C H) direct overexpression of miR-142 I) quantification of tube formation assays. Error bars represent standard deviation.

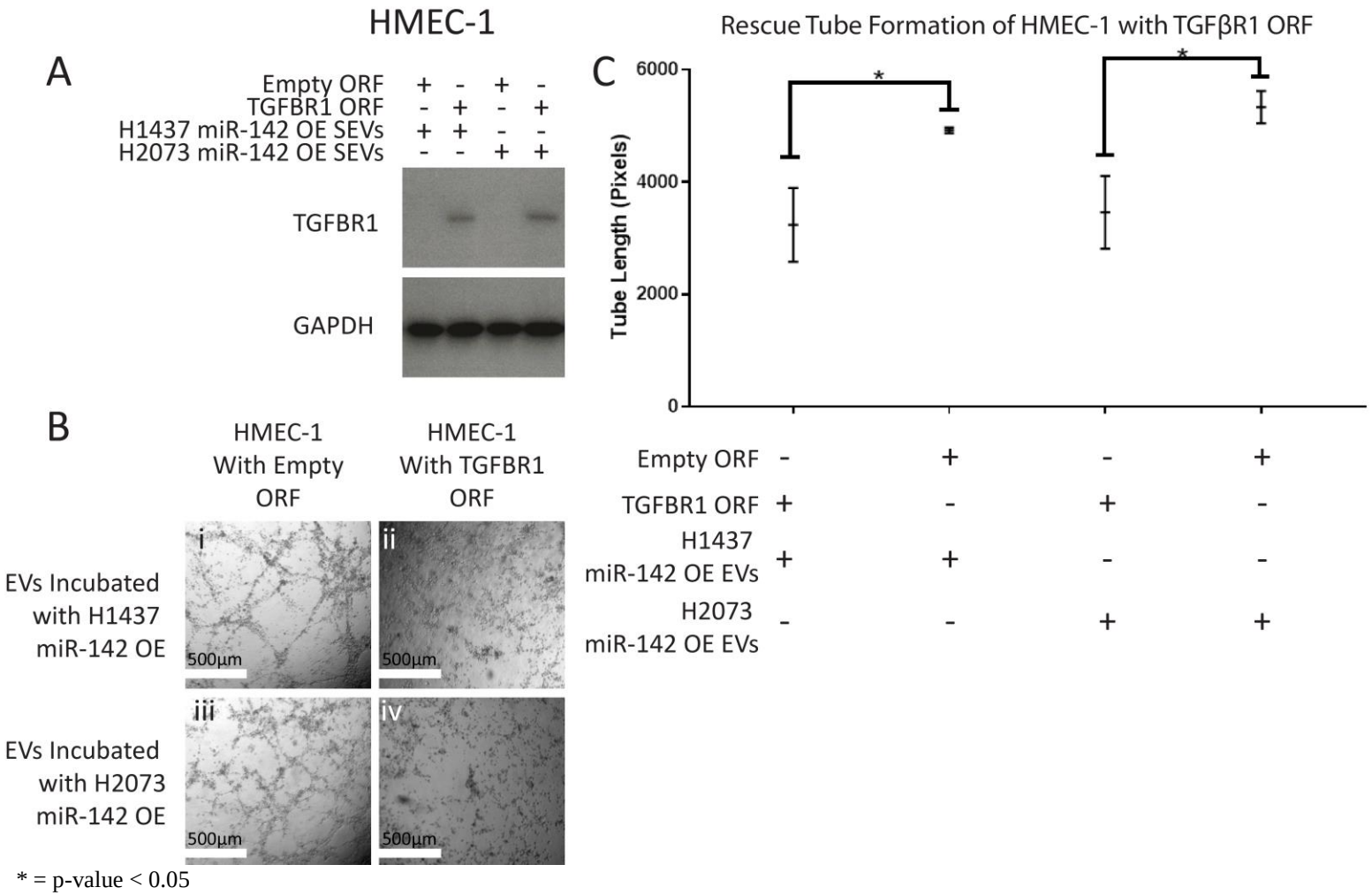

* = p-value < 0.05

Figure 4.5 Rescue of HMEC-1 cells using TGFβR1 ORF A) Western blot of TGFβR1 and GAPDH in HMEC-1 cells with either a control ORF or TGFβR1 ORF incubated with miR-142 OE extracellular vesicles from H1437 or H2073 cell lines B i-iv)) tube formation images of TGFβR1 ORF rescue in HMEC-1 C) quantification of rescue tube formation (B i-iv). Error bars represent standard deviation.

4.3.3 MiR-142-3p containing EVs promote CAF phenotype

Fibroblasts are the most abundant tumour microenvironment cell type in solid tumours, and mainly reside in a CAF state due to reprogramming by the adjacent tumour[278]. To determine if secreted miR-142-3p also had an impact on lung fibroblast cells, we incubated WI-38 lung fibroblast cells with miR-C and miR-142 OE EVs for 72 hours from H1437 and H2073 cells. Protein was extracted and western blots were performed for known CAF markers α-SMA, and PDGFR-β (Figure 4.6A), which are positively correlated with fibroblast activation and CAF transformation[279]. An increase in the cytoskeleton protein α-SMA and the growth factor receptor PDGFR-β were observed. In contrast to endothelial cells no significant changes were observed for the protein TGFβR1 in fibroblast cells upon addition of the LAC EVs and subsequent increase in miR-142-3p (Figure 4.6B). We next aimed to determine whether the CAF phenotype as seen by an increase in CAF markers, was caused by an increase in TGFβ signaling, a common pathway for CAF phenotype activation[280]. To investigation activation of TGFβ signaling we examined the levels of phosphorylation (p) on the proteins SMAD Family Member 2 & 3 (SMAD2/3) (Figure 4.7). When TGFβ signaling is activated both SMAD 2 and 3 are phosphorylated on serine residues and act as transducers for TGFβ signaling. These proteins associate with SMAD4 which, causes translocation to the nucleus where it binds to promoters and recruits proteins in other areas to act as repressors[281]. We saw typical induction of CAF markers PDGFR-β and αSMA in both WI-38 and IMR90 cells when treated with EVs and TGFβ (Figure 4.7). WI-38 and IMR90 cells that were treated with TGFβ showed increased pSMAD2/3 which, indicates signaling by TGFβ (Figure 4.7). We did not see SMAD2/3 phosphorylation in WI-38 and IMR90 cells incubated with any EV treatment, indicating the mechanism by which lung fibroblast cells are promoted to the CAF phenotype is independent of TGFβ signaling.

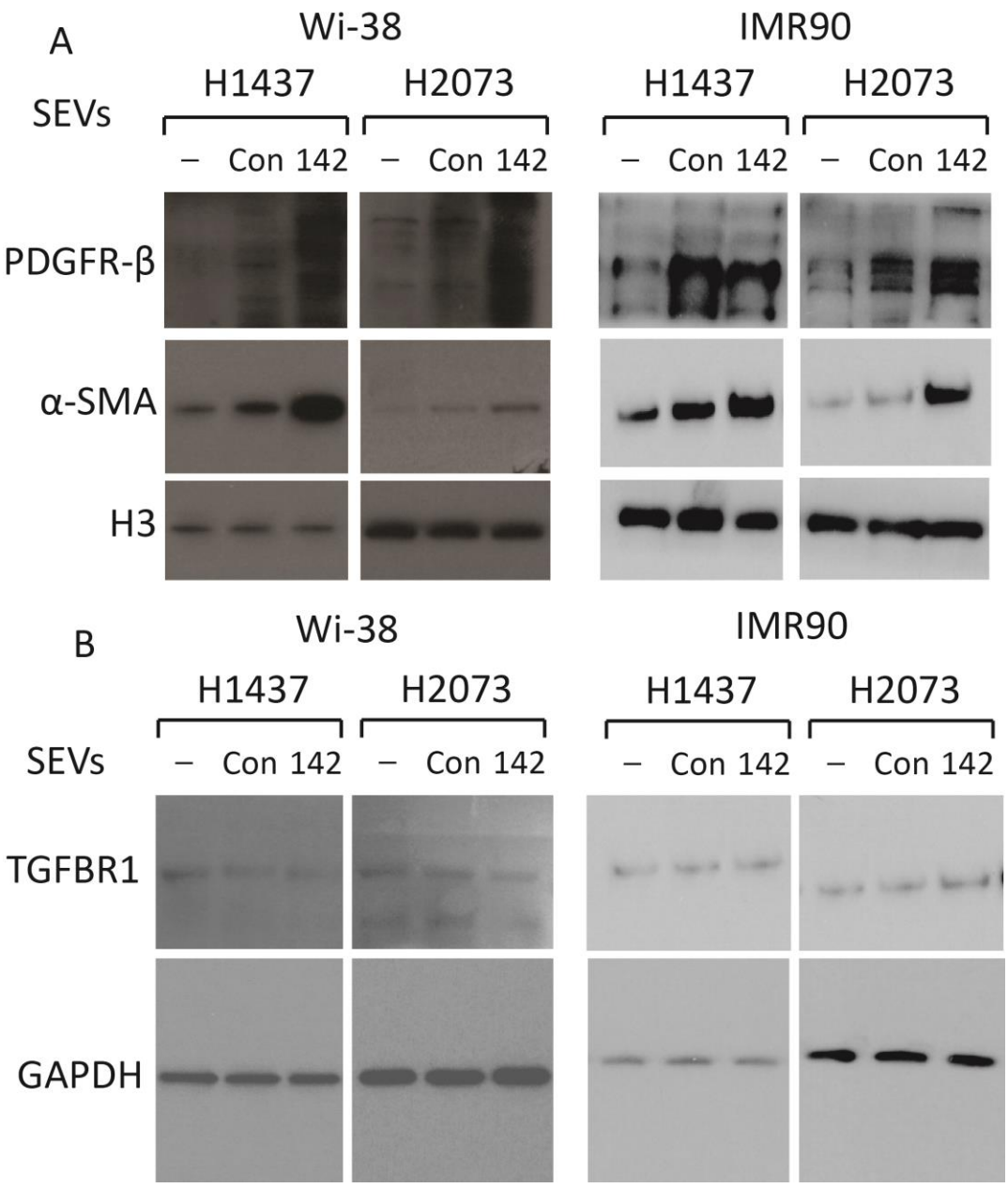

Figure 4.6 Western blot analysis of WI-38 and IMR90 cells incubated with EVs from H1437 and H2073 cell lines A) Western blot of PDGF-β, α-SMA and H3 in WI-38 and IMR90 after EV incubation B) Western blot of TGFβ and GAPDH in WI-38 and IMR90 cells after EV incubation

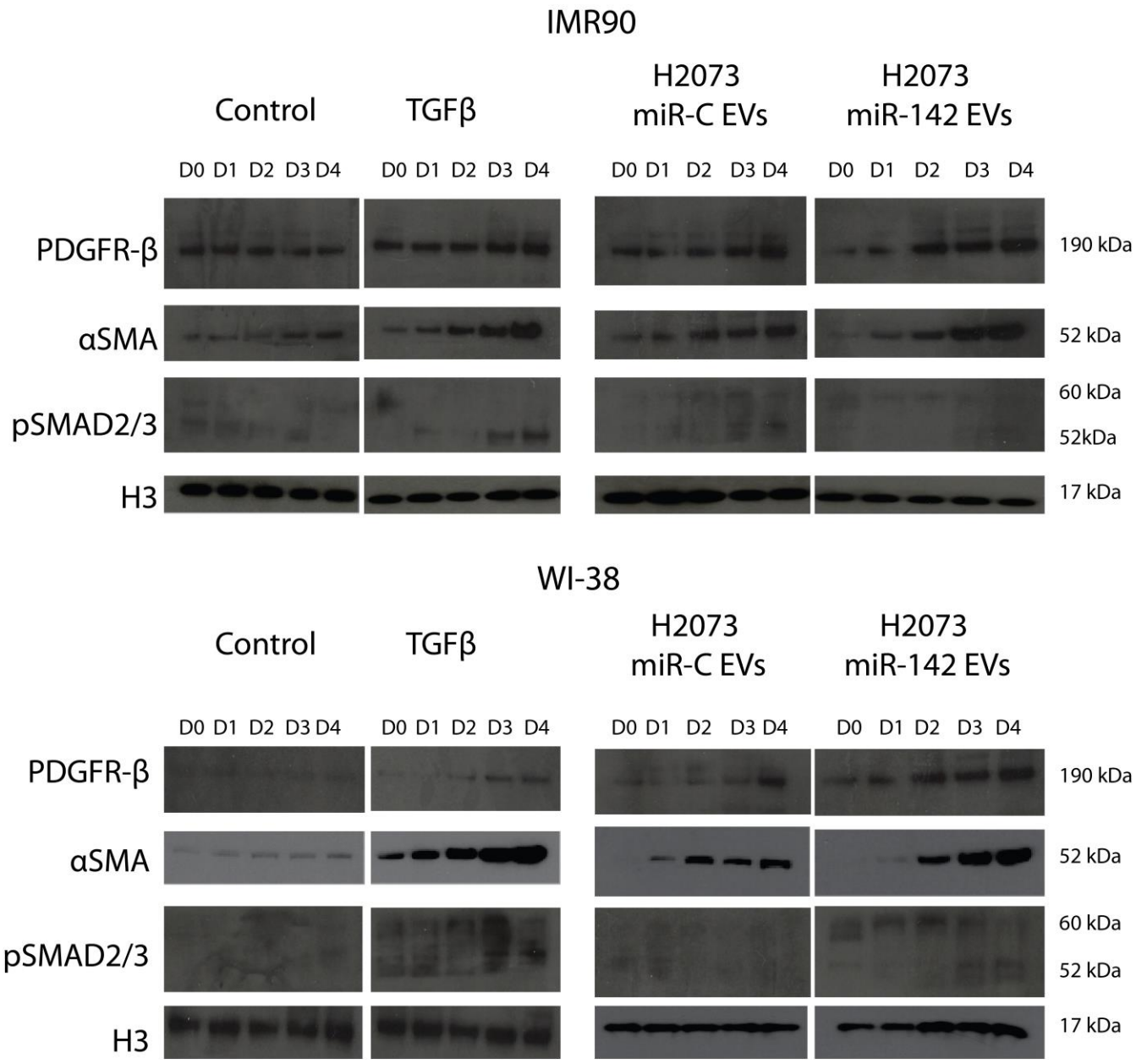

Figure 4.7 Western blot of WI-38 and IMR90 cells incubated with EVs or TGFβ for PDGFR-β, αSMA, pSMAD2/3 and H3

4.3.4 Secreted miR-142-3p promotes cancer associated fibroblast transformation

The results above suggest that EVs containing enriched miR-142-3p contributes to fibroblast activation through a pathway independent of TGFβ. This is expected as a large decrease in TGFβR1 would be expected to inhibit CAF formation as TGFβ signaling is a known activator of the CAF phenotype[282,283].

We next sought to determine whether the miR-142-3p containing EVs were able to promote migration of fibroblast cells, another characteristic of the CAF phenotype. Using a scratch assay, a scratch 1mm in diameter was made in a 24 well plate using a p1000 pipette tip, and either EVs, TFGβ or no treatment was incubated with the cells for 48 hours. WI-38 and IMR90 cells that were incubated with EVs showed higher wound closure ability compared to cells that received no treatment (Figure 4.8 and Figure 4.9). MiR-142 EVs showed significantly higher wound healing ability than miR-C EVs in WI-38 cells at 18 hours for both H1437 and H2073 EVs ($p<0.05$). At 24 hours H1437 miR-142 OE EVs remained significantly better at wound healing than H1437 miR-C EVs (~60% wound closure and ~40% wound closure respectively $p<0.05$), but H2073 miR-142 OE EVs no longer remained significantly better at wound healing compared to miR-C EVs. At 48 hours both H1437 and H2073 miR-142 OE EVs were no longer significantly different from miR-C EVs (Figure 4.8 and Figure 4.9). In IMR90 cells H2073 miR-142 OE EVs were significantly better at wound healing than H2073 miR-C EVs starting at 18 hours (H2073 18 hours: miR-142 OE EVs 30% wound closure, miR-C EVs 24% wound closure, p-value<0.05, 24 hours: miR-142 OE EVs ~48% wound closure miR-C EVs 41% wound closure, p-value<0.05, 48 hours: miR-142 OE EVs 88% wound closure, miR-C EVs 75% wound closure, p-value<0.05). H1437 miR-142 OE EVs however, were only significantly better at wound healing than H1437 miR-C EVs at 48 hours (18 hours: miR-142 OE

EVs 28% wound closure miR-C EVs 24% wound closure, p-value>0.50, 24 hours: miR-142 OE EVs 45% wound closure miR-C EVs 39% wound closure, p-value>0.50). At 48 hours H1437 miR-142 OE EVs had 85% wound closure while miR-C EVs had 75% wound closure (p-value>0.05), this could suggest that H1437 EVs are not as strong inducers of IMR90 migration, or that miR-142-3p within H1437 EVs is not an important early inducer of migration in IMR90 cells and that miR-142-3p is acting secondary to another inducer until 48 hours (Figure 4.8 and Figure 4.9). For both WI-38 and IMR90 cells, miR-142 OE EVs showed significantly higher wound closure compared to standard TGFβ treatment at all time points (p-values>0.05) (Figure 4.8 and Figure 4.9). This suggests that the EVs that have a higher enrichment of miR-142 from the LAC lines are better able to promote fibroblast migration compared to TGFβ alone. While miR-142 OE EVs were strong inducers of fibroblast migration, miR-C EVs showed higher variability in response. In IMR90 cells, H2073 and H1437 miR-C EVs had a significantly higher wound closure than TGFβ treatment at only 18 hours (24%, 24% and 16% wound closure respectively, p-value<0.001). At longer time points (24 and 48 hours), these miR-C EVs became non-significant. In WI-38 cells, H1437 miR-C EVs had a significant difference at only 18 hours compared to TGFβ (26% vs 23% wound closure respectively p-value<0.05) however, in H2073 miR-C EVs a significant difference was seen only at 48 hours compared to TGFβ treatment (100% vs 60% wound closure, p-value <0.001). These results suggest that miR-C EVs, which contains endogenous levels of miRNAs within their EVs, are still strong inducers of fibroblast migration and are comparable to a known strong inducer of the CAF phenotype TGFβ. Together, these results demonstrate the ability for LAC derived EVs to promote the wound healing ability of CAFs, and that LAC derived EVs containing enrichment of miR-142-3p are regulators of the CAF phenotype *in vitro*.

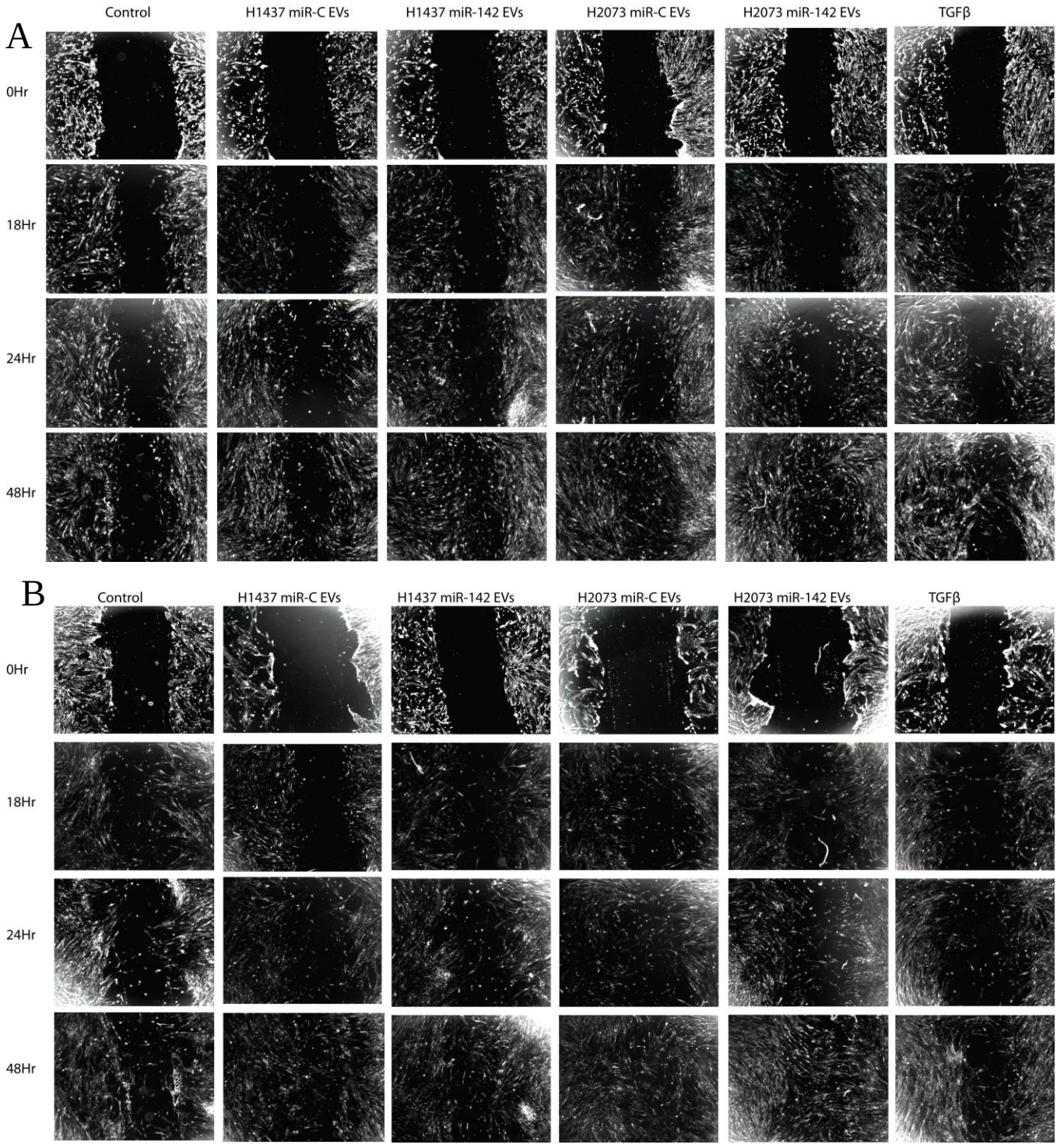

Figure 4.8 Wound healing assays of A) WI-38 and B) IMR90 with extracellular vesicle and TGFβ treatment

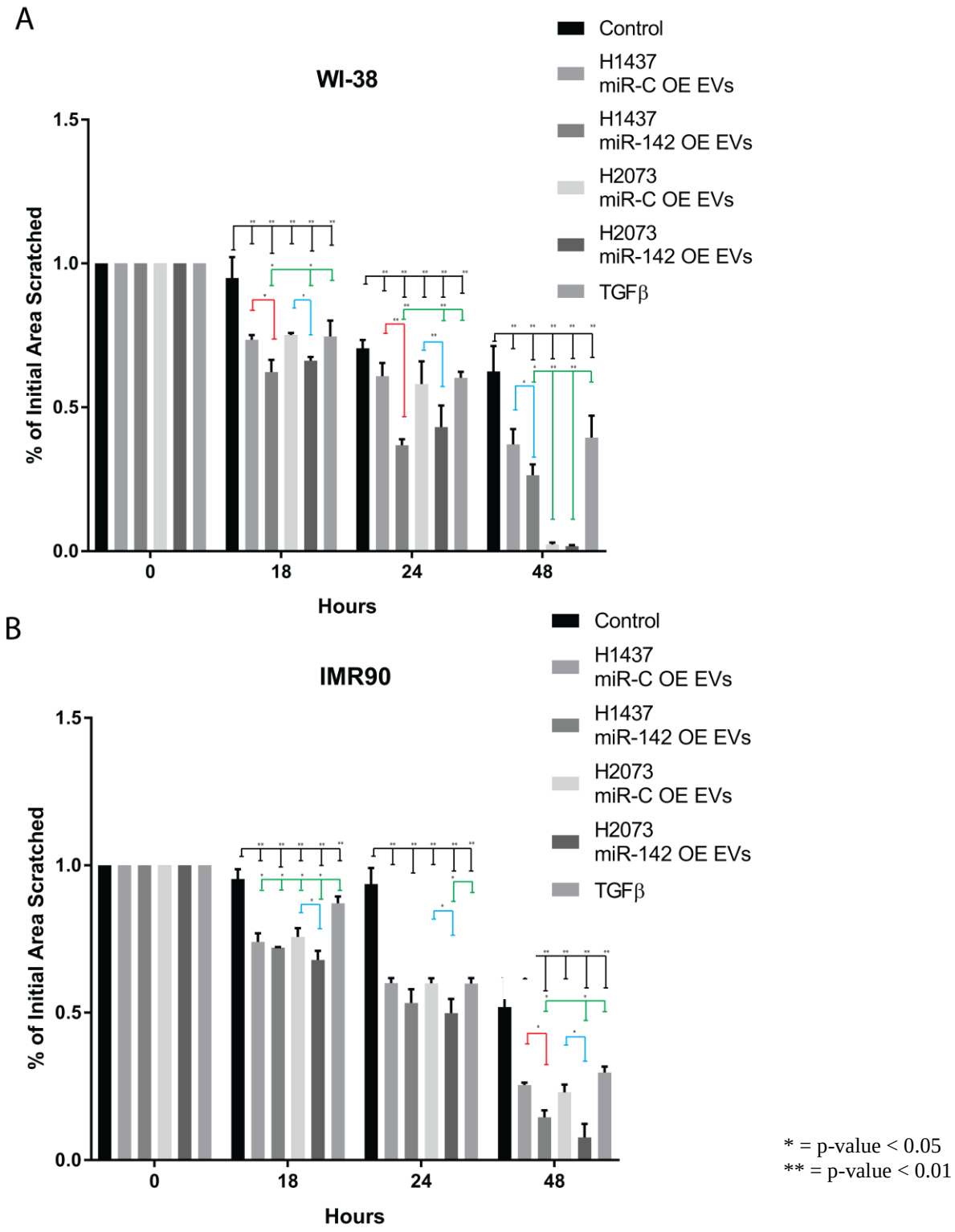

Figure 4.9 Graphs of wound healing assay for A) WI-38 and B) IMR90 cell lines. Error bars represent standard deviation.

4.4 Discussion

MiR-142-3p is highly deregulated in many tumor tissues including colon, breast, lung, osteosarcoma, pancreatic and cervical cancers where it shows decreased tumor tissue expression compared to normal tissue[284-287]. In these tumor types miR-142-3p has been classified as a tumor suppressor, with several known mRNA targets in addition to TGFβR1 such as WASL, TGAV, cytoskeleton-associated molecules, CD133, Lgr5, ABCG2 and Rac1, that can impact tumorigenesis[286-288]. miR-142-3p overexpression has also been shown to decrease HIF-1α expression in the tumor microenvironment leading to reduced invasion of cells and proliferation[285].

However, miR-142-3p has also been classified as an oncomiR in several tumor types such as renal cell carcinoma, T-cell acute lymphoblastic leukemia, nasopharyngeal carcinoma and gastric cancers where it is shown to be upregulated[289-292]. In renal cell carcinoma tissue miR-142-3p was found to be elevated compared to adjacent normal tissue and functioned as an oncogenic miRNA, as when miR-142-3p was inhibited proliferation and migration were reduced and apoptosis was promoted[291]. In nasopharyngeal cancer miR-142-3p inhibition led to a decrease in proliferation and cell cycle progression *in vitro* and suppressed tumor growth in mouse models[289]. In T-Cell acute lymphoblastic leukemia, miR-142-3p at high levels reduced cyclic adenosine monophosphate (cAMP) and protein kinase A (PKA) levels and relieved the inhibitory effect of PKA on proliferation[290]. Its oncogenic role is further supported by its tumor promoting activity in gastric cancer through targeting of FOXO4[292]. This suggests that miR-142-3p can serve as both tumor suppressor and oncogene depending on the cell type in which it is present.

In LAC miR-142-3p has been reported as a tumor suppressor and is frequently decreased in tumor compared to normal tissue[272]. TGFβR1 and HMGB1, two well-known oncogenes, are validated targets of miR-142-3p in NSCLC[251,272]. Inhibition of HMGB1 by miR-142-3p resulted in increased apoptosis and decreased growth, and upregulation of TGFβR1 has been shown to promote NSCLC tumorigenesis[272,273]. In our model system miR-142-3p was not detectable within the cellular fraction by qRT-PCR in three of the cell lines used (H1437, H2073, H2347), however enrichment of this miRNA was observed in the EVs derived from these lines indicating an efficient packaging mechanism for miR-142-3p into EVs. This efficient packaging may serve several functions, one to eliminate suppressive miRNAs from the tumor cells and two to serve as cell-cell communicators thereby creating a more favorable tumor microenvironment.

EVs are cell-cell communicators and are known to be released from tumors and enter the serum of the patient, which has led to the interest of circulating miRNAs as serum biomarkers. The majority of miRNAs in circulation are packaged within EVs which grants them stability and protects them from RNase digestion[114]. miR-142-3p has been predominantly found within 120 nm particles (associated with microvesicles and exosomes) and found at elevated levels in the serum of LAC patients[213]. This was associated with higher risk of relapse in patients with adjuvant therapy[213]. Furthermore, an increase of miR-142-3p in the plasma was associated with aggressive NSCLC disease[293]. Considering miR-142-3p is elevated within LAC cell line EVs and is found elevated in the serum of LAC and NSCLC patients suggests that miR-142-3p is secreted from tumors and enter the serum, to be used as communicators for distant signaling or local signaling.

MiRNAs within EVs are important regulators of tumor physiology, playing roles in immune regulation, modifying tumor microenvironment to facilitate tumor progression, angiogenesis, metastasis and chemotherapy resistance. Angiogenesis is essential for tumor development as establishing blood flow to the tumor is important for tumor growth and metastasis, for example in leukemia exosomal miR-92a was found to be transferred into endothelial cells and causing increased migration as well as tube formation[157]. In regulating the immune system, tumor derived EVs have been shown to both activate and suppress the immune response to tumors. In glioma, treatment of dendritic cells with tumor derived EVs were able to induce glioma-specific CD8(+) cytotoxic T-lymphocyte response against autologous glioma cells *in vitro*[294]. This data along with other publications demonstrate the tumor suppressive role of EVs, however anti-T Cell and anti-Natural Killer cell effects have been found as a result of tumor EV transfer[295,296]. Changes in monocyte differentiation were found to be caused by circulating microvesicles released from the tumor, which promoted the generation of myeloid suppressive cell subsets[297]. MiR-21 containing exosomes were shown to promote recurrence and distant metastasis in esophageal cancer through targeting and repression of programmed cell death 4 (PDCD4)[298]. Chemotherapy resistance has been found to be mediated by the transfer of miRNA EVs. In breast cancer the transfer of EVs from docetaxel resistant cells to non-resistant cells resulted in an increase of chemoresistance to docetaxel. Taken together EVs have been shown to be critical in promoting many hallmarks of cancer and their communication mechanism must be further studied to determine potential therapeutic interventions.

EVs are known as potent cell to cell communicators transferring mRNA, proteins and miRNAs. One important aspect of miRNA function is that one single miRNA can have many targets in a single cell[299]. This feature of miRNAs allows for it to have different targets

depending on the cell type the miRNA is present within. For example, in certain cell types a miRNA may act to target a tumor suppressor however, in another cell with minimal expression of the tumor suppressor gene that miRNA may effect different targets as the tumor suppressor gene is not abundant enough. Due to this unique feature we sought to investigate the function of miR-142-3p and its targets in endothelial cells and fibroblasts.

Currently the role of miR-142-3p is not well established within fibroblasts and endothelial cells. In endothelial cells we reported TGFβR1 is inhibited by miR-142-3p containing EVs. When TGFβR1 was inhibited, angiogenesis was promoted, showing miR-142-3p is a promoter of angiogenesis in endothelial cells *in vitro*. We report here that miR-142-3p containing EVs produced by early LAC cell lines promote the CAF phenotype, as the protein levels of α-SMA and PDGFR-β were elevated (Figure 4.6). Additionally, fibroblast migration, another phenotype associated with myofibroblasts, was significantly increased by incubation with miR-142 OE EVs. It was most evident compared to WI-38 and IMR90 cells incubated with TGFβ, where significant increases in migration were seen across all time points. This could indicate that miR-142-3p when elevated within EVs is a strong inducer of fibroblast migration and may be a driving force for the CAF phenotype. While miR-C EVs did not impact migration as much as miR-142 OE EVs, they still showed significant increases in migration compared to TGFβ incubation in IMR90 fibroblasts at early time points coming from both H1437 and H2073 cell lines (Figure 4.9). This may indicate that EVs from LAC cells are important initiators of fibroblast migration and can accelerate the early processes of cellular migration in IMR90 cells but are eclipsed by other factors. In WI-38 cells, we found that miR-C EVs from H2073 cells were strong inducers of migration but only after 48 hours. These results may indicate that specific fibroblast cell lines will respond differently to EVs and that the cell line of origin for the EVs is equally as important.

In our fibroblast cell lines, we found that TGFβR1 was not the target of miR-142-3p, and that the mechanism by which miR-142-3p induced the CAF phenotype was independent of TGFβ signaling as was shown by a lack of phospho-SMAD2/3. The role of SMAD2/3 in fibroblast activation was previously established, as constitutively active TGFβR1 mutant resulted

in increased phospho-SMAD2/3 and caused an increase in myofibroblast markers[300]. In addition, sustained phospho-SMAD2/3 has been found in fibroblasts of models for fibrosis, which again indicates the importance of transducing the TGFβ signal to induce myofibroblast changes[301]. We did not see activation of the TGFβ signaling mechanism after incubation with miR-142-3p containing EVs, thus the CAF phenotype is being promoted through a different mechanism. Altogether these results demonstrate that the function of miR-142-3p is dependent on the cell type it is within and that miR-142-3p packaging within LAC cell line EVs may be a method of promoting pro-tumorigenic effects to both endothelial and fibroblast cells.

With the role that miRNAs play within EVs and cancer it is logical that they may be an avenue for therapeutics. One proposed method of therapeutic intervention consists of EV removal from the circulatory system using an affinity plasmapheresis platform[302]. This removes tumor produced EVs from circulation, which is expected to reduce metastasis and tumor intercellular signaling. Clinical trials have currently begun by Aethlon Medical on this platform. Other methods of EV reduction such as by targeting EV production genes like neutral sphingomyelinase 2 (nSMase2) and RAB27B with siRNAs in breast cancer has suppressed invasion through the blood brain barrier[238]. We demonstrate that LAC EVs are important in the tumor microenvironment, so targeting of EV production either by removal or inhibition may be a useful mechanism to treat LAC.

In summary the role of miR-142-3p in LAC is complex (Figure 4.10). We provide evidence that EVs from LAC cell lines can enter endothelial and fibroblast cell lines to promote angiogenesis and the CAF phenotype. This is mediated by TGFβR1 targeting through miR-142-3p in endothelial cells leading to promotion of angiogenesis but is not mediated by TGFβR1 targeting in fibroblasts to cause features of the CAF phenotype. In conclusion miR-142-3p when secreted in LAC EVs can promote tumorigenesis through signaling to the surrounding stromal cells and may represent a mechanism to interrupt to reduce cancer development.

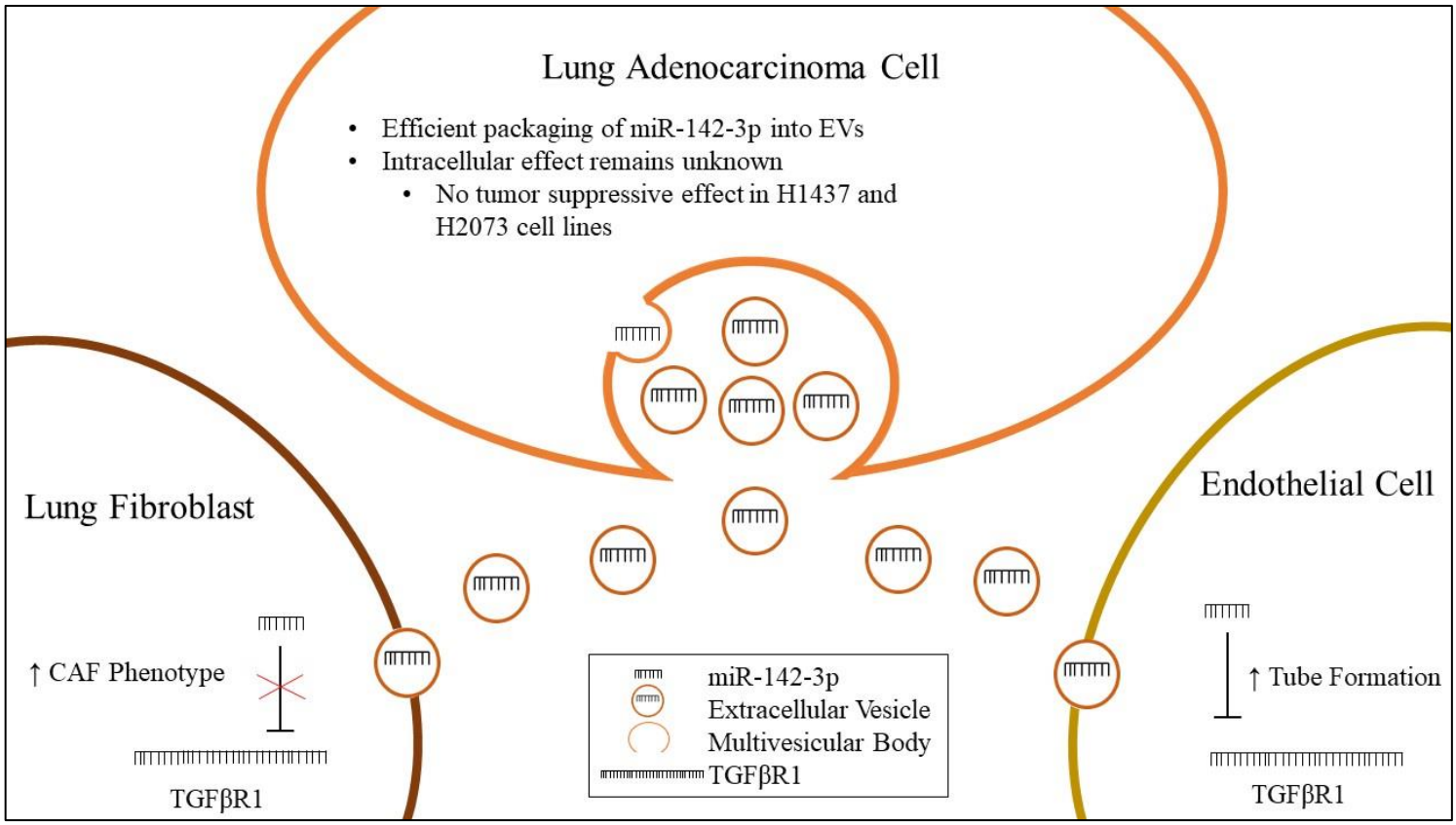

Figure 4.10 Summary of the role of miR-142-3p in LAC.

Chapter 5: Discussion and Conclusion

5.1 Discussing Rationale and Thesis Concepts

LAC is the most common subtype of lung cancer worldwide and its dismal 5-year survival rate of ~15% is generally caused by its late stage of diagnosis. The development of LAC is mainly caused by tobacco smoke and develops in the periphery of the lung where it can remain with no symptoms for a long period of time. By the time diagnostic procedures are conducted a metastasized tumor is generally found and there are few options for treatment. Determining a method for early detection of the disease and understanding early tumor development will allow for us to improve survival in LAC patients. Thus, an in-depth analysis of tumor released miRNAs may provide information on the function of EVs in LAC development and be a useful non-invasive biomarker for early disease detection. The work within this thesis presents serum miRNA profiling of LAC patients and high-risk non-cancer controls, in addition to the functional characterization of EV associated miR-143-3p, miR-145-5p and miR-142-3p in the surrounding tumor stroma.

5.1.1 Tumor released factors promote tumorigenesis

Tumor cells are potent communicators, sending growth factors, immunosuppressive factors, invasion promoters and metastasis promoters to surrounding and distant cells to promote their own growth. Many of these factors end up in the tumor microenvironment, which is a collection of non-tumor cells surrounding and integrated within the cancer. The factors can have a variety of functions. To facilitate angiogenesis within the tumor, cancer cells can secrete VEGF to stimulate endothelial cells to form new blood vessels[303]. In breast cancer the secretion of

exosomes containing TGF-β has been shown to cause immunosuppression by suppressing the proliferation of T cells[303-307]. In oral, breast, head and neck cancers, the secretion of the proteins MMP-9 to the tumor microenvironment is implicated in degrading extracellular matrices which contributes to invasion and metastasis[304-306,308]. MMP-9 functions by degrading type IV collagen, which is one of the initial steps in tumor invasion. Together tumor secreted factors play many roles in promoting tumorigenesis and facilitating the growth of the tumor.

5.1.2 Tumor released miRNAs contribute to cancer development

One type of tumor secreted factor are miRNAs. As previously discussed in the introduction, miRNAs are released from tumor cells mainly enclosed within EVs. These EVs can then be transferred to stromal cells locally or distant cells through the blood. The miRNAs can have a variety of actions once transferred including promoting angiogenesis, immunosuppression, promoting invasion and metastasis. miR-1245 has recently been implicated as an immunosuppressive miRNA due to its targeting of natural-killer group 2, member D (NKG2D) in natural killer cells, which reduced their efficacy[309]. Other secreted miRNAs like miR-21 and miR-29a have been shown to bind to toll-like receptors (TLR) and trigger a TLR mediated pro-metastatic inflammatory response, and thus contributes to the cancers growth and/or metastasis[155]. Our results add to this understanding of tumor released miRNAs in LAC, we demonstrate in Chapter 3 and 4 the ability of miR-142-3p, miR-143-3p and miR-145-5p to contribute to tumorigenesis through promotion of angiogenesis, and the CAF phenotype. Considering the roles in miRNAs within the tumor it is not surprising that expression of miRNAs within tumors are deregulated.

Tumors have differing expression of miRNAs compared to their normal counter parts. In NSCLC some miRNAs have been shown to be down regulated within the tumor cells. MiR-145-5p was shown to be reduced in the NSCLC cells which mirrored results in colon cancers[310,311].The reduction of miR-145-5p within the cells may not be an indication of the levels of miR-145-5p total expression. In our results miR-145-5p was found almost entirely within LAC EVs, which indicted that this miRNA may only be found within the EVs due to efficient shuttling of this miRNA. Other miRNAs such as miR-21-5p was shown to be upregulated in NSCLC in addition to others[310]. This deregulation of miRNAs contributes to the cancer development by reducing the expression of tumor suppressing miRNAs and increasing the expression of oncogenic miRNAs[312]. Considering that tumor miRNAs are deregulated we would expect to see differences in secreted miRNAs and therefore differences in the miRNA serum profiles of cancer patients compared to non-cancer patients.

5.2 Summary of Findings

5.2.1 Serum miRNAs as biomarkers in the detection of LAC

One of the goals our research was to determine whether differences in serum miRNAs could be detected in the serum profiles of LAC patients compared to high-risk non-cancer patients. In chapter 2, I provide a comprehensive profiling of serum miRNAs in early stage LAC patients and high-risk non-cancer controls. Within the chapter I initially profile for 742 different miRNAs and find a set of miRNAs that are able to distinguish LAC from non-cancer. This method of biomarker detection has a number of strengths associated with it. First, the profiling of serum miRNAs by qRT-PCR is highly sensitive and with our stringent selection of candidates by eliminating any miRNA affected by hemolysis offers a robust selection of miRNAs for use as

candidates. These factors of selection are clinically relevant data, since hemolysis contamination is a common problem in blood draws. In addition, we validated across platforms suggesting that these miRNAs are highly sensitive and could be used in a clinic regardless of platform. One of the more unique aspects of my study is that we utilize early stage LAC serum samples which are difficult to obtain but offer the potential to find early indications of LAC development. In general, these samples would show smaller changes in miRNAs as on average they have lower cell numbers that are able to secrete miRNA containing EVs. Additionally, early stage LAC tumors would have limited access to both the lymph and circulatory systems to secrete EVs into for detection compared to later stage disseminated tumors. However, they are more relevant to the clinic considering it is easier to treat early stages of LAC and early stages of LAC are generally asymptomatic. These early stages of LAC offer a high yield reward if we can detect LAC presence early. Finally, the use of high-risk non-cancer serum samples as our comparator offers a highly clinically relevant examination of high-risk patients who are more likely to be screened. These samples mimic what would occur in the clinic and therefore more relevant that many previous studies which use healthy patient controls. This type of patient data is not commonly used as a comparison, and therefor is quite rare.

There are however some limitations to our data and analysis, first, in patient serum data there is a significant difference in age between patients in our training data and considering age is a factor in serum miRNAs this may create a bias based on age between LAC and non-cancer[227]. Although there is a difference in age it is mainly seen in serum that is greater than 10 years of age apart, and therefore may not present a large factor[227].

Another limitation within our profiling of LAC serum miRNAs, is that we changed qRT-PCR platforms for validation of our miRNA candidates. Doing so, we saw that miR-197 and miR-142-3p did not show similar values in our validation samples compared to our training data. This suggests that the platform significantly affected the levels of miRNAs detected. To become more confident in our biomarker selection, initial profiling of serum miRNAs on the TaqMan platform, would have given us a stronger miRNA signature with a higher chance of validating as expected. However, given this limitation once miRNAs that failed to validate were eliminated the discriminate equations were reproducible across two platforms.

The results of this biomarker examination show specific miRNAs including miR-27b, miR-582-5p, miR-497, miR-92b could be used as indicators of LAC presence in both sexes using the SYBR Green platform. However, when we attempted to validate using the TaqMan platform on a separate set of samples the accuracy dropped considerably. After finding that sex played a role in serum miRNA levels, I separated the samples based on sex to construct sex-specific miRNA signatures. I found two unique signatures that separated LAC from non-cancer in each sex. The signature in females had low sensitivity and specificity compared to males and when validated on the TaqMan panels tended to call LAC over non-cancer. In males we saw a similar trend which additionally favored calling LAC, however after examining paired samples we found that miR-142-3p showed significantly different detection in paired samples and was thus removed from analysis. A new male sex specific signature was determined and validated which had the highest sensitivity and specificity. This male specific miRNA signature may offer a non-invasive method of screening for LAC in high risk patients. Further validation must be conducted on a larger sample size to confirm these results. In the future, examining these patient miRNA profiles with tumor grading changed according to the new guidelines and follow up survival may allow for us to determine if the miRNA signatures are associated with stage or survival, and further allow for us to stratify the patient miRNA profiles.

5.2.2 Function of LAC secreted miRNAs

The second goal of this thesis was to determine the function of specific miRNAs within LAC EVs in the tumor stroma. In chapter 3 we profiled LAC cell line EVs to determine what miRNAs were enriched within them. This does raise a limitation to our research as the early LAC cell lines utilized are stage I – IIIa but are well established as coming from patients with

advanced disease, thus our cell lines may not properly represent early LAC tumors. However, there are very few staged early LAC cell lines and we utilized the best cell lines available for our *in vitro* research. After determining the miRNAs frequently enriched we selected miR-143-3p and miR-145-5p for further functional validation as they were additionally found to be enriched in serum draining directly from LAC tumor beds. This represented a major strength of this thesis chapter as these samples are extremely rare and offer the highest concentration of tumor secreted miRNAs and allow for us to more accurately determine miRNAs that are secreted from LAC tumors. Although this data does not utilize miR-Seq, the data in this thesis represents a comprehensive interrogation of tumor secreted miRNAs, as it analyzes 742 of the most abundant human miRNAs and presents a highly sensitive analysis of these miRNAs. The detection of miR-143-3p and miR-145-5p within these rare serum samples lead us to follow up on the function that these miRNAs may have when released from LAC cells. A further investigation of these miRNAs demonstrated that the miRNAs promoted angiogenesis *in vivo* in endothelial cells when directly overexpressed and when transferred through EVs, which was mediated by the targeting of CAMK1D. Going forward deletion of these miRNAs within LAC cell lines may present a robust method for examining the exact role miR-143-3p and miR-145-5p play in tumor development. By utilizing CRISPR, miR-143-3p and miR-145-5p could be deleted in LAC cell lines and then injected into mice for *in vivo* analysis. Once injected and allowed to grow, examination of angiogenesis in an *in vivo* model will allow for a strong conclusion about the role that these miRNAs play in tumorigenesis.

In chapter 4 we investigate miR-142-3p due to its common enrichment in oral cancer cell EVs and due to its abundance in LAC EVs. I investigated its function which revealed that miR-142-3p targets TGFβR1 in endothelial cells and promotes angiogenesis through this effect. When

transferred through EVs these miRNAs with the additional EVs contents can induce angiogenesis. However, in fibroblast cells miR-142-3p did not target TGFβR1 but promoted the CAF phenotype through an unidentified mechanism which increased CAF markers αSMA and PDGFR. This research presented itself with a limitation due to the inability to identify the target of miR-142-3p in the fibroblast cells. In the future, overexpressing miR-142-3p within fibroblast cells and conducting proteomic analysis on overexpression and control cell lines may offer a narrowed list of miR-142-3p targets in fibroblasts. Once narrowed, western blots could be conducted for validation followed by luciferase assays for target confirmation. If a target is confirmed to be inhibited by miR-142-3p then further examination of the role the target plays in CAF formation could be examined and a more defined role for miR-142-3p could be given.

5.3 Conclusions Regarding Hypothesis

For this thesis the hypotheses were: 1) A miRNA signature in the serum of LAC patients will allow for discrimination between LAC and non-cancer 2) LAC EV miRNAs promote tumorigenic changes in stromal cells to promote tumorigenesis.

Hypothesis 1 was examined in Chapter 2 of this thesis where I identified a unique miRNA signature that could reasonably separate LAC patient serum from high-risk non-cancer controls. This signature allows for discrimination of LAC and non-cancer confirming my hypothesis.

Hypothesis 2 was examined in Chapter 3 and 4, where the results demonstrated that miR-142-3p, miR-143-3p and miR-145-5p were able to be transferred from LAC cell lines within EVs to stromal cells where they promoted cancer associated features. In Chapter 3 specifically the role of miR-143-3p and miR-145-5p were outlined as promoting cancer associated features

through inducing angiogenesis and therefore supporting the hypothesis. Chapter 4 additionally supported this hypothesis as we examined the role miR-142-3p played on both endothelial cells and fibroblasts where it was able to promote angiogenesis and features of the CAF phenotype, both of which promote tumorigenesis.

5.4 Overall Significance

The goal of this research was to identify tumor secreted miRNAs from LAC and determine whether they could be used as biomarkers in the serum and to determine their function when transferred to the surrounding stroma. In our investigation we present the detailed analysis of secreted miRNAs from LAC.

Chapter 2 presents the analysis of miRNAs within patient serum samples taken from patients with LAC and high-risk non-cancer controls. We first establish a method for normalizing serum miRNAs using miR-23a. Throughout the analysis we find a miRNA signature that was able to distinguish LAC from non-cancer 68% of the time, while this is a relatively decent detection rate, we were able to find a stronger signature in male patients only. This male specific signature had the highest sensitivity and specificity compared to the other signatures, making the signature a strong candidate for use in the clinic. Further follow up and larger validation cohorts are required to validate the determined LAC classifiers to determine their use in the clinic.

The analysis of EV-associated miRNAs in LAC is the first to show that specific miRNAs are selectively packaged into EVs in LAC. To date many studies on LAC EVs utilizes the cell line A549 cells which, is a highly mutated model of LAC or utilize late stage LAC cell lines (Table 4.1). This is extremely important as stromal changes and microenvironment

transformation occur at all stages of cancer development to support the growing tumor. Utilizing early LAC cell lines allow for the identification of miRNAs that are important early in development of the cancer to potentially intervene at a stage before metastasis. In our research of early LAC cell lines, we demonstrate that EVs from LAC are able to enter into endothelial cells and fibroblast cells where they are able to affect the function of these cells. In Chapter 3 we demonstrate that miR-143-3p and miR-145-5p increase tube formation through inhibition of CAMK1D, this was the first time LAC EVs were shown to increase angiogenesis within endothelial cells. This data demonstrated that LAC EVs are functional *in vitro* and increase the tumor associated changes in the endothelial and fibroblast cells.

We also present the function of miR-142-3p in LAC EVs. We identify the target of miR-142-3p in endothelial cells as TGFβR1, and which when targeted increases tube formation. In addition, we investigate the target of miR-142-3p in fibroblast cells, however we find that TGFβR1 is not a target in fibroblasts. This demonstrates the ability of miR-142-3p to have differing functions and targets when entering specific types of stromal cells.

Bibliography

1 Song, H. *et al.* Functional characterization of pulmonary neuroendocrine cells in lung development, injury, and tumorigenesis. *Proc Natl Acad Sci U S A* **109**, 17531-17536, doi:10.1073/pnas.1207238109 (2012).

2 Canadian Cancer Society's Steering Committee for Canadian Cancer, S. (2017).

3 Zhang, Y. *et al.* Secreted monocytic miR-150 enhances targeted endothelial cell migration. *Mol Cell* **39**, 133-144, doi:10.1016/j.molcel.2010.06.010 (2010).

4 Dela Cruz, C. S., Tanoue, L. T. & Matthay, R. A. Lung cancer: epidemiology, etiology, and prevention. *Clin Chest Med* **32**, 605-644, doi:10.1016/j.ccm.2011.09.001 (2011).

5 Hsu, C. *et al.* Regulation of exosome secretion by Rab35 and its GTPase-activating proteins TBC1D10A-C. *The Journal of cell biology* **189**, 223-232, doi:10.1083/jcb.200911018 (2010).

6 Detterbeck, F. C., Boffa, D. J., Kim, A. W. & Tanoue, L. T. The Eighth Edition Lung Cancer Stage Classification. *Chest* **151**, 193-203, doi:10.1016/j.chest.2016.10.010 (2017).

7 Sulu, E. *et al.* Delays in the diagnosis and treatment of non-small-cell lung cancer. *Tumori* **97**, 693-697, doi:10.1700/1018.11083 (2011).

8 Ellis, P. M. & Vandermeer, R. Delays in the diagnosis of lung cancer. *J Thorac Dis* **3**, 183-188, doi:10.3978/j.issn.2072-1439.2011.01.01 (2011).

9 Ruano-Ravina, A., Figueiras, A. & Barros-Dios, J. M. Lung cancer and related risk factors: an update of the literature. *Public Health* **117**, 149-156, doi:10.1016/S0033-3506(02)00023-9 (2003).

10 Shaper, A. G., Wannamethee, S. G. & Walker, M. Pipe and cigar smoking and major cardiovascular events, cancer incidence and all-cause mortality in middle-aged British men. *Int J Epidemiol* **32**, 802-808 (2003).

11 Henley, S. J., Thun, M. J., Chao, A. & Calle, E. E. Association between exclusive pipe smoking and mortality from cancer and other diseases. *J Natl Cancer Inst* **96**, 853-861 (2004).

12 Sabari, J. K., Lok, B. H., Laird, J. H., Poirier, J. T. & Rudin, C. M. Unravelling the biology of SCLC: implications for therapy. *Nat Rev Clin Oncol* **14**, 549-561, doi:10.1038/nrclinonc.2017.71 (2017).

13 Pignon, J. P. *et al.* A meta-analysis of thoracic radiotherapy for small-cell lung cancer. *N Engl J Med* **327**, 1618-1624, doi:10.1056/NEJM199212033272302 (1992).

14 Wang, S. *et al.* Survival changes in patients with small cell lung cancer and disparities between different sexes, socioeconomic statuses and ages. *Sci Rep* **7**, 1339, doi:10.1038/s41598-017-01571-0 (2017).

15 Hanna, J. M. & Onaitis, M. W. Cell of origin of lung cancer. *J Carcinog* **12**, 6, doi:10.4103/1477-3163.109033 (2013).

16 Cheng, C. Y. & Nikitin, A. Y. Neuroendocrine cells: potential cells of origin for small cell lung carcinoma. *Cell Cycle* **10**, 3629-3630, doi:10.4161/cc.10.21.18034 (2011).

17 Travis, W. D. Update on small cell carcinoma and its differentiation from squamous cell carcinoma and other non-small cell carcinomas. *Mod Pathol* **25 Suppl 1**, S18-30, doi:10.1038/modpathol.2011.150 (2012).

18 Barbareschi, M. *et al.* Heterogeneity of large cell carcinoma of the lung: an immunophenotypic and miRNA-based analysis. *Am J Clin Pathol* **136**, 773-782, doi:10.1309/AJCPYY79XAGRAYCJ (2011).
19 Varela, G. & Thomas, P. A. Surgical management of advanced non-small cell lung cancer. *J Thorac Dis* **6 Suppl 2**, S217-223, doi:10.3978/j.issn.2072-1439.2014.04.34 (2014).
20 Bareschino, M. A. *et al.* Treatment of advanced non small cell lung cancer. *J Thorac Dis* **3**, 122-133, doi:10.3978/j.issn.2072-1439.2010.12.08 (2011).
21 Chan, B. A. & Hughes, B. G. Targeted therapy for non-small cell lung cancer: current standards and the promise of the future. *Transl Lung Cancer Res* **4**, 36-54, doi:10.3978/j.issn.2218-6751.2014.05.01 (2015).
22 Lauro, S., Onesti, C. E., Righini, R. & Marchetti, P. The use of bevacizumab in non-small cell lung cancer: an update. *Anticancer Res* **34**, 1537-1545 (2014).
23 Travis, W. D., Travis, L. B. & Devesa, S. S. Lung cancer. *Cancer* **75**, 191-202 (1995).
24 Rowbotham, S. P. & Kim, C. F. Diverse cells at the origin of lung adenocarcinoma. *Proc Natl Acad Sci U S A* **111**, 4745-4746, doi:10.1073/pnas.1401955111 (2014).
25 Pikor, L. A., Ramnarine, V. R., Lam, S. & Lam, W. L. Genetic alterations defining NSCLC subtypes and their therapeutic implications. *Lung Cancer* **82**, 179-189, doi:10.1016/j.lungcan.2013.07.025 (2013).
26 Jiang, X., de Groh, M., Liu, S., Liang, H. & Morrison, H. Rising incidence of adenocarcinoma of the lung in Canada. *Lung Cancer* **78**, 16-22, doi:10.1016/j.lungcan.2012.06.002 (2012).
27 Goldstraw, P. *et al.* The IASLC Lung Cancer Staging Project: Proposals for Revision of the TNM Stage Groupings in the Forthcoming (Eighth) Edition of the TNM Classification for Lung Cancer. *J Thorac Oncol* **11**, 39-51, doi:10.1016/j.jtho.2015.09.009 (2016).
28 Borchert, G. M., Lanier, W. & Davidson, B. L. RNA polymerase III transcribes human microRNAs. *Nat Struct Mol Biol* **13**, 1097-1101, doi:10.1038/nsmb1167 (2006).
29 Lee, Y. *et al.* MicroRNA genes are transcribed by RNA polymerase II. *EMBO J* **23**, 4051-4060, doi:10.1038/sj.emboj.7600385 (2004).
30 Gregory, R. I. *et al.* The Microprocessor complex mediates the genesis of microRNAs. *Nature* **432**, 235-240, doi:10.1038/nature03120 (2004).
31 Lee, Y. *et al.* The nuclear RNase III Drosha initiates microRNA processing. *Nature* **425**, 415-419, doi:10.1038/nature01957 (2003).
32 Han, J. *et al.* The Drosha-DGCR8 complex in primary microRNA processing. *Genes Dev* **18**, 3016-3027, doi:10.1101/gad.1262504 (2004).
33 Westholm, J. O. & Lai, E. C. Mirtrons: microRNA biogenesis via splicing. *Biochimie* **93**, 1897-1904, doi:10.1016/j.biochi.2011.06.017 (2011).
34 Diederichs, S. & Haber, D. A. Dual role for argonautes in microRNA processing and posttranscriptional regulation of microRNA expression. *Cell* **131**, 1097-1108, doi:10.1016/j.cell.2007.10.032 (2007).
35 Baek, D. *et al.* The impact of microRNAs on protein output. *Nature* **455**, 64-71, doi:10.1038/nature07242 (2008).

36 Tay, Y., Zhang, J., Thomson, A. M., Lim, B. & Rigoutsos, I. MicroRNAs to Nanog, Oct4 and Sox2 coding regions modulate embryonic stem cell differentiation. *Nature* **455**, 1124-1128, doi:10.1038/nature07299 (2008).
37 Creemers, E. E., Tijsen, A. J. & Pinto, Y. M. Circulating microRNAs: novel biomarkers and extracellular communicators in cardiovascular disease? *Circ Res* **110**, 483-495, doi:10.1161/CIRCRESAHA.111.247452 (2012).
38 Trams, E. G., Lauter, C. J., Salem, N., Jr. & Heine, U. Exfoliation of membrane ecto-enzymes in the form of micro-vesicles. *Biochim Biophys Acta* **645**, 63-70 (1981).
39 Doherty, G. J. & McMahon, H. T. Mechanisms of endocytosis. *Annu Rev Biochem* **78**, 857-902, doi:10.1146/annurev.biochem.78.081307.110540 (2009).
40 Baumgart, T., Capraro, B. R., Zhu, C. & Das, S. L. Thermodynamics and mechanics of membrane curvature generation and sensing by proteins and lipids. *Annual review of physical chemistry* **62**, 483-506, doi:10.1146/annurev.physchem.012809.103450 (2011).
41 Gruenberg, J. The endocytic pathway: a mosaic of domains. *Nature reviews. Molecular cell biology* **2**, 721-730, doi:10.1038/35096054 (2001).
42 Mellman, I. Endocytosis and molecular sorting. *Annual review of cell and developmental biology* **12**, 575-625, doi:10.1146/annurev.cellbio.12.1.575 (1996).
43 Mayor, S., Presley, J. F. & Maxfield, F. R. Sorting of membrane components from endosomes and subsequent recycling to the cell surface occurs by a bulk flow process. *The Journal of cell biology* **121**, 1257-1269 (1993).
44 Dunn, K. W., McGraw, T. E. & Maxfield, F. R. Iterative fractionation of recycling receptors from lysosomally destined ligands in an early sorting endosome. *The Journal of cell biology* **109**, 3303-3314 (1989).
45 Grosshans, B. L., Ortiz, D. & Novick, P. Rabs and their effectors: achieving specificity in membrane traffic. *Proc Natl Acad Sci U S A* **103**, 11821-11827, doi:10.1073/pnas.0601617103 (2006).
46 Gorvel, J. P., Chavrier, P., Zerial, M. & Gruenberg, J. rab5 controls early endosome fusion in vitro. *Cell* **64**, 915-925 (1991).
47 Bucci, C. *et al.* The small GTPase rab5 functions as a regulatory factor in the early endocytic pathway. *Cell* **70**, 715-728 (1992).
48 van der Sluijs, P. *et al.* The small GTP-binding protein rab4 controls an early sorting event on the endocytic pathway. *Cell* **70**, 729-740 (1992).
49 Daro, E., van der Sluijs, P., Galli, T. & Mellman, I. Rab4 and cellubrevin define different early endosome populations on the pathway of transferrin receptor recycling. *Proc Natl Acad Sci U S A* **93**, 9559-9564 (1996).
50 Jovic, M., Sharma, M., Rahajeng, J. & Caplan, S. The early endosome: a busy sorting station for proteins at the crossroads. *Histology and histopathology* **25**, 99-112 (2010).
51 Zeigerer, A. *et al.* Rab5 is necessary for the biogenesis of the endolysosomal system in vivo. *Nature* **485**, 465-470, doi:10.1038/nature11133 (2012).
52 Gautreau, A., Oguievetskaia, K. & Ungermann, C. Function and regulation of the endosomal fusion and fission machineries. *Cold Spring Harb Perspect Biol* **6**, doi:10.1101/cshperspect.a016832 (2014).
53 Antonin, W., Holroyd, C., Tikkanen, R., Honing, S. & Jahn, R. The R-SNARE endobrevin/VAMP-8 mediates homotypic fusion of early endosomes and late endosomes. *Molecular biology of the cell* **11**, 3289-3298 (2000).

54 Keller, S., Sanderson, M. P., Stoeck, A. & Altevogt, P. Exosomes: from biogenesis and secretion to biological function. *Immunology letters* **107**, 102-108, doi:10.1016/j.imlet.2006.09.005 (2006).
55 Rink, J., Ghigo, E., Kalaidzidis, Y. & Zerial, M. Rab conversion as a mechanism of progression from early to late endosomes. *Cell* **122**, 735-749, doi:10.1016/j.cell.2005.06.043 (2005).
56 Ostrowski, M. *et al.* Rab27a and Rab27b control different steps of the exosome secretion pathway. *Nature cell biology* **12**, 19-30; sup pp 11-13, doi:10.1038/ncb2000 (2010).
57 Savina, A., Vidal, M. & Colombo, M. I. The exosome pathway in K562 cells is regulated by Rab11. *Journal of cell science* **115**, 2505-2515 (2002).
58 Colombo, M. *et al.* Analysis of ESCRT functions in exosome biogenesis, composition and secretion highlights the heterogeneity of extracellular vesicles. *Journal of cell science* **126**, 5553-5565, doi:10.1242/jcs.128868 (2013).
59 Hurley, J. H. & Hanson, P. I. Membrane budding and scission by the ESCRT machinery: it's all in the neck. *Nature reviews. Molecular cell biology* **11**, 556-566, doi:10.1038/nrm2937 (2010).
60 Wollert, T., Wunder, C., Lippincott-Schwartz, J. & Hurley, J. H. Membrane scission by the ESCRT-III complex. *Nature* **458**, 172-177, doi:10.1038/nature07836 (2009).
61 Kojima, K. *et al.* ESCRT-0 protein hepatocyte growth factor-regulated tyrosine kinase substrate (Hrs) is targeted to endosomes independently of signal-transducing adaptor molecule (STAM) and the complex formation with STAM promotes its endosomal dissociation. *J Biol Chem* **290**, 8065-8066, doi:10.1074/jbc.A114.578245 (2015).
62 Ghazi-Tabatabai, S. *et al.* Structure and disassembly of filaments formed by the ESCRT-III subunit Vps24. *Structure* **16**, 1345-1356, doi:10.1016/j.str.2008.06.010 (2008).
63 Lata, S. *et al.* Helical structures of ESCRT-III are disassembled by VPS4. *Science* **321**, 1354-1357, doi:10.1126/science.1161070 (2008).
64 Saksena, S., Wahlman, J., Teis, D., Johnson, A. E. & Emr, S. D. Functional reconstitution of ESCRT-III assembly and disassembly. *Cell* **136**, 97-109, doi:10.1016/j.cell.2008.11.013 (2009).
65 Hanson, P. I., Roth, R., Lin, Y. & Heuser, J. E. Plasma membrane deformation by circular arrays of ESCRT-III protein filaments. *The Journal of cell biology* **180**, 389-402, doi:10.1083/jcb.200707031 (2008).
66 Wollert, T. & Hurley, J. H. Molecular mechanism of multivesicular body biogenesis by ESCRT complexes. *Nature* **464**, 864-869, doi:10.1038/nature08849 (2010).
67 Stuffers, S., Sem Wegner, C., Stenmark, H. & Brech, A. Multivesicular endosome biogenesis in the absence of ESCRTs. *Traffic* **10**, 925-937, doi:10.1111/j.1600-0854.2009.00920.x (2009).
68 Trajkovic, K. *et al.* Ceramide triggers budding of exosome vesicles into multivesicular endosomes. *Science* **319**, 1244-1247, doi:10.1126/science.1153124 (2008).
69 Akers, J. C., Gonda, D., Kim, R., Carter, B. S. & Chen, C. C. Biogenesis of extracellular vesicles (EV): exosomes, microvesicles, retrovirus-like vesicles, and apoptotic bodies. *J Neurooncol* **113**, 1-11, doi:10.1007/s11060-013-1084-8 (2013).
70 Nabhan, J. F., Hu, R., Oh, R. S., Cohen, S. N. & Lu, Q. Formation and release of arrestin domain-containing protein 1-mediated microvesicles (ARMMs) at plasma membrane by

recruitment of TSG101 protein. *Proc Natl Acad Sci U S A* **109**, 4146-4151, doi:10.1073/pnas.1200448109 (2012).
71 Minciacchi, V. R., Freeman, M. R. & Di Vizio, D. Extracellular vesicles in cancer: exosomes, microvesicles and the emerging role of large oncosomes. *Semin Cell Dev Biol* **40**, 41-51, doi:10.1016/j.semcdb.2015.02.010 (2015).
72 Szatanek, R., Baran, J., Siedlar, M. & Baj-Krzyworzeka, M. Isolation of extracellular vesicles: Determining the correct approach (Review). *Int J Mol Med* **36**, 11-17, doi:10.3892/ijmm.2015.2194 (2015).
73 Yuana, Y., Levels, J., Grootemaat, A., Sturk, A. & Nieuwland, R. Co-isolation of extracellular vesicles and high-density lipoproteins using density gradient ultracentrifugation. *J Extracell Vesicles* **3**, doi:10.3402/jev.v3.23262 (2014).
74 Cantin, R., Diou, J., Belanger, D., Tremblay, A. M. & Gilbert, C. Discrimination between exosomes and HIV-1: purification of both vesicles from cell-free supernatants. *J Immunol Methods* **338**, 21-30, doi:10.1016/j.jim.2008.07.007 (2008).
75 Vlassov, A. V., Magdaleno, S., Setterquist, R. & Conrad, R. Exosomes: current knowledge of their composition, biological functions, and diagnostic and therapeutic potentials. *Biochim Biophys Acta* **1820**, 940-948, doi:10.1016/j.bbagen.2012.03.017 (2012).
76 Fitzner, D. *et al.* Selective transfer of exosomes from oligodendrocytes to microglia by macropinocytosis. *Journal of cell science* **124**, 447-458, doi:10.1242/jcs.074088 (2011).
77 Boing, A. N. *et al.* Single-step isolation of extracellular vesicles by size-exclusion chromatography. *J Extracell Vesicles* **3**, doi:10.3402/jev.v3.23430 (2014).
78 Yanez-Mo, M. *et al.* Biological properties of extracellular vesicles and their physiological functions. *J Extracell Vesicles* **4**, 27066, doi:10.3402/jev.v4.27066 (2015).
79 Filipe, V., Hawe, A. & Jiskoot, W. Critical evaluation of Nanoparticle Tracking Analysis (NTA) by NanoSight for the measurement of nanoparticles and protein aggregates. *Pharm Res* **27**, 796-810, doi:10.1007/s11095-010-0073-2 (2010).
80 Lotvall, J. *et al.* Minimal experimental requirements for definition of extracellular vesicles and their functions: a position statement from the International Society for Extracellular Vesicles. *J Extracell Vesicles* **3**, 26913, doi:10.3402/jev.v3.26913 (2014).
81 Mateescu, B. *et al.* Obstacles and opportunities in the functional analysis of extracellular vesicle RNA - an ISEV position paper. *J Extracell Vesicles* **6**, 1286095, doi:10.1080/20013078.2017.1286095 (2017).
82 Bellingham, S. A., Coleman, B. M. & Hill, A. F. Small RNA deep sequencing reveals a distinct miRNA signature released in exosomes from prion-infected neuronal cells. *Nucleic Acids Res* **40**, 10937-10949, doi:10.1093/nar/gks832 (2012).
83 Balaj, L. *et al.* Tumour microvesicles contain retrotransposon elements and amplified oncogene sequences. *Nat Commun* **2**, 180, doi:10.1038/ncomms1180 (2011).
84 Kahlert, C. *et al.* Identification of double-stranded genomic DNA spanning all chromosomes with mutated KRAS and p53 DNA in the serum exosomes of patients with pancreatic cancer. *J Biol Chem* **289**, 3869-3875, doi:10.1074/jbc.C113.532267 (2014).
85 Thakur, B. K. *et al.* Double-stranded DNA in exosomes: a novel biomarker in cancer detection. *Cell Res* **24**, 766-769, doi:10.1038/cr.2014.44 (2014).

86 Tauro, B. J. *et al.* Comparison of ultracentrifugation, density gradient separation, and immunoaffinity capture methods for isolating human colon cancer cell line LIM1863-derived exosomes. *Methods* **56**, 293-304, doi:10.1016/j.ymeth.2012.01.002 (2012).
87 Heijnen, H. F., Schiel, A. E., Fijnheer, R., Geuze, H. J. & Sixma, J. J. Activated platelets release two types of membrane vesicles: microvesicles by surface shedding and exosomes derived from exocytosis of multivesicular bodies and alpha-granules. *Blood* **94**, 3791-3799 (1999).
88 Melo, S. A. *et al.* Cancer exosomes perform cell-independent microRNA biogenesis and promote tumorigenesis. *Cancer Cell* **26**, 707-721, doi:10.1016/j.ccell.2014.09.005 (2014).
89 Goldie, B. J. *et al.* Activity-associated miRNA are packaged in Map1b-enriched exosomes released from depolarized neurons. *Nucleic Acids Res* **42**, 9195-9208, doi:10.1093/nar/gku594 (2014).
90 Guduric-Fuchs, J. *et al.* Selective extracellular vesicle-mediated export of an overlapping set of microRNAs from multiple cell types. *BMC Genomics* **13**, 357, doi:10.1186/1471-2164-13-357 (2012).
91 Villarroya-Beltri, C. *et al.* Sumoylated hnRNPA2B1 controls the sorting of miRNAs into exosomes through binding to specific motifs. *Nat Commun* **4**, 2980, doi:10.1038/ncomms3980 (2013).
92 Gibbings, D. J., Ciaudo, C., Erhardt, M. & Voinnet, O. Multivesicular bodies associate with components of miRNA effector complexes and modulate miRNA activity. *Nature cell biology* **11**, 1143-1149, doi:10.1038/ncb1929 (2009).
93 Buccheri, G. & Ferrigno, D. Lung cancer: clinical presentation and specialist referral time. *Eur Respir J* **24**, 898-904, doi:10.1183/09031936.04.00113603 (2004).
94 Detterbeck, F. C., Lewis, S. Z., Diekemper, R., Addrizzo-Harris, D. & Alberts, W. M. Executive Summary: Diagnosis and management of lung cancer, 3rd ed: American College of Chest Physicians evidence-based clinical practice guidelines. *Chest* **143**, 7S-37S, doi:10.1378/chest.12-2377 (2013).
95 Lindeman, N. I. *et al.* Molecular testing guideline for selection of lung cancer patients for EGFR and ALK tyrosine kinase inhibitors: guideline from the College of American Pathologists, International Association for the Study of Lung Cancer, and Association for Molecular Pathology. *J Mol Diagn* **15**, 415-453, doi:10.1016/j.jmoldx.2013.03.001 (2013).
96 Tammemagi, M. C. *et al.* Participant selection for lung cancer screening by risk modelling (the Pan-Canadian Early Detection of Lung Cancer [PanCan] study): a single-arm, prospective study. *Lancet Oncol*, doi:10.1016/S1470-2045(17)30597-1 (2017).
97 Canadian Task Force on Preventive Health, C. *et al.* Recommendations on screening for lung cancer. *CMAJ* **188**, 425-432, doi:10.1503/cmaj.151421 (2016).
98 National Lung Screening Trial Research, T. *et al.* Reduced lung-cancer mortality with low-dose computed tomographic screening. *N Engl J Med* **365**, 395-409, doi:10.1056/NEJMoa1102873 (2011).
99 Hubers, A. J., Prinsen, C. F., Sozzi, G., Witte, B. I. & Thunnissen, E. Molecular sputum analysis for the diagnosis of lung cancer. *Br J Cancer* **109**, 530-537, doi:10.1038/bjc.2013.393 (2013).

100 Xie, Y. *et al.* Altered miRNA expression in sputum for diagnosis of non-small cell lung cancer. *Lung Cancer* **67**, 170-176, doi:10.1016/j.lungcan.2009.04.004 (2010).
101 Xing, L. *et al.* Sputum microRNA biomarkers for identifying lung cancer in indeterminate solitary pulmonary nodules. *Clin Cancer Res* **21**, 484-489, doi:10.1158/1078-0432.CCR-14-1873 (2015).
102 Mitchell, P. S. *et al.* Circulating microRNAs as stable blood-based markers for cancer detection. *Proc Natl Acad Sci U S A* **105**, 10513-10518, doi:10.1073/pnas.0804549105 (2008).
103 Roth, C. *et al.* Circulating microRNAs as blood-based markers for patients with primary and metastatic breast cancer. *Breast Cancer Res* **12**, R90, doi:10.1186/bcr2766 (2010).
104 Gezer, U. *et al.* Abundant circulating microRNAs in breast cancer patients fluctuate considerably during neoadjuvant chemotherapy. *Oncol Lett* **8**, 845-848, doi:10.3892/ol.2014.2188 (2014).
105 Redova, M., Sana, J. & Slaby, O. Circulating miRNAs as new blood-based biomarkers for solid cancers. *Future Oncol* **9**, 387-402, doi:10.2217/fon.12.192 (2013).
106 Nadal, E. *et al.* A Novel Serum 4-microRNA Signature for Lung Cancer Detection. *Sci Rep* **5**, 12464, doi:10.1038/srep12464 (2015).
107 Wozniak, M. B. *et al.* Circulating MicroRNAs as Non-Invasive Biomarkers for Early Detection of Non-Small-Cell Lung Cancer. *PLoS One* **10**, e0125026, doi:10.1371/journal.pone.0125026 (2015).
108 Halvorsen, A. R. *et al.* A unique set of 6 circulating microRNAs for early detection of non-small cell lung cancer. *Oncotarget* **7**, 37250-37259, doi:10.18632/oncotarget.9363 (2016).
109 Tang, D. *et al.* Identification of plasma microRNAs as novel noninvasive biomarkers for early detection of lung cancer. *Eur J Cancer Prev* **22**, 540-548, doi:10.1097/CEJ.0b013e32835f3be9 (2013).
110 Shen, J. & Jiang, F. Applications of MicroRNAs in the Diagnosis and Prognosis of Lung Cancer. *Expert opinion on medical diagnostics* **6**, 197-207, doi:10.1517/17530059.2012.672970 (2012).
111 Del Vescovo, V., Grasso, M., Barbareschi, M. & Denti, M. A. MicroRNAs as lung cancer biomarkers. *World journal of clinical oncology* **5**, 604-620, doi:10.5306/wjco.v5.i4.604 (2014).
112 Huang, Y. *et al.* MicroRNAs in body fluids as biomarkers for non-small cell lung cancer: a systematic review. *Technology in cancer research & treatment* **13**, 277-287, doi:10.7785/tcrt.2012.500377 (2014).
113 Wang, H. *et al.* Clinical use of microRNAs as potential non-invasive biomarkers for detecting non-small cell lung cancer: a meta-analysis. *Respirology* **20**, 56-65, doi:10.1111/resp.12444 (2015).
114 Chen, X. *et al.* Characterization of microRNAs in serum: a novel class of biomarkers for diagnosis of cancer and other diseases. *Cell Res* **18**, 997-1006, doi:10.1038/cr.2008.282 (2008).
115 Bianchi, F. *et al.* A serum circulating miRNA diagnostic test to identify asymptomatic high-risk individuals with early stage lung cancer. *EMBO Mol Med* **3**, 495-503, doi:10.1002/emmm.201100154 (2011).

116 Dou, H., Wang, Y., Su, G. & Zhao, S. Decreased plasma let-7c and miR-152 as noninvasive biomarker for non-small-cell lung cancer. *Int J Clin Exp Med* **8**, 9291-9298 (2015).
117 Fan, L. *et al.* Identification of serum miRNAs by nano-quantum dots microarray as diagnostic biomarkers for early detection of non-small cell lung cancer. *Tumour Biol* **37**, 7777-7784, doi:10.1007/s13277-015-4608-3 (2016).
118 Hu, Z. *et al.* Serum microRNA signatures identified in a genome-wide serum microRNA expression profiling predict survival of non-small-cell lung cancer. *J Clin Oncol* **28**, 1721-1726, doi:10.1200/JCO.2009.24.9342 (2010).
119 Silva, J. *et al.* Vesicle-related microRNAs in plasma of nonsmall cell lung cancer patients and correlation with survival. *Eur Respir J* **37**, 617-623, doi:10.1183/09031936.00029610 (2011).
120 Wang, C. *et al.* A Five-miRNA Panel Identified From a Multicentric Case-control Study Serves as a Novel Diagnostic Tool for Ethnically Diverse Non-small-cell Lung Cancer Patients. *EBioMedicine* **2**, 1377-1385, doi:10.1016/j.ebiom.2015.07.034 (2015).
121 Chen, X. *et al.* Identification of ten serum microRNAs from a genome-wide serum microRNA expression profile as novel noninvasive biomarkers for nonsmall cell lung cancer diagnosis. *Int J Cancer* **130**, 1620-1628, doi:10.1002/ijc.26177 (2012).
122 Foss, K. M. *et al.* miR-1254 and miR-574-5p: serum-based microRNA biomarkers for early-stage non-small cell lung cancer. *J Thorac Oncol* **6**, 482-488, doi:10.1097/JTO.0b013e318208c785 (2011).
123 Giallombardo, M. *et al.* Exosomal miRNA Analysis in Non-small Cell Lung Cancer (NSCLC) Patients' Plasma Through qPCR: A Feasible Liquid Biopsy Tool. *J Vis Exp*, doi:10.3791/53900 (2016).
124 Hennessey, P. T. *et al.* Serum microRNA biomarkers for detection of non-small cell lung cancer. *PLoS One* **7**, e32307, doi:10.1371/journal.pone.0032307 (2012).
125 Li, Z. H. *et al.* Prognostic significance of serum microRNA-210 levels in nonsmall-cell lung cancer. *J Int Med Res* **41**, 1437-1444, doi:10.1177/0300060513497560 (2013).
126 Wang, K. *et al.* Comparing the MicroRNA spectrum between serum and plasma. *PLoS One* **7**, e41561, doi:10.1371/journal.pone.0041561 (2012).
127 Yuxia, M., Zhennan, T. & Wei, Z. Circulating miR-125b is a novel biomarker for screening non-small-cell lung cancer and predicts poor prognosis. *J Cancer Res Clin Oncol* **138**, 2045-2050, doi:10.1007/s00432-012-1285-0 (2012).
128 Abd-El-Fattah, A. A., Sadik, N. A., Shaker, O. G. & Aboulftouh, M. L. Differential microRNAs expression in serum of patients with lung cancer, pulmonary tuberculosis, and pneumonia. *Cell Biochem Biophys* **67**, 875-884, doi:10.1007/s12013-013-9575-y (2013).
129 Arab, A. *et al.* Potential circulating miRNA signature for early detection of NSCLC. *Cancer Genet* **216-217**, 150-158, doi:10.1016/j.cancergen.2017.07.006 (2017).
130 Franchina, T. *et al.* Circulating miR-22, miR-24 and miR-34a as novel predictive biomarkers to pemetrexed-based chemotherapy in advanced non-small cell lung cancer. *J Cell Physiol* **229**, 97-99, doi:10.1002/jcp.24422 (2014).
131 Liu, Q. *et al.* Circulating exosomal microRNAs as prognostic biomarkers for non-small-cell lung cancer. *Oncotarget* **8**, 13048-13058, doi:10.18632/oncotarget.14369 (2017).

132 Powrozek, T. *et al.* The diagnostic role of plasma circulating precursors of miRNA-944 and miRNA-3662 for non-small cell lung cancer detection. *Pathol Res Pract* **213**, 1384-1387, doi:10.1016/j.prp.2017.09.011 (2017).
133 Roth, C., Kasimir-Bauer, S., Pantel, K. & Schwarzenbach, H. Screening for circulating nucleic acids and caspase activity in the peripheral blood as potential diagnostic tools in lung cancer. *Mol Oncol* **5**, 281-291, doi:10.1016/j.molonc.2011.02.002 (2011).
134 Shen, J. *et al.* Diagnosis of lung cancer in individuals with solitary pulmonary nodules by plasma microRNA biomarkers. *BMC Cancer* **11**, 374, doi:10.1186/1471-2407-11-374 (2011).
135 Yang, J. S. *et al.* Serum miR-152, miR-148a, miR-148b, and miR-21 as novel biomarkers in non-small cell lung cancer screening. *Tumour Biol* **36**, 3035-3042, doi:10.1007/s13277-014-2938-1 (2015).
136 Zhang, L. *et al.* Serum MicroRNA-150 Predicts Prognosis for Early-Stage Non-Small Cell Lung Cancer and Promotes Tumor Cell Proliferation by Targeting Tumor Suppressor Gene SRCIN1. *Clin Pharmacol Ther*, doi:10.1002/cpt.870 (2017).
137 Zheng, D. *et al.* Plasma microRNAs as novel biomarkers for early detection of lung cancer. *Int J Clin Exp Pathol* **4**, 575-586 (2011).
138 Sun, Y., Mei, H., Xu, C., Tang, H. & Wei, W. Circulating microRNA-339-5p and -21 in plasma as an early detection predictors of lung adenocarcinoma. *Pathol Res Pract*, doi:10.1016/j.prp.2017.10.011 (2017).
139 MacLellan, S. A., MacAulay, C., Lam, S. & Garnis, C. Pre-profiling factors influencing serum microRNA levels. *BMC clinical pathology* **14**, 27 (2014).
140 Kirschner, M. B. *et al.* The Impact of Hemolysis on Cell-Free microRNA Biomarkers. *Frontiers in genetics* **4**, 94, doi:10.3389/fgene.2013.00094 (2013).
141 Kirschner, M. B. *et al.* Haemolysis during sample preparation alters microRNA content of plasma. *PLoS One* **6**, e24145, doi:10.1371/journal.pone.0024145 (2011).
142 Wang, R. J., Zheng, Y. H., Wang, P. & Zhang, J. Z. Serum miR-125a-5p, miR-145 and miR-146a as diagnostic biomarkers in non-small cell lung cancer. *Int J Clin Exp Pathol* **8**, 765-771 (2015).
143 Wang, P. *et al.* Early Detection of Lung Cancer in Serum by a Panel of MicroRNA Biomarkers. *Clin Lung Cancer* **16**, 313-319 e311, doi:10.1016/j.cllc.2014.12.006 (2015).
144 Mo, D. *et al.* miR-1290 is a potential prognostic biomarker in non-small cell lung cancer. *J Thorac Dis* **7**, 1570-1579, doi:10.3978/j.issn.2072-1439.2015.09.38 (2015).
145 Jin, X. *et al.* Evaluation of Tumor-Derived Exosomal miRNA as Potential Diagnostic Biomarkers for Early-Stage Non-Small Cell Lung Cancer Using Next-Generation Sequencing. *Clin Cancer Res* **23**, 5311-5319, doi:10.1158/1078-0432.CCR-17-0577 (2017).
146 Gallo, A., Tandon, M., Alevizos, I. & Illei, G. G. The majority of microRNAs detectable in serum and saliva is concentrated in exosomes. *PLoS One* **7**, e30679, doi:10.1371/journal.pone.0030679 (2012).
147 Wu, C. *et al.* Serum levels of miR-19b and miR-146a as prognostic biomarkers for non-small cell lung cancer. *Tohoku J Exp Med* **232**, 85-95 (2014).
148 Munagala, R., Aqil, F. & Gupta, R. C. Exosomal miRNAs as biomarkers of recurrent lung cancer. *Tumour Biol* **37**, 10703-10714, doi:10.1007/s13277-016-4939-8 (2016).

149 Wang, M. *et al.* Role of tumor microenvironment in tumorigenesis. *J Cancer* **8**, 761-773, doi:10.7150/jca.17648 (2017).
150 Balkwill, F. R., Capasso, M. & Hagemann, T. The tumor microenvironment at a glance. *Journal of cell science* **125**, 5591-5596, doi:10.1242/jcs.116392 (2012).
151 Lerner, I. *et al.* Heparanase powers a chronic inflammatory circuit that promotes colitis-associated tumorigenesis in mice. *J Clin Invest* **121**, 1709-1721, doi:10.1172/JCI43792 (2011).
152 Becker, A. *et al.* Extracellular Vesicles in Cancer: Cell-to-Cell Mediators of Metastasis. *Cancer Cell* **30**, 836-848, doi:10.1016/j.ccell.2016.10.009 (2016).
153 Xiao, X. *et al.* Exosomes: decreased sensitivity of lung cancer A549 cells to cisplatin. *PLoS ONE* **9**, e89534 (2014).
154 Rana, S., Malinowska, K. & Zoller, M. Exosomal tumor microRNA modulates premetastatic organ cells. *Neoplasia* **15**, 281-295 (2013).
155 Fabbri, M. *et al.* MicroRNAs bind to Toll-like receptors to induce prometastatic inflammatory response. *Proceedings of the National Academy of Sciences* **109**, E2110-E2116 (2012).
156 Kosaka, N. *et al.* Neutral Sphingomyelinase 2 (nSMase2)-dependent Exosomal Transfer of Angiogenic MicroRNAs Regulate Cancer Cell Metastasis. *J Biol Chem* **288**, 10849-10859, doi:10.1074/jbc.M112.446831 (2013).
157 Umezu, T., Ohyashiki, K., Kuroda, M. & Ohyashiki, J. Leukemia cell to endothelial cell communication via exosomal miRNAs. *Oncogene* **32**, 2747-2755 (2013).
158 Baroni, S. *et al.* Exosome-mediated delivery of miR-9 induces cancer-associated fibroblast-like properties in human breast fibroblasts. *Cell Death & Disease* **7**, e2312 (2016).
159 Zhang, L. *et al.* Microenvironment-induced PTEN loss by exosomal microRNA primes brain metastasis outgrowth. *nature* **527**, 100-104 (2015).
160 Ruffell, B., Affara, N. I. & Coussens, L. M. Differential macrophage programming in the tumor microenvironment. *Trends in immunology* **33**, 119-126 (2012).
161 Xing, F., Saidou, J. & Watabe, K. Cancer associated fibroblasts (CAFs) in tumor microenvironment. *Frontiers in bioscience: a journal and virtual library* **15**, 166 (2010).
162 Kerbel, R. S. Tumor angiogenesis: past, present and the near future. *Carcinogenesis* **21**, 505-515 (2000).
163 Lopes-Bastos, B. M., Jiang, W. G. & Cai, J. Tumour-Endothelial Cell Communications: Important and Indispensable Mediators of Tumour Angiogenesis. *Anticancer Res* **36**, 1119-1126 (2016).
164 Bremnes, R. M., Camps, C. & Sirera, R. Angiogenesis in non-small cell lung cancer: the prognostic impact of neoangiogenesis and the cytokines VEGF and bFGF in tumours and blood. *Lung Cancer* **51**, 143-158, doi:10.1016/j.lungcan.2005.09.005 (2006).
165 Peters, S. *et al.* Metastatic non-small-cell lung cancer (NSCLC): ESMO Clinical Practice Guidelines for diagnosis, treatment and follow-up. *Annals of oncology : official journal of the European Society for Medical Oncology / ESMO* **23 Suppl 7**, vii56-64, doi:10.1093/annonc/mds226 (2012).
166 De Palma, M., Biziato, D. & Petrova, T. V. Microenvironmental regulation of tumour angiogenesis. *Nat Rev Cancer* **17**, 457-474, doi:10.1038/nrc.2017.51 (2017).

167 Lombardo, G. *et al.* Activated Stat5 trafficking Via Endothelial Cell-derived Extracellular Vesicles Controls IL-3 Pro-angiogenic Paracrine Action. *Sci Rep* **6**, 25689, doi:10.1038/srep25689 (2016).
168 Zernecke, A. *et al.* Delivery of microRNA-126 by apoptotic bodies induces CXCL12-dependent vascular protection. *Sci Signal* **2**, ra81, doi:10.1126/scisignal.2000610 (2009).
169 Cantaluppi, V. *et al.* Microvesicles derived from endothelial progenitor cells protect the kidney from ischemia-reperfusion injury by microRNA-dependent reprogramming of resident renal cells. *Kidney Int* **82**, 412-427, doi:10.1038/ki.2012.105 (2012).
170 van Balkom, B. W. *et al.* Endothelial cells require miR-214 to secrete exosomes that suppress senescence and induce angiogenesis in human and mouse endothelial cells. *Blood* **121**, 3997-4006, S3991-3915, doi:10.1182/blood-2013-02-478925 (2013).
171 Liang, X., Zhang, L., Wang, S., Han, Q. & Zhao, R. C. Exosomes secreted by mesenchymal stem cells promote endothelial cell angiogenesis by transferring miR-125a. *Journal of cell science* **129**, 2182-2189, doi:10.1242/jcs.170373 (2016).
172 Kang, T. *et al.* Adipose-Derived Stem Cells Induce Angiogenesis via Microvesicle Transport of miRNA-31. *Stem Cells Transl Med* **5**, 440-450, doi:10.5966/sctm.2015-0177 (2016).
173 Li, J. *et al.* Microvesicle-mediated transfer of microRNA-150 from monocytes to endothelial cells promotes angiogenesis. *J Biol Chem* **288**, 23586-23596, doi:10.1074/jbc.M113.489302 (2013).
174 Zou, X. *et al.* Human mesenchymal stromal cell-derived extracellular vesicles alleviate renal ischemic reperfusion injury and enhance angiogenesis in rats. *Am J Transl Res* **8**, 4289-4299 (2016).
175 Brill, A., Dashevsky, O., Rivo, J., Gozal, Y. & Varon, D. Platelet-derived microparticles induce angiogenesis and stimulate post-ischemic revascularization. *Cardiovasc Res* **67**, 30-38, doi:10.1016/j.cardiores.2005.04.007 (2005).
176 Ma, J. *et al.* Exosomes Derived from Akt-Modified Human Umbilical Cord Mesenchymal Stem Cells Improve Cardiac Regeneration and Promote Angiogenesis via Activating Platelet-Derived Growth Factor D. *Stem Cells Transl Med* **6**, 51-59, doi:10.5966/sctm.2016-0038 (2017).
177 Lopatina, T. *et al.* Platelet-derived growth factor regulates the secretion of extracellular vesicles by adipose mesenchymal stem cells and enhances their angiogenic potential. *Cell Commun Signal* **12**, 26, doi:10.1186/1478-811X-12-26 (2014).
178 Taraboletti, G. *et al.* Shedding of the matrix metalloproteinases MMP-2, MMP-9, and MT1-MMP as membrane vesicle-associated components by endothelial cells. *Am J Pathol* **160**, 673-680, doi:10.1016/S0002-9440(10)64887-0 (2002).
179 Fang, T. *et al.* Tumor-derived exosomal miR-1247-3p induces cancer-associated fibroblast activation to foster lung metastasis of liver cancer. *Nat Commun* **9**, 191, doi:10.1038/s41467-017-02583-0 (2018).
180 Sidhu, S. S., Mengistab, A. T., Tauscher, A. N., LaVail, J. & Basbaum, C. The microvesicle as a vehicle for EMMPRIN in tumor-stromal interactions. *Oncogene* **23**, 956-963, doi:10.1038/sj.onc.1207070 (2004).
181 Webber, J., Steadman, R., Mason, M. D., Tabi, Z. & Clayton, A. Cancer exosomes trigger fibroblast to myofibroblast differentiation. *Cancer Res* **70**, 9621-9630, doi:10.1158/0008-5472.CAN-10-1722 (2010).

182 Webber, J. P. *et al.* Differentiation of tumour-promoting stromal myofibroblasts by cancer exosomes. *Oncogene* **34**, 290-302, doi:10.1038/onc.2013.560 (2015).
183 Pang, W. *et al.* Pancreatic cancer-secreted miR-155 implicates in the conversion from normal fibroblasts to cancer-associated fibroblasts. *Cancer Sci* **106**, 1362-1369, doi:10.1111/cas.12747 (2015).
184 Rubin, G. D. Lung nodule and cancer detection in computed tomography screening. *J Thorac Imaging* **30**, 130-138, doi:10.1097/RTI.0000000000000140 (2015).
185 Ge, Z. *et al.* Computer-aided detection of lung nodules: false positive reduction using a 3D gradient field method and 3D ellipsoid fitting. *Med Phys* **32**, 2443-2454, doi:10.1118/1.1944667 (2005).
186 Dietel, M. *et al.* Diagnostic procedures for non-small-cell lung cancer (NSCLC): recommendations of the European Expert Group. *Thorax* **71**, 177-184, doi:10.1136/thoraxjnl-2014-206677 (2016).
187 Heerink, W. J. *et al.* Complication rates of CT-guided transthoracic lung biopsy: meta-analysis. *Eur Radiol* **27**, 138-148, doi:10.1007/s00330-016-4357-8 (2017).
188 Glinge, C. *et al.* Stability of Circulating Blood-Based MicroRNAs - Pre-Analytic Methodological Considerations. *PLoS One* **12**, e0167969, doi:10.1371/journal.pone.0167969 (2017).
189 Huan, J. *et al.* RNA trafficking by acute myelogenous leukemia exosomes. *Cancer Res* **73**, 918-929, doi:10.1158/0008-5472.CAN-12-2184 (2013).
190 Hunter, M. P. *et al.* Detection of microRNA expression in human peripheral blood microvesicles. *PLoS One* **3**, e3694, doi:10.1371/journal.pone.0003694 (2008).
191 Cheng, L., Sharples, R. A., Scicluna, B. J. & Hill, A. F. Exosomes provide a protective and enriched source of miRNA for biomarker profiling compared to intracellular and cell-free blood. *J Extracell Vesicles* **3**, doi:10.3402/jev.v3.23743 (2014).
192 Lawrie, C. H. MicroRNA expression in lymphoma. *Expert Opin Biol Ther* **7**, 1363-1374, doi:10.1517/14712598.7.9.1363 (2007).
193 Lawrie, C. H. *et al.* Detection of elevated levels of tumour-associated microRNAs in serum of patients with diffuse large B-cell lymphoma. *Br J Haematol* **141**, 672-675, doi:10.1111/j.1365-2141.2008.07077.x (2008).
194 Tan, L. *et al.* Genome-wide serum microRNA expression profiling identifies serum biomarkers for Alzheimer's disease. *J Alzheimers Dis* **40**, 1017-1027, doi:10.3233/JAD-132144 (2014).
195 Adachi, T. *et al.* Plasma microRNA 499 as a biomarker of acute myocardial infarction. *Clin Chem* **56**, 1183-1185, doi:10.1373/clinchem.2010.144121 (2010).
196 Sun, X. Y. *et al.* A preliminary analysis of microRNA as potential clinical biomarker for schizophrenia. *Am J Med Genet B Neuropsychiatr Genet* **168B**, 170-178, doi:10.1002/ajmg.b.32292 (2015).
197 Mundalil Vasu, M. *et al.* Serum microRNA profiles in children with autism. *Mol Autism* **5**, 40, doi:10.1186/2040-2392-5-40 (2014).
198 Wang, J. *et al.* Circulating microRNAs are promising novel biomarkers for drug-resistant epilepsy. *Sci Rep* **5**, 10201, doi:10.1038/srep10201 (2015).
199 Arroyo, J. D. *et al.* Argonaute2 complexes carry a population of circulating microRNAs independent of vesicles in human plasma. *Proc Natl Acad Sci U S A* **108**, 5003-5008, doi:10.1073/pnas.1019055108 (2011).

200 Turchinovich, A., Weiz, L., Langheinz, A. & Burwinkel, B. Characterization of extracellular circulating microRNA. *Nucleic Acids Res* **39**, 7223-7233, doi:10.1093/nar/gkr254 (2011).
201 Zhang, J. *et al.* Exosome and exosomal microRNA: trafficking, sorting, and function. *Genomics Proteomics Bioinformatics* **13**, 17-24, doi:10.1016/j.gpb.2015.02.001 (2015).
202 King, H. W., Michael, M. Z. & Gleadle, J. M. Hypoxic enhancement of exosome release by breast cancer cells. *BMC Cancer* **12**, 421, doi:10.1186/1471-2407-12-421 (2012).
203 Mazurov, D., Barbashova, L. & Filatov, A. Tetraspanin protein CD9 interacts with metalloprotease CD10 and enhances its release via exosomes. *FEBS J* **280**, 1200-1213, doi:10.1111/febs.12110 (2013).
204 Andreasen, D. *et al.* Improved microRNA quantification in total RNA from clinical samples. *Methods* **50**, S6-9, doi:10.1016/j.ymeth.2010.01.006 (2010).
205 Liu, C. J. *et al.* Increase of microRNA miR-31 level in plasma could be a potential marker of oral cancer. *Oral Dis* **16**, 360-364, doi:10.1111/j.1601-0825.2009.01646.x (2010).
206 Komatsu, S. *et al.* Circulating microRNAs in plasma of patients with oesophageal squamous cell carcinoma. *Br J Cancer* **105**, 104-111, doi:10.1038/bjc.2011.198 (2011).
207 Benjamini, Y. & Hochberg, Y. Controlling the False Discovery Rate: A Practical and Powerful Approach to Multiple Testing. *Journal of the Royal Statistical Society. Series B (Methodological)* **57**, 289-300 (1995).
208 McDonald, J. S., Milosevic, D., Reddi, H. V., Grebe, S. K. & Algeciras-Schimnich, A. Analysis of circulating microRNA: preanalytical and analytical challenges. *Clin Chem* **57**, 833-840, doi:10.1373/clinchem.2010.157198 (2011).
209 Benz, F. *et al.* U6 is unsuitable for normalization of serum miRNA levels in patients with sepsis or liver fibrosis. *Exp Mol Med* **45**, e42, doi:10.1038/emm.2013.81 (2013).
210 Bockmeyer, C. L. *et al.* Comparison of different normalization strategies for the analysis of glomerular microRNAs in IgA nephropathy. *Sci Rep* **6**, 31992, doi:10.1038/srep31992 (2016).
211 Vandesompele, J. *et al.* Accurate normalization of real-time quantitative RT-PCR data by geometric averaging of multiple internal control genes. *Genome Biol* **3**, RESEARCH0034 (2002).
212 Andersen, C. L., Jensen, J. L. & Orntoft, T. F. Normalization of real-time quantitative reverse transcription-PCR data: a model-based variance estimation approach to identify genes suited for normalization, applied to bladder and colon cancer data sets. *Cancer Res* **64**, 5245-5250, doi:10.1158/0008-5472.CAN-04-0496 (2004).
213 Kaduthanam, S. *et al.* Serum miR-142-3p is associated with early relapse in operable lung adenocarcinoma patients. *Lung Cancer* **80**, 223-227, doi:10.1016/j.lungcan.2013.01.013 (2013).
214 Schopman, N. C., Heynen, S., Haasnoot, J. & Berkhout, B. A miRNA-tRNA mix-up: tRNA origin of proposed miRNA. *RNA Biol* **7**, 573-576, doi:10.4161/rna.7.4.13141 (2010).
215 Fichtlscherer, S. *et al.* Circulating microRNAs in patients with coronary artery disease. *Circ Res* **107**, 677-684, doi:10.1161/CIRCRESAHA.109.215566 (2010).

216 Zhu, G. F. *et al.* microRNA-155 is inversely associated with severity of coronary stenotic lesions calculated by the Gensini score. *Coron Artery Dis* **25**, 304-310, doi:10.1097/MCA.0000000000000088 (2014).
217 Corral-Fernandez, N. E. *et al.* Dysregulated miR-155 expression in peripheral blood mononuclear cells from patients with type 2 diabetes. *Exp Clin Endocrinol Diabetes* **121**, 347-353, doi:10.1055/s-0033-1341516 (2013).
218 Backes, C., Meese, E. & Keller, A. Specific miRNA Disease Biomarkers in Blood, Serum and Plasma: Challenges and Prospects. *Mol Diagn Ther* **20**, 509-518, doi:10.1007/s40291-016-0221-4 (2016).
219 Wang, Y. T., Tsai, P. C., Liao, Y. C., Hsu, C. Y. & Juo, S. H. Circulating microRNAs have a sex-specific association with metabolic syndrome. *J Biomed Sci* **20**, 72, doi:10.1186/1423-0127-20-72 (2013).
220 Zhi, F. *et al.* A serum 6-miRNA panel as a novel non-invasive biomarker for meningioma. *Sci Rep* **6**, 32067, doi:10.1038/srep32067 (2016).
221 Mestdagh, P. *et al.* Evaluation of quantitative miRNA expression platforms in the microRNA quality control (miRQC) study. *Nat Methods* **11**, 809-815, doi:10.1038/nmeth.3014 (2014).
222 Yu, L. *et al.* Early detection of lung adenocarcinoma in sputum by a panel of microRNA markers. *Int J Cancer* **127**, 2870-2878, doi:10.1002/ijc.25289 (2010).
223 He, W. J. *et al.* MicroRNAs level as an initial screening method for early-stage lung cancer: a bivariate diagnostic random-effects meta-analysis. *Int J Clin Exp Med* **8**, 12317-12326 (2015).
224 Cazzoli, R. *et al.* microRNAs derived from circulating exosomes as noninvasive biomarkers for screening and diagnosing lung cancer. *J Thorac Oncol* **8**, 1156-1162, doi:10.1097/JTO.0b013e318299ac32 (2013).
225 Zhu, Z. *et al.* Comprehensive characterization of serum microRNA profile in response to the emerging avian influenza A (H7N9) virus infection in humans. *Viruses* **6**, 1525-1539, doi:10.3390/v6041525 (2014).
226 Chang, X. *et al.* Ethnic differences in microRNA-375 expression level and DNA methylation status in type 2 diabetes of Han and Kazak populations. *J Diabetes Res* **2014**, 761938, doi:10.1155/2014/761938 (2014).
227 Noren Hooten, N. *et al.* Age-related changes in microRNA levels in serum. *Aging (Albany NY)* **5**, 725-740, doi:10.18632/aging.100603 (2013).
228 Xiang, M. *et al.* U6 is not a suitable endogenous control for the quantification of circulating microRNAs. *Biochem Biophys Res Commun* **454**, 210-214, doi:10.1016/j.bbrc.2014.10.064 (2014).
229 Siegel, R., Ward, E., Brawley, O. & Jemal, A. Cancer statistics, 2011: the impact of eliminating socioeconomic and racial disparities on premature cancer deaths. *CA: a cancer journal for clinicians* **61**, 212-236, doi:10.3322/caac.20121 (2011).
230 Sculier, J. P. Nonsmall cell lung cancer. *European respiratory review : an official journal of the European Respiratory Society* **22**, 33-36, doi:10.1183/09059180.00007012 (2013).
231 Crino, L., Weder, W., van Meerbeeck, J. & Felip, E. Early stage and locally advanced (non-metastatic) non-small-cell lung cancer: ESMO Clinical Practice Guidelines for diagnosis, treatment and follow-up. *Annals of oncology : official journal of the European*

Society for Medical Oncology / ESMO **21 Suppl 5**, v103-115, doi:10.1093/annonc/mdq207 (2010).
232 Lee, T. H. *et al.* Microvesicles as mediators of intercellular communication in cancer--the emerging science of cellular 'debris'. *Seminars in immunopathology* **33**, 455-467, doi:10.1007/s00281-011-0250-3 (2011).
233 Katsuda, T., Kosaka, N. & Ochiya, T. The roles of extracellular vesicles in cancer biology: toward the development of novel cancer biomarkers. *Proteomics* **14**, 412-425, doi:10.1002/pmic.201300389 (2014).
234 Minciacchi, V. R., Freeman, M. R. & Di Vizio, D. in *Seminars in cell & developmental biology*. 41-51 (Elsevier).
235 Kawamata, T. & Tomari, Y. Making RISC. *Trends in biochemical sciences* **35**, 368-376, doi:10.1016/j.tibs.2010.03.009 (2010).
236 He, L. & Hannon, G. J. MicroRNAs: small RNAs with a big role in gene regulation. *Nature reviews. Genetics* **5**, 522-531, doi:10.1038/nrg1379 (2004).
237 Zhang, W., Liu, J. & Wang, G. The role of microRNAs in human breast cancer progression. *Tumour Biol* **35**, 6235-6244, doi:10.1007/s13277-014-2202-8 (2014).
238 Tominaga, N. *et al.* Brain metastatic cancer cells release microRNA-181c-containing extracellular vesicles capable of destructing blood-brain barrier. *Nat Commun* **6**, 6716, doi:10.1038/ncomms7716 (2015).
239 Chen, W. X. *et al.* Exosomes from drug-resistant breast cancer cells transmit chemoresistance by a horizontal transfer of microRNAs. *PLoS One* **9**, e95240, doi:10.1371/journal.pone.0095240 (2014).
240 Liu, Y. *et al.* STAT3-regulated exosomal miR-21 promotes angiogenesis and is involved in neoplastic processes of transformed human bronchial epithelial cells. *Cancer letters* **370**, 125-135, doi:10.1016/j.canlet.2015.10.011 (2016).
241 Huang, Z. & Feng, Y. Exosomes derived from hypoxic colorectal cancer cells promotes angiogenesis through Wnt4 induced beta-catenin signaling in endothelial cells. *Oncology research*, doi:10.3727/096504016X14752792816791 (2016).
242 Mineo, M. *et al.* Exosomes released by K562 chronic myeloid leukemia cells promote angiogenesis in a Src-dependent fashion. *Angiogenesis* **15**, 33-45, doi:10.1007/s10456-011-9241-1 (2012).
243 Janas, T., Janas, M. M. & Sapon, K. Mechanisms of RNA loading into exosomes. *FEBS letters* **589**, 1391-1398, doi:10.1016/j.febslet.2015.04.036 (2015).
244 Rani, S. *et al.* in *Gene Expression Profiling* 181-195 (Springer, 2011).
245 Mestdagh, P. *et al.* A novel and universal method for microRNA RT-qPCR data normalization. *Genome Biol* **10**, R64 (2009).
246 Montagne, R. *et al.* MET receptor variant R970C favors calpain-dependent generation of a fragment promoting epithelial cell scattering. *Oncotarget* **8**, 11268-11283, doi:10.18632/oncotarget.14499 (2017).
247 Koivunen, J. P. *et al.* EML4-ALK fusion gene and efficacy of an ALK kinase inhibitor in lung cancer. *Clin Cancer Res* **14**, 4275-4283, doi:10.1158/1078-0432.CCR-08-0168 (2008).
248 Forbes, S. A. *et al.* COSMIC: somatic cancer genetics at high-resolution. *Nucleic Acids Res* **45**, D777-D783, doi:10.1093/nar/gkw1121 (2017).

249 Dimitrova, N. *et al.* Stromal Expression of miR-143/145 Promotes Neoangiogenesis in Lung Cancer Development. *Cancer discovery* **6**, 188-201, doi:10.1158/2159-8290.CD-15-0854 (2016).
250 Hannafon, B. N. *et al.* Plasma exosome microRNAs are indicative of breast cancer. *Breast Cancer Res* **18**, 90, doi:10.1186/s13058-016-0753-x (2016).
251 Lei, Z. *et al.* MiR-142-3p represses TGF-beta-induced growth inhibition through repression of TGFbetaR1 in non-small cell lung cancer. *FASEB J* **28**, 2696-2704, doi:10.1096/fj.13-247288 (2014).
252 Wang, W. H. *et al.* MiR-150-5p suppresses colorectal cancer cell migration and invasion through targeting MUC4. *Asian Pacific journal of cancer prevention : APJCP* **15**, 6269-6273 (2014).
253 Wang, J. *et al.* Downregulation of miR-486-5p contributes to tumor progression and metastasis by targeting protumorigenic ARHGAP5 in lung cancer. *Oncogene* **33**, 1181-1189, doi:10.1038/onc.2013.42 (2014).
254 Wang, R. *et al.* MicroRNA-451 functions as a tumor suppressor in human non-small cell lung cancer by targeting ras-related protein 14 (RAB14). *Oncogene* **30**, 2644-2658, doi:10.1038/onc.2010.642 (2011).
255 Chen, X. *et al.* Role of miR-143 targeting KRAS in colorectal tumorigenesis. *Oncogene* **28**, 1385-1392, doi:10.1038/onc.2008.474 (2009).
256 Su, J. *et al.* MiR-143 and MiR-145 regulate IGF1R to suppress cell proliferation in colorectal cancer. *PLoS One* **9**, e114420, doi:10.1371/journal.pone.0114420 (2014).
257 Cho, W. C., Chow, A. S. & Au, J. S. MiR-145 inhibits cell proliferation of human lung adenocarcinoma by targeting EGFR and NUDT1. *RNA Biol* **8**, 125-131 (2011).
258 Jung, H. J. & Suh, Y. Regulation of IGF -1 signaling by microRNAs. *Frontiers in genetics* **5**, 472, doi:10.3389/fgene.2014.00472 (2014).
259 Xiao, J., Lin, H., Luo, X. & Wang, Z. miR-605 joins p53 network to form a p53:miR-605:Mdm2 positive feedback loop in response to stress. *EMBO J* **30**, 5021, doi:10.1038/emboj.2011.463 (2011).
260 Cui, S. Y., Wang, R. & Chen, L. B. MicroRNA-145: a potent tumour suppressor that regulates multiple cellular pathways. *Journal of cellular and molecular medicine* **18**, 1913-1926, doi:10.1111/jcmm.12358 (2014).
261 He, Z. *et al.* MiR-143-3p functions as a tumor suppressor by regulating cell proliferation, invasion and epithelial-mesenchymal transition by targeting QKI-5 in esophageal squamous cell carcinoma. *Molecular cancer* **15**, 51, doi:10.1186/s12943-016-0533-3 (2016).
262 Lin, T. *et al.* MicroRNA-143 as a tumor suppressor for bladder cancer. *The Journal of urology* **181**, 1372-1380, doi:10.1016/j.juro.2008.10.149 (2009).
263 Liu, L. *et al.* miR-143 is downregulated in cervical cancer and promotes apoptosis and inhibits tumor formation by targeting Bcl-2. *Molecular medicine reports* **5**, 753-760, doi:10.3892/mmr.2011.696 (2012).
264 Wang, Z., Chen, J. Q., Liu, J. L. & Tian, L. Exosomes in tumor microenvironment: novel transporters and biomarkers. *J Transl Med* **14**, 297, doi:10.1186/s12967-016-1056-9 (2016).
265 Taylor, D. D. & Gercel-Taylor, C. MicroRNA signatures of tumor-derived exosomes as diagnostic biomarkers of ovarian cancer. *Gynecologic oncology* **110**, 13-21 (2008).

266 Rabinowits, G., Gerçel-Taylor, C., Day, J. M., Taylor, D. D. & Kloecker, G. H. Exosomal microRNA: a diagnostic marker for lung cancer. *Clinical lung cancer* **10**, 42-46 (2009).
267 Michael, A. *et al.* Exosomes from human saliva as a source of microRNA biomarkers. *Oral diseases* **16**, 34-38 (2010).
268 Valadi, H. *et al.* Exosome-mediated transfer of mRNAs and microRNAs is a novel mechanism of genetic exchange between cells. *Nature cell biology* **9**, 654-659, doi:10.1038/ncb1596 (2007).
269 Dickman, C. T. *et al.* Selective extracellular vesicle exclusion of miR-142-3p by oral cancer cells promotes both internal and extracellular malignant phenotypes. *Oncotarget* **8**, 15252-15266, doi:10.18632/oncotarget.14862 (2017).
270 Sukma Dewi, I. *et al.* Exosomal miR-142-3p is increased during cardiac allograft rejection and augments vascular permeability through down-regulation of endothelial RAB11FIP2 expression. *Cardiovasc Res* **113**, 440-452, doi:10.1093/cvr/cvw244 (2017).
271 Cancer Genome Atlas Research, N. Comprehensive molecular profiling of lung adenocarcinoma. *Nature* **511**, 543-550, doi:10.1038/nature13385 (2014).
272 Xiao, P. & Liu, W. L. MiR-142-3p functions as a potential tumor suppressor directly targeting HMGB1 in non-small-cell lung carcinoma. *Int J Clin Exp Pathol* **8**, 10800-10807 (2015).
273 Kim, W. *et al.* TFAP2C-mediated upregulation of TGFBR1 promotes lung tumorigenesis and epithelial-mesenchymal transition. *Exp Mol Med* **48**, e273, doi:10.1038/emm.2016.125 (2016).
274 Geback, T., Schulz, M. M., Koumoutsakos, P. & Detmar, M. TScratch: a novel and simple software tool for automated analysis of monolayer wound healing assays. *Biotechniques* **46**, 265-274, doi:10.2144/000113083 (2009).
275 Lawson, J. *et al.* Selective secretion of microRNAs from lung cancer cells via extracellular vesicles promotes CAMK1D-mediated tube formation in endothelial cells. *Oncotarget* **8**, 83913-83924, doi:10.18632/oncotarget.19996 (2017).
276 Cao, X. C. *et al.* miR-142-3p inhibits cancer cell proliferation by targeting CDC25C. *Cell Prolif* **49**, 58-68, doi:10.1111/cpr.12235 (2016).
277 Xu, S. *et al.* Effect of miR-142-3p on the M2 macrophage and therapeutic efficacy against murine glioblastoma. *Journal of the National Cancer Institute* **106**, dju162 (2014).
278 Klemm, F. & Joyce, J. A. Microenvironmental regulation of therapeutic response in cancer. *Trends Cell Biol* **25**, 198-213, doi:10.1016/j.tcb.2014.11.006 (2015).
279 Shiga, K. *et al.* Cancer-associated fibroblasts: their characteristics and their roles in tumor growth. *Cancers* **7**, 2443-2458 (2015).
280 Calon, A., Tauriello, D. V. & Batlle, E. TGF-beta in CAF-mediated tumor growth and metastasis. *Semin Cancer Biol* **25**, 15-22, doi:10.1016/j.semcancer.2013.12.008 (2014).
281 Shi, Y. & Massague, J. Mechanisms of TGF-beta signaling from cell membrane to the nucleus. *Cell* **113**, 685-700 (2003).
282 Li, Q. *et al.* MiR-21/Smad 7 signaling determines TGF-β1-induced CAF formation. *Sci Rep* **3**, 2038 (2013).
283 Rønnov-Jessen, L. & Petersen, O. W. Induction of alpha-smooth muscle actin by transforming growth factor-beta 1 in quiescent human breast gland fibroblasts.

Implications for myofibroblast generation in breast neoplasia. *Laboratory investigation; a journal of technical methods and pathology* **68**, 696-707 (1993).
284 Cao, X. C. *et al.* miR-142-3p inhibits cancer cell proliferation by targeting CDC25C. *Cell Proliferat* **49**, 58-68, doi:10.1111/cpr.12235 (2016).
285 Lu, Y. B. *et al.* MiR-142 modulates human pancreatic cancer proliferation and invasion by targeting hypoxia-inducible factor 1 (HIF-1 alpha) in the tumor microenvironments. *Biol Open* **6**, 252-259, doi:10.1242/bio.021774 (2017).
286 Zheng, Z. H. *et al.* miR-142 acts as a tumor suppressor in osteosarcoma cell lines by targeting Rac1. *Oncol Rep* **33**, 1291-1299, doi:10.3892/or.2014.3687 (2015).
287 Shen, W. W., Zeng, Z., Zhu, W. X. & Fu, G. H. MiR-142-3p functions as a tumor suppressor by targeting CD133, ABCG2, and Lgr5 in colon cancer cells. *J Mol Med (Berl)* **91**, 989-1000, doi:10.1007/s00109-013-1037-x (2013).
288 Schwickert, A. *et al.* microRNA miR-142-3p Inhibits Breast Cancer Cell Invasiveness by Synchronous Targeting of WASL, Integrin Alpha V, and Additional Cytoskeletal Elements. *PLoS One* **10**, e0143993, doi:10.1371/journal.pone.0143993 (2015).
289 Qi, X., Li, J., Zhou, C., Lv, C. & Tian, M. MiR-142-3p Suppresses SOCS6 Expression and Promotes Cell Proliferation in Nasopharyngeal Carcinoma. *Cell Physiol Biochem* **36**, 1743-1752, doi:10.1159/000430147 (2015).
290 Lv, M. *et al.* An oncogenic role of miR-142-3p in human T-cell acute lymphoblastic leukemia (T-ALL) by targeting glucocorticoid receptor-alpha and cAMP/PKA pathways. *Leukemia* **26**, 769-777, doi:10.1038/leu.2011.273 (2012).
291 Li, Y. F. *et al.* Oncogenic microRNA-142-3p is associated with cellular migration, proliferation and apoptosis in renal cell carcinoma. *Oncology Letters* **11**, 1235-1241, doi:10.3892/ol.2015.4021 (2016).
292 Zhu, J. J., Tian, X. X., Zhang, Y., Bai, Y. L. & Pei, K. MiR-142-3p is a tumor promoter by directly targeting FOXO4 to promote gastric cancer cell growth and suppress cell apoptosis in gastric cancer. *Int J Clin Exp Patho* **9**, 12079-12087 (2016).
293 Boeri, M. *et al.* MicroRNA signatures in tissues and plasma predict development and prognosis of computed tomography detected lung cancer. *Proc Natl Acad Sci U S A* **108**, 3713-3718, doi:10.1073/pnas.1100048108 (2011).
294 Bu, N. *et al.* Exosome-loaded dendritic cells elicit tumor-specific CD8+ cytotoxic T cells in patients with glioma. *J Neurooncol* **104**, 659-667, doi:10.1007/s11060-011-0537-1 (2011).
295 Taylor, D. D., Gercel-Taylor, C., Lyons, K. S., Stanson, J. & Whiteside, T. L. T-cell apoptosis and suppression of T-cell receptor/CD3-zeta by Fas ligand-containing membrane vesicles shed from ovarian tumors. *Clin Cancer Res* **9**, 5113-5119 (2003).
296 Andreola, G. *et al.* Induction of lymphocyte apoptosis by tumor cell secretion of FasL-bearing microvesicles. *J Exp Med* **195**, 1303-1316 (2002).
297 Valenti, R. *et al.* Human tumor-released microvesicles promote the differentiation of myeloid cells with transforming growth factor-beta-mediated suppressive activity on T lymphocytes. *Cancer Res* **66**, 9290-9298, doi:10.1158/0008-5472.CAN-06-1819 (2006).
298 Liao, J., Liu, R., Shi, Y. J., Yin, L. H. & Pu, Y. P. Exosome-shuttling microRNA-21 promotes cell migration and invasion-targeting PDCD4 in esophageal cancer. *Int J Oncol* **48**, 2567-2579, doi:10.3892/ijo.2016.3453 (2016).

299 Krek, A. *et al.* Combinatorial microRNA target predictions. *Nat Genet* **37**, 495-500, doi:10.1038/ng1536 (2005).
300 Guido, C. *et al.* Metabolic reprogramming of cancer-associated fibroblasts by TGF-beta drives tumor growth: connecting TGF-beta signaling with "Warburg-like" cancer metabolism and L-lactate production. *Cell Cycle* **11**, 3019-3035, doi:10.4161/cc.21384 (2012).
301 Takagawa, S. *et al.* Sustained activation of fibroblast transforming growth factor-beta/Smad signaling in a murine model of scleroderma. *J Invest Dermatol* **121**, 41-50, doi:10.1046/j.1523-1747.2003.12308.x (2003).
302 Marleau, A. M., Chen, C. S., Joyce, J. A. & Tullis, R. H. Exosome removal as a therapeutic adjuvant in cancer. *J Transl Med* **10**, 134, doi:10.1186/1479-5876-10-134 (2012).
303 Decaussin, M. *et al.* Expression of vascular endothelial growth factor (VEGF) and its two receptors (VEGF-R1-Flt1 and VEGF-R2-Flk1/KDR) in non-small cell lung carcinomas (NSCLCs): correlation with angiogenesis and survival. *J Pathol* **188**, 369-377, doi:10.1002/(SICI)1096-9896(199908)188:4<369::AID-PATH381>3.0.CO;2-X (1999).
304 Charous, S. J., Stricklin, G. P., Nanney, L. B., Netterville, J. L. & Burkey, B. B. Expression of matrix metalloproteinases and tissue inhibitor of metalloproteinases in head and neck squamous cell carcinoma. *Ann Otol Rhinol Laryngol* **106**, 271-278, doi:10.1177/000348949710600402 (1997).
305 Kurahara, S. *et al.* Expression of MMPS, MT-MMP, and TIMPs in squamous cell carcinoma of the oral cavity: correlations with tumor invasion and metastasis. *Head Neck* **21**, 627-638 (1999).
306 Ikebe, T. *et al.* Gelatinolytic activity of matrix metalloproteinase in tumor tissues correlates with the invasiveness of oral cancer. *Clin Exp Metastasis* **17**, 315-323 (1999).
307 Rong, L., Li, R., Li, S. & Luo, R. Immunosuppression of breast cancer cells mediated by transforming growth factor-beta in exosomes from cancer cells. *Oncol Lett* **11**, 500-504, doi:10.3892/ol.2015.3841 (2016).
308 Mehner, C. *et al.* Tumor cell-produced matrix metalloproteinase 9 (MMP-9) drives malignant progression and metastasis of basal-like triple negative breast cancer. *Oncotarget* **5**, 2736-2749, doi:10.18632/oncotarget.1932 (2014).
309 Espinoza, J. L. *et al.* Human microRNA-1245 down-regulates the NKG2D receptor in natural killer cells and impairs NKG2D-mediated functions. *Haematologica* **97**, 1295-1303, doi:10.3324/haematol.2011.058529 (2012).
310 Wang, Y. *et al.* Role of deregulated microRNAs in non-small cell lung cancer progression using fresh-frozen and formalin-fixed, paraffin-embedded samples. *Oncol Lett* **11**, 801-808, doi:10.3892/ol.2015.3976 (2016).
311 Michael, M. Z., SM, O. C., van Holst Pellekaan, N. G., Young, G. P. & James, R. J. Reduced accumulation of specific microRNAs in colorectal neoplasia. *Mol Cancer Res* **1**, 882-891 (2003).
312 Zhang, B., Pan, X., Cobb, G. P. & Anderson, T. A. microRNAs as oncogenes and tumor suppressors. *Dev Biol* **302**, 1-12, doi:10.1016/j.ydbio.2006.08.028 (2007).